70 P.

Final Report IN-14321

for

NASA Grant NAG 1-216

Experimental Study Using Nearfield Acoustic Holography of Sound Transmission through Fuselage Sidewall Structures

PJ304292

J. D. Maynard
Department of Physics
The Pennsylvania State University
University Park, PA 16802

(NASA-CR-177162) EXPERIMENTAL STUDY USING NEARFIELD ACOUSTIC HOLOGRAPHY OF SOUND TRANSMISSION THROUGH FUSELAGE SIDEWALL STRUCTURES Final Report (Pennsylvania State Univ.) 70 p HC A04/MF A01 CSCL 20A G3/71 N86-28702 Unclas 43421

I. INTRODUCTION

The reduction of cabin noise in lightweight, propeller-driven aircraft is an especially difficult problem in noise control. The cabin noise spectrum contains low frequency tonal components which are generated by the propeller blades (which may pass close to the cabin sidewalls) and possibly by the engines. The acoustic energy of these components is transmitted through the air or aircraft structure to the cabin sidewalls where it is radiated into the interior. The difficulty in reducing this low frequency radiation arises from the weight limitations of the aircraft which preclude the use of conventional low frequency treatments such as heavy mass addition, stiffening, damping, or cabin isolation. A more sophisticated solution to the problem requires a detailed understanding of acoustic energy transmission to and re-radiation by the aircraft sidewalls and the effects of structure changes and treatments. With such a thorough understanding, an efficient quieting technique may be found.

Such a detailed understanding of how a complex vibrator radiates sound may be achieved through a visualization of the acoustic vector intensity field generated by the vibrator. In order to probe the subtle interactions which occur near a complex vibrator, a high density of data points is necessary; obtaining such a mass of data with conventional point-by-point probes would require a prohibitively long time. However, such data may be obtained efficiently through the use of acoustic holography. With the technique of holography, data measured on a two-dimensional surface may be used to reconstruct an entire three-dimensional radiated sound field and all associated energy fields. The great power of the technique arises from the enormous increase in the amount of information which occurs in going from a two-dimensional measured field to several fields reconstructed in three dimensions. However, it is usually assumed in holography that the spatial resolution of a reconstructed

field is limited by the wavelength of the radiation, and a large number of sound radiation problems, including noise radiation from aircraft panels, involve low frequency, long wavelength (and therefore poorly resolved) components. Because of this, acoustical holography has been rejected as a means of precisely locating and quantifying low frequency acoustic energy sources. However, the wavelength resolution limitation is not intrinsic to the fundamental principles of holography but rather is due to experimental limitations which are present in optical holography but are not necessarily present in acoustical holography. At the Pennsylvania State University we have developed a new technique, called Nearfield Acoustic Holography (NAH), which is free from the limitations of conventional holography, and we have applied the new technique to the study of sound radiation from several samples of lightweight aircraft sidewall panels. This study involved the use of NAH to determine the mode of vibration and acoustic intensity for panels which differed in:

1) Construction (number of stiffening ribs, size of stiffening ribs, construction material, panel surface curvature, etc.).

2) Boundary support condition (free edge condition or clamped edge condition).

3) Mode of excitation (structural-borne forces or airborne forces).

It had been predicted[1] that the last feature, mode of excitation, would be particularly interesting.

In Section II of this paper we present a brief description of the NAH technique (details may be found in the references).[2-9] In Section III we describe the different samples of aircraft panels and discuss the measurement of their natural response frequencies under the various boundary support and excitation conditions. Finally in Section IV we present figures showing the results of the NAH measurements.

II. NEARFIELD ACOUSTIC HOLOGRAPHY (NAH) TECHNIQUE

The details of the Nearfield Acoustic Holography (NAH) technique may be found in references 2-9; in this section only a brief outline is presented.

The NAH technique is based on the principles of holography in which measurements on a two-dimensional surface are used to reconstruct an entire three-dimensional wave field. The nearfield acoustic technique differs from conventional holographic systems in a crucial way and, as a result, has several significant advantages, such as having a high spatial resolution (not limited by the wavelength of the radiation) and being able to determine the acoustic vector intensity field.[2] Experimentally the technique involves recording the sound pressure field close to the source with a plane array of microphones, digitally processing the data with an on-line mini-computer and array processor, and displaying the results with computer graphics. With a single measurement one can determine the sound pressure field, the particle velocity field, and the vector intensity field in a large region next to the source. From the particle velocity field one can visualize the surface vibration of the source; with the vector intensity field one can locate the energy producing areas of a vibrating structure, trace the flow of acoustic energy away from the source, determine the farfield radiation pattern and the total power radiated (into a half-space), and identify regions of high spatial correlation (circulating energy flow fields). The advantage of nearfield acoustic holograrphy lies in its ability to furnish a large amount of information in a short time; the three components of the vector intensity can be determined at more than 4000 points in space in less than 30 minutes.

III. DESCRIPTION OF THE AIRCRAFT PANELS, SUPPORT SYSTEM, AND EXCITATION SYSTEM

A total of six samples of lightweight aircraft panels were examined in the study; some of the features of these are summarized in Figure 1 and Table 1. All of the panels were rectangular with a length of 1.0 m and a width of 0.76 m. Three of the panels had flat surfaces while three were curved, with a displacement of 2.5 cm at the long centerline. Four of the panels were stiffened with individual ribs, while two involved a sandwiched honeycomb construction. The individual ribs were fastened to the panel skin with rivits and eopxy. As will be discussed in Section IV, the NAH measurements revealed that the epoxy bonding was not uniform.

The panel samples were studied under two different support conditions; free-edge and clamped-edge. The free-edge condition was obtained by simply placing the panels on a large, flat, soft foam cushion, approximatly 15 cm thick. It had been found in earlier research with vibrating plates that while the foam damped the plate vibration amplitude, it did so uniformly so that the surface vibration pattern and radiated sound field were not affected by the foam support. The clamped-edge condition was obtained (approximately) by fastening the panels to a box with massive walls, illustrated in Figure 2. The walls of the box in immediate contact with the panel were made of 1.9 cm thick aluminum and were sufficiently massive to present a large impedance change at the panel edge which approximated a clamped boundary condition. The panel samples were fastned to the aluminum box walls with a large number of machine screws (with a spacing of 2.5 cm). The short walls had a curvature which matched that of the curved panels; for mounting the flat panels, an adapter with a matching concave curvature was positioned between the flat panel and the box wall. For all panel mountings an airtight seal was obtained with a stiff, high temperature wax.

The remainder of the mounting box, below the aluminum walls (see Figure 2) was constructed with thick (2.5 cm) plywood; the main panel was rendered more stiff and massive by using three thicknesses glued together. Attached to the main panel are nine individual boxes which enclose nine audio speakers sealed in holes in the main panel; the nine individual boxes inhibit sound radiation from the back of the speakers and avoid resonances which would be present if a single enclosing box had been used. When an aircraft panel is mounted, the aluminum walls, main wood panel, and speakers from a sealed box; activating the speakers produces a uniform pressure on the aircraft panel which simulates excitation by low frequency airborne sound.

As discussed in the Introduction, the panels were measured using structure borne and airborne excitation. The structure borne excitation wss simulated by mounting (using a threaded stud and epoxy adhesive) an electromechanical shaker directly to the aircraft panel surface. The airborne excitation was simulated with the sealed box described above; the airborne excitation was only used with the clamped boundary condition.

Before making the measurements with the NAH system, the natural frequencies of vibration (within a 100-2000 Hz range) for each of the aircraft panels were determined using a Hewlett-Packard Model 3580A spectrum analyzer. The frequency spectra were measured for each of the two modes of excitation (structure borne and airborne) and found to be different; this was expected since different distributions of excitation forces may couple in different ways to different normal modes of vibration. This mechanism also accounts for the different levels of sound radiation from the panels for the different modes of excitation.

The measured frequency spectra are shown in Figures 3-15. The frequency scale is shown in each figure; the vertical scale is in arbitrary units since the drive levels were not calibrated. The panel numbers (1-6) and mode of excitation are indicated in each figure.

IV. RESULTS OF NEARFIELD ACOUSTIC HOLOGRAPHY MEASUREMENTS

The Nearfield Acoustic Holography technique generates such an enormous amount of data that it is possible to reproduce only a sample of it in this report. Usually the output is reviewed rapidly with a high-speed online computer graphics system. For purposes of comparing the sound radiation from the different aircraft panels under the different modes of excitation, the most useful method is to use the plots of the surface acoustic intensity; other NAH reconstructed fields may be obtained by request from the author of this report.

The NAH data is shown in the figures appended to this report. The first three letters of the figure labels indicate the type of panel and mode of excitation as indicated in Table II. The three digits in the figure label indicate the frequency of excitation in Hertz. The lack of symmetry in the reconstructions above the panels indicates the non-uniformity of the rib bonding epoxy.

REFERENCES

1. M. C. McGary and W. H. Mayes, Noise Control Eng. 20, 21 (1983).
2. J. D. Maynard, E. G. Williams and Y. Lee, J. Acoust. Soc. Am. 78, 1395 (1985).
3. W. A. Veronesi and J. D. Maynard, to be published in J. Acoust. Soc. Am.
4. J. D. Maynard, J. Acoust. Soc. Am. 74, S37 (1983).
5. D. J. Bowen and J. D. Maynard, J. Acoust. Soc. Am. 75, S71 (1984).
6. Y. Huang, W. A. Veronsei and J. D. Maynard, J. Acoust. Soc. Am. 75, S71 (1984).
7. W. A. Veronsei and J. D. Maynard, J. Acoust Soc. Am. 75, S71 (1984).
8. Y. Lee and J. D. Maynard, J. Acoust. Soc. Am. 75, S71 (1984).
9. W. A. Veronsei and J. D. Maynard, J. Acoust. Soc. Am. 75, S71 (1984).

Table I. Lightweight aircraft panel sample characteristics.

Panel number	Number of ribs	Rib dimensions (A × B × C) (cm)	Rib Spacing D.(cm)	Number of rivits per rib	Rivit Spacing (cm)	Panel description
1	6	4.4 × 10.0 × 65.4	16.5	6	27.6	Curved
2	11	4.4 × 5.0 × 65.4	7.6	6	27.6	Curved
3	0	-	-	-	-	Curved honeycomb
4	6	4.4 × 10.0 × 65.7	16.2	6	27.6	Flat
5	0	-	-	-	-	Flat honeycomb
6	6	4.4 × 10.0 × 65.7	16.2	6	27.6	Flat with graphite composite ribs

Table II. Label codes for appended figures of NAH data

ARS	Panel No. 1 (6 ribs), structure borne excitation
ARB	Panel No. 1 (6 ribs), airborne excitation
ARM	Panel No. 2 (11 ribs), structure borne excitation
ARL	Panel No. 2 (11 ribs), airborne excitation

FIGURE CAPTIONS

Fig. 1. Illustration of generic lightweight aircraft panel sample. Dimensions are in centimeters. Dimensions A-D are given in Table I.

Fig. 2. Mounting box for damped edge conditions and airborne sound excitations.

Fig. 3-16. Aircraft panel response frequency spectra. Panel number and mode of excitation are indicated in the figure.

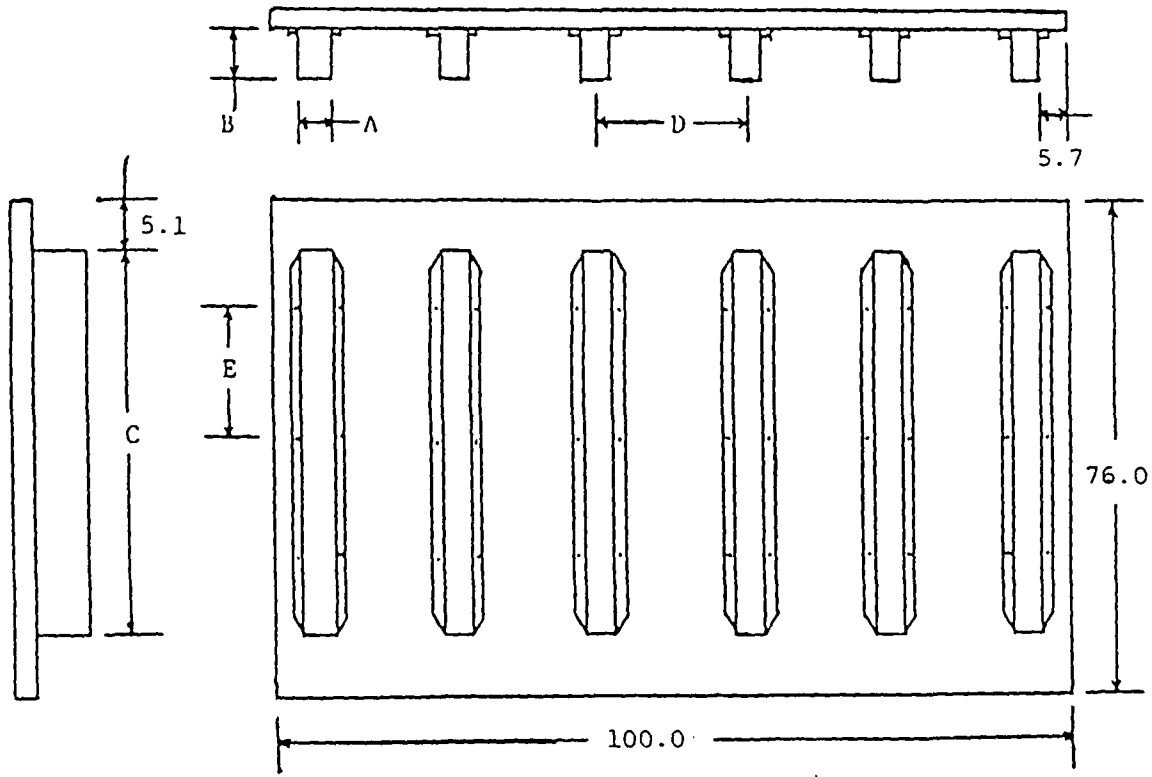

Figure 1. Illustration of generic lightweight aircraft panel sample. Dimensions are in centimeters. Dimensions A-D are given in Table I.

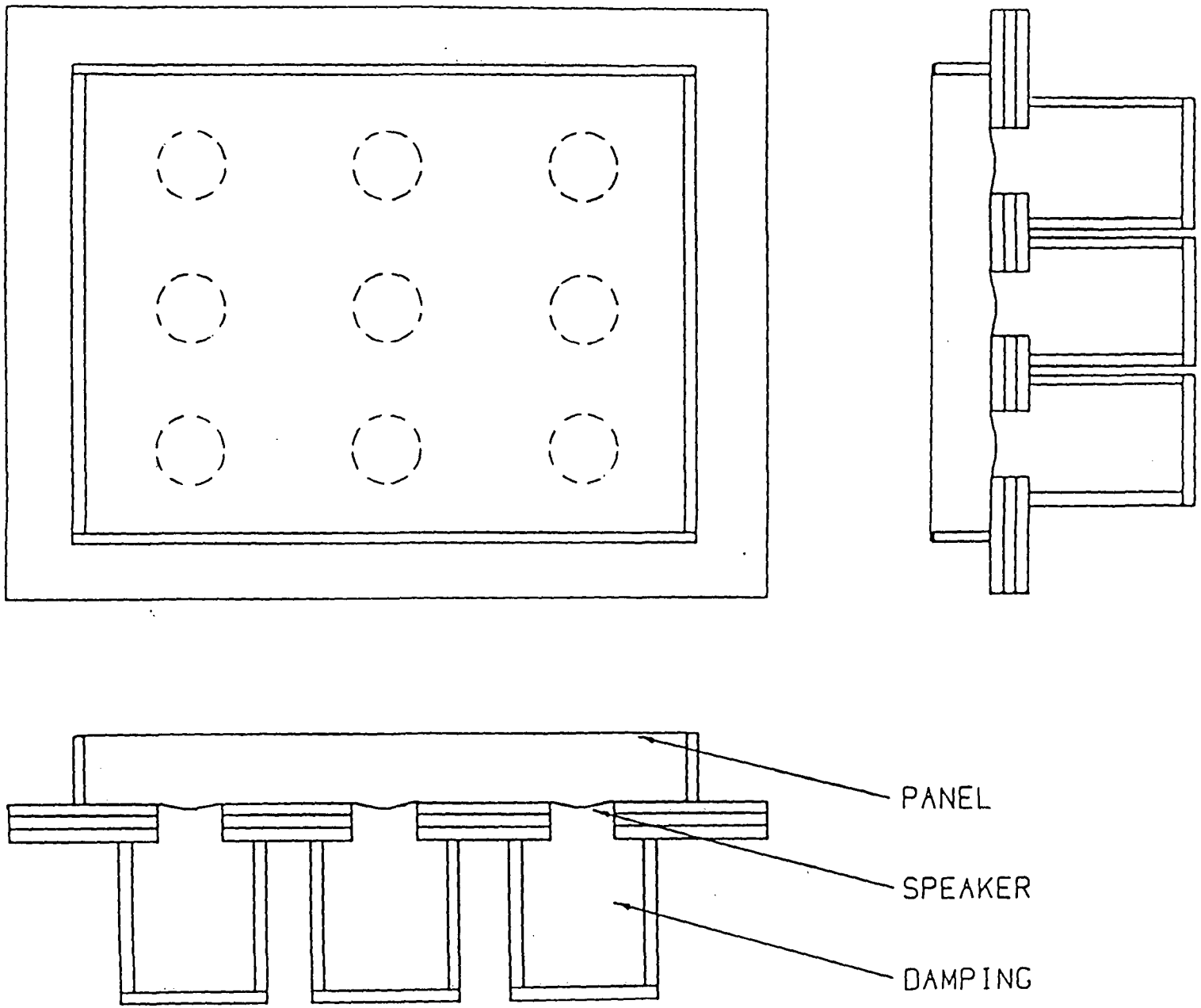

Figure 2. Mounting box for clamped edge condition and airborne sound excitation.

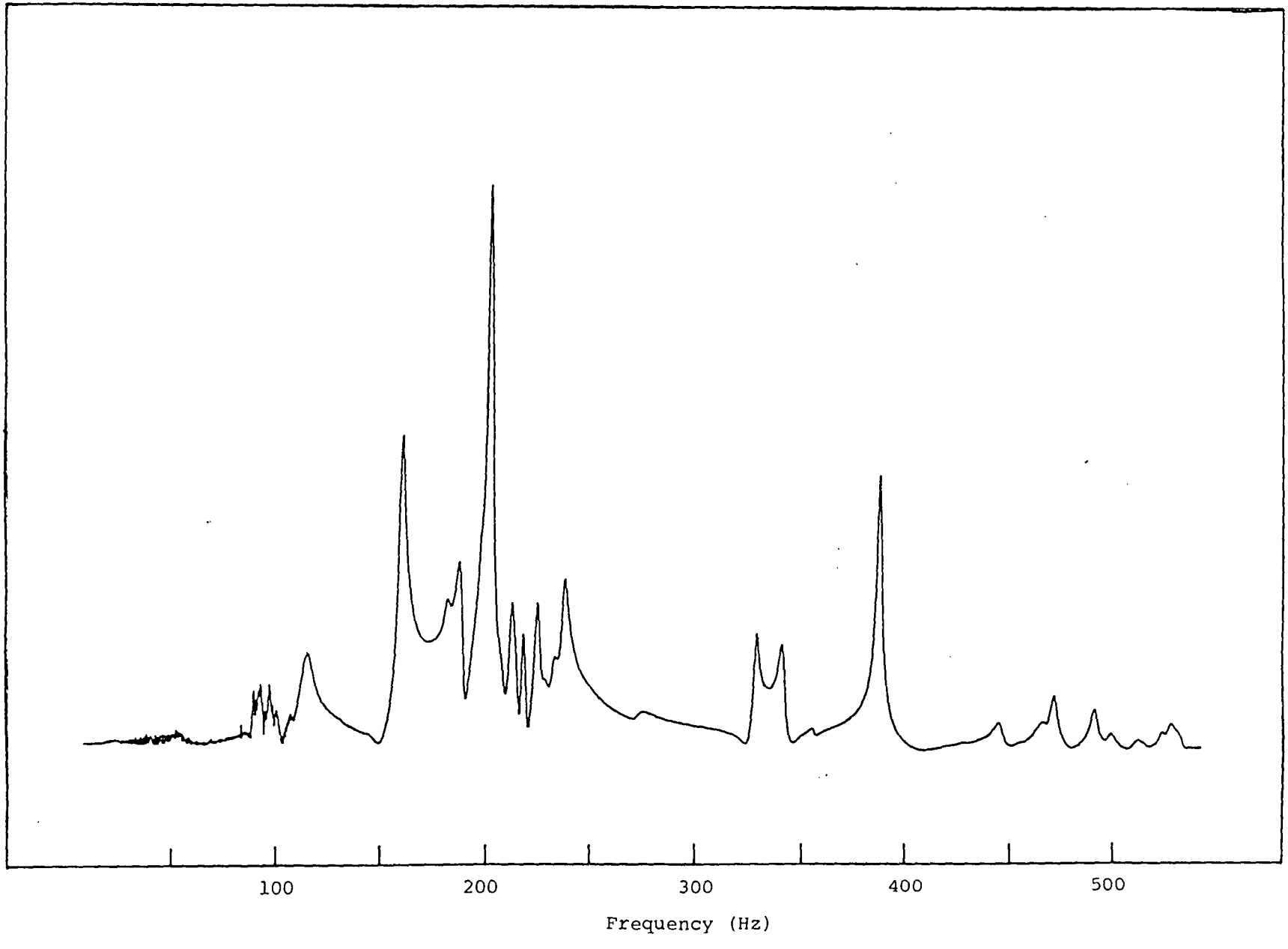

Figure 3. Frequency response of aircraft panel No. 1 with structure borne excitation.

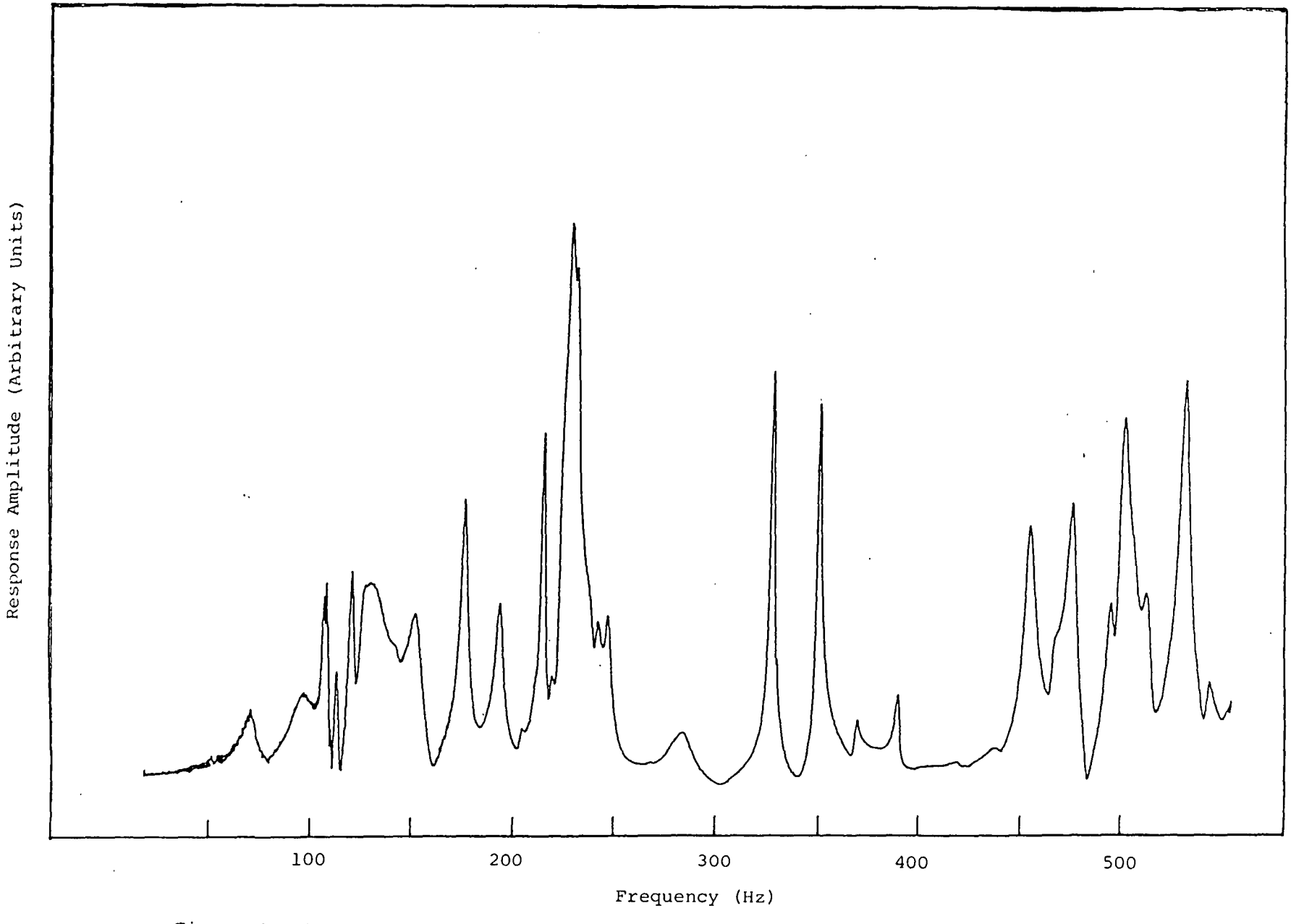

Figure 4. Frequency response of aircraft panel No. 2 with airborne excitation.

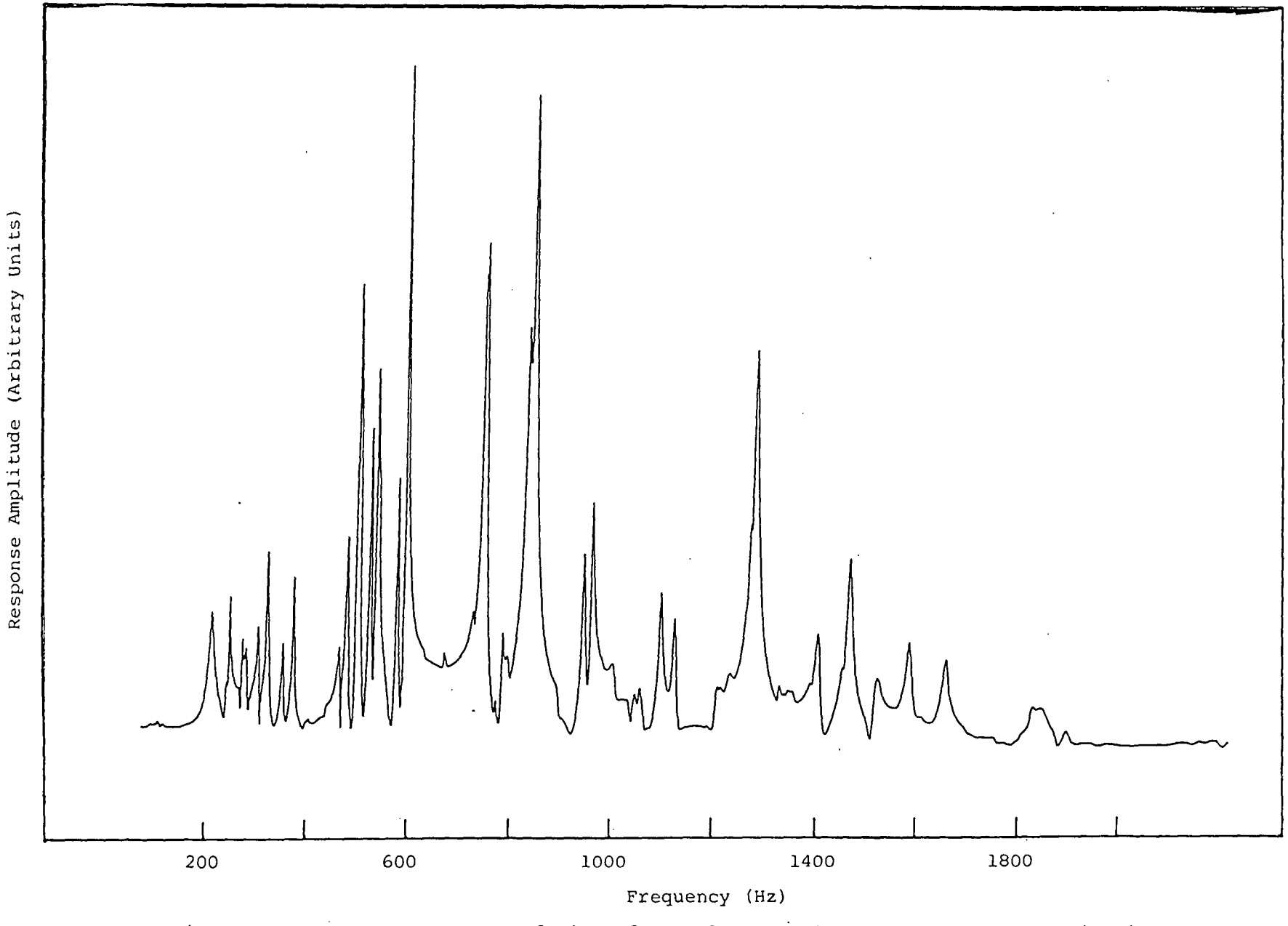

Figure 5. Frequency response of aircraft panel No. 2 with structure borne excitation.

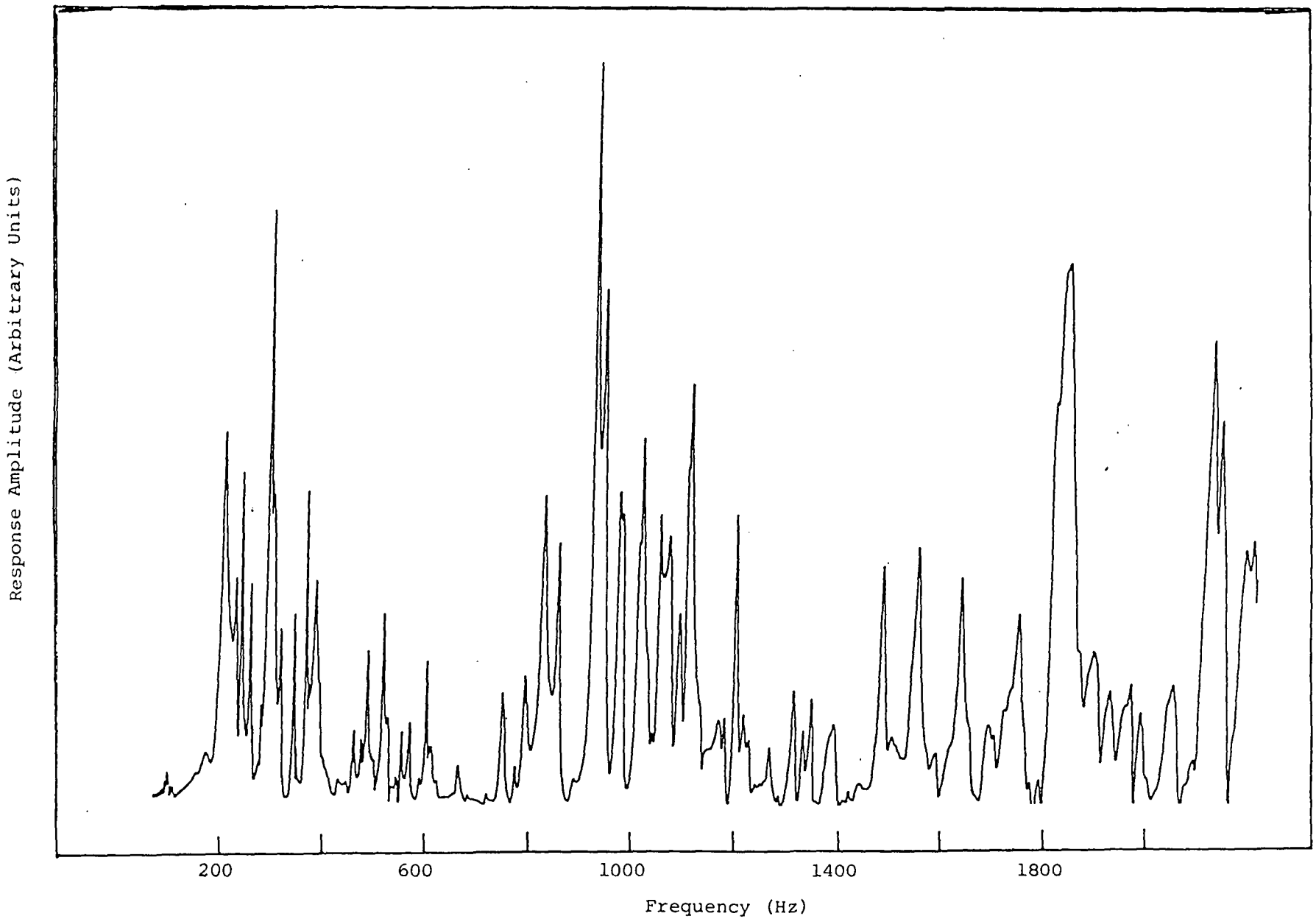

Figure 6. Frequency response of aircraft panel No. 2 with airborne excitation.

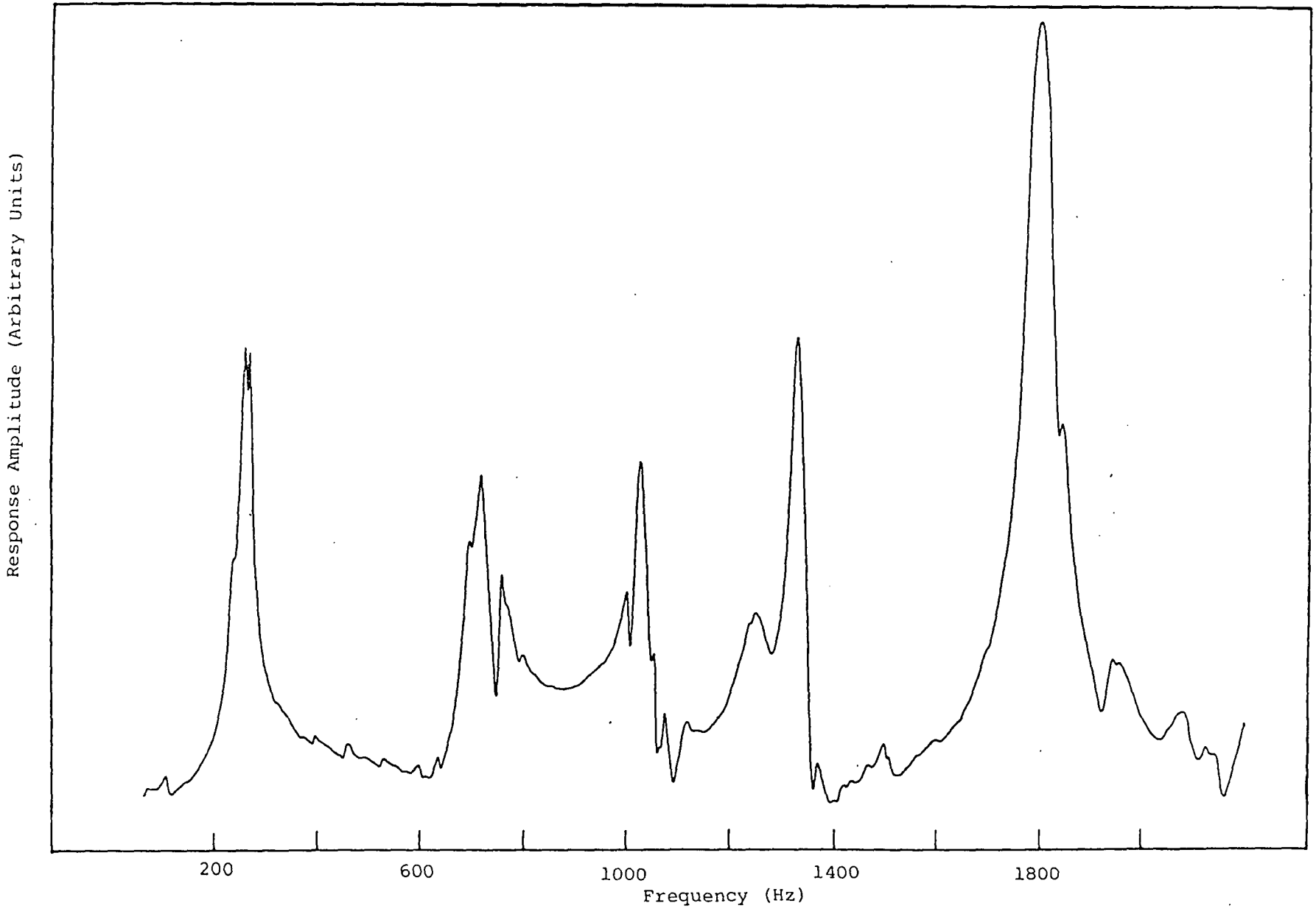

Figure 7. Frequency response of aircraft panel No. 3 with structure borne excitation.

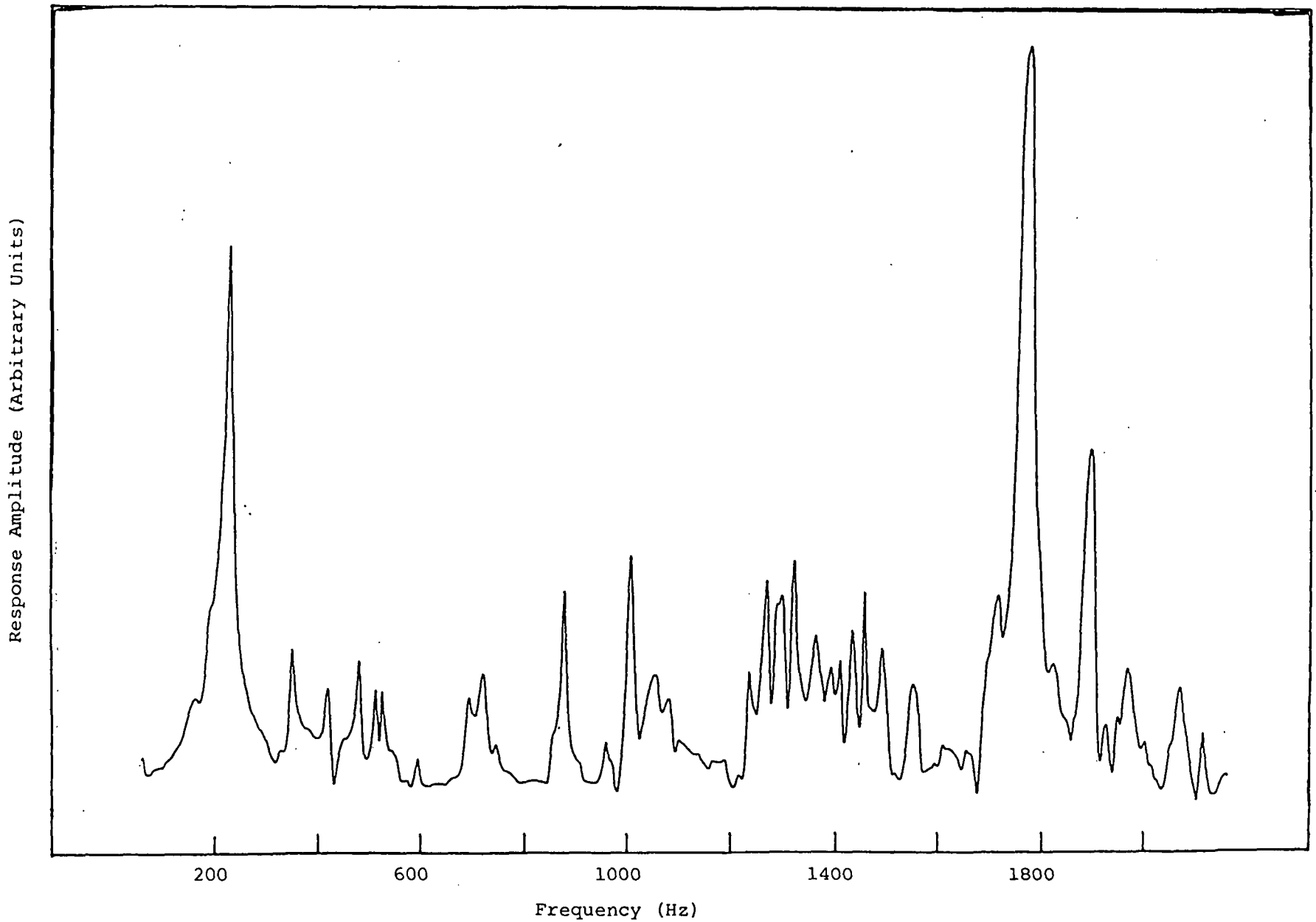

Figure 8. Frequency response of aircraft panel No. 3 with airborne excitation.

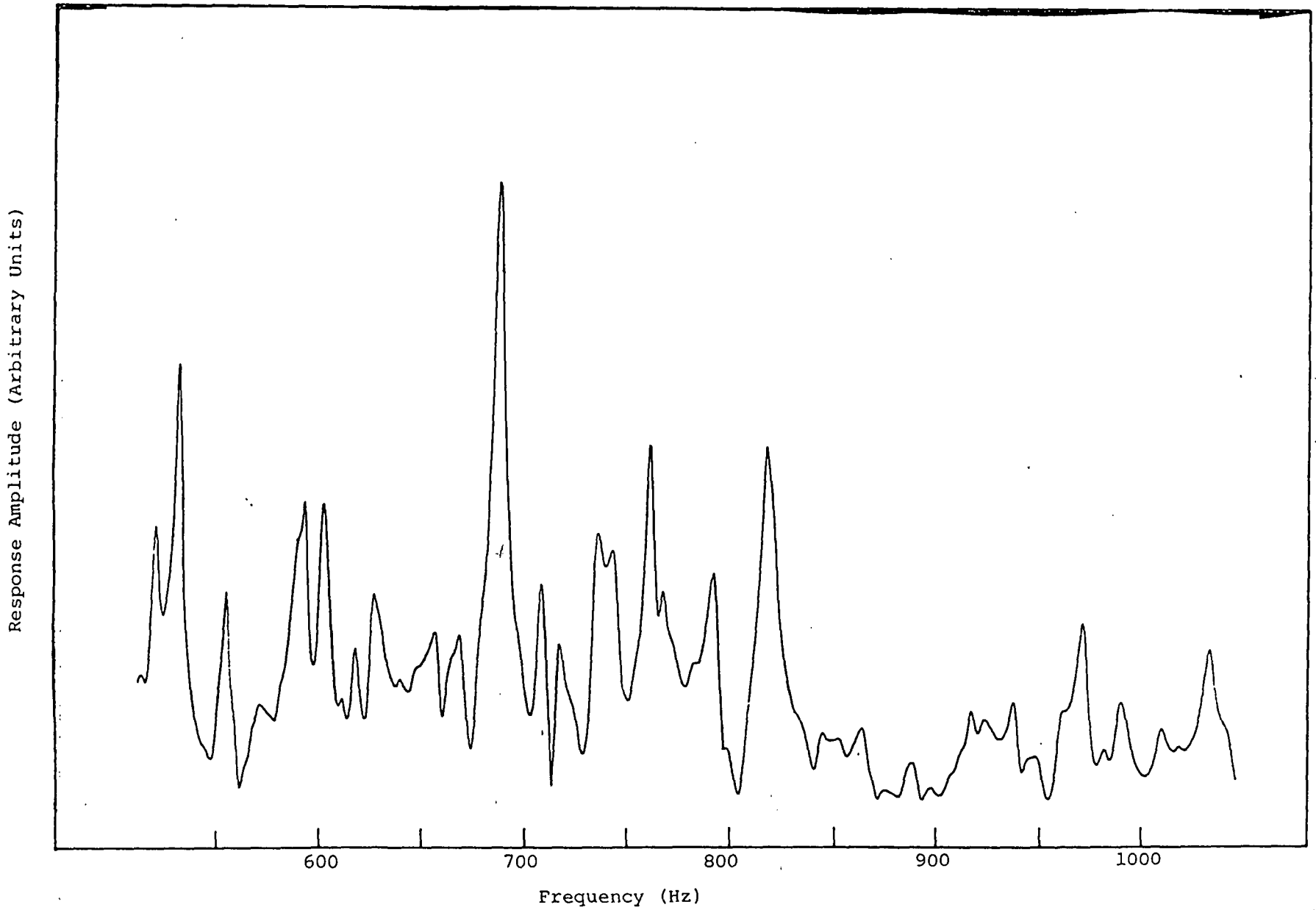

Figure 9. Frequency response of aircraft panel No. 4 with structure borne excitation.

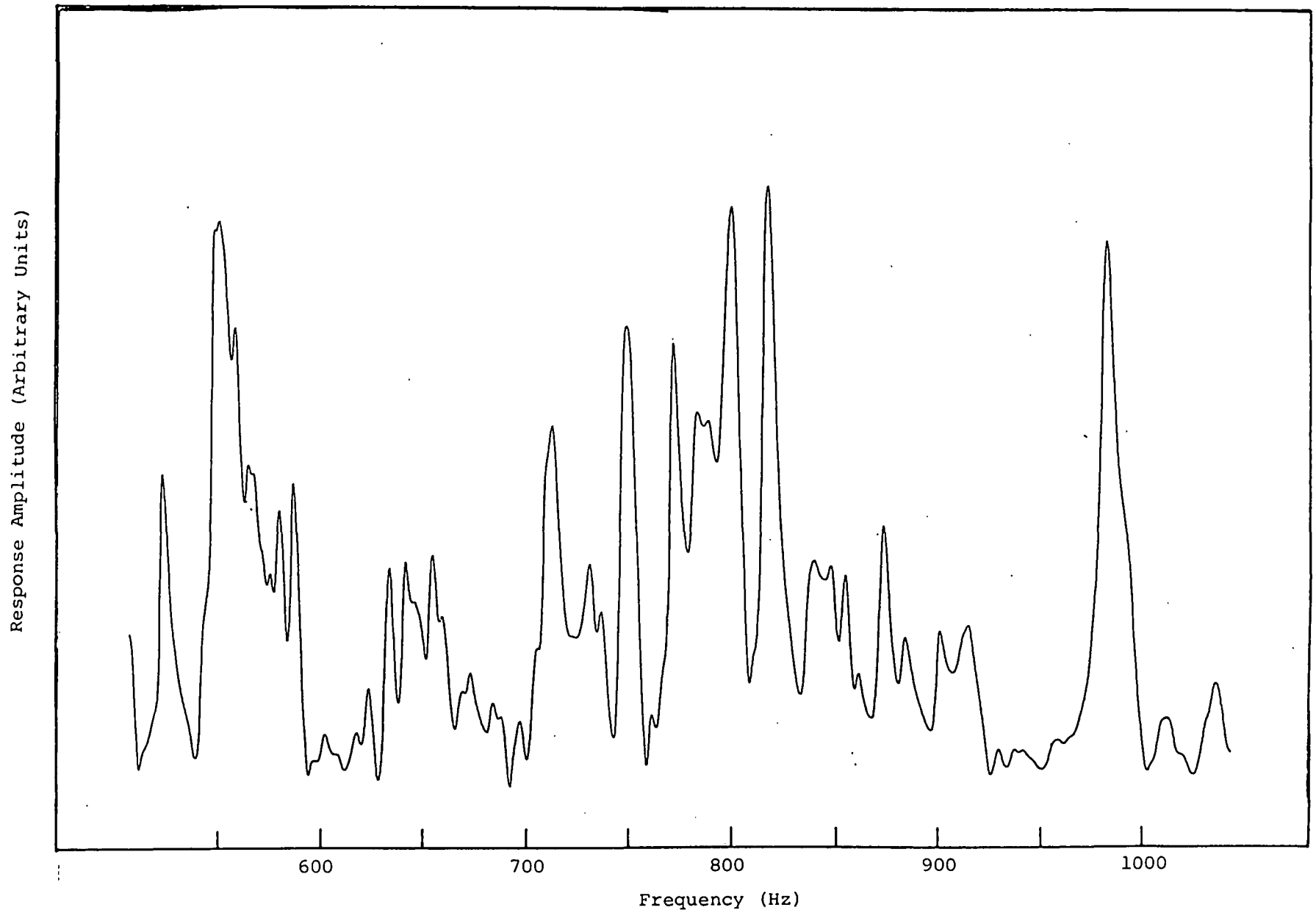

Figure 10. Frequency response of aircraft panel No. 4 with airborne excitation.

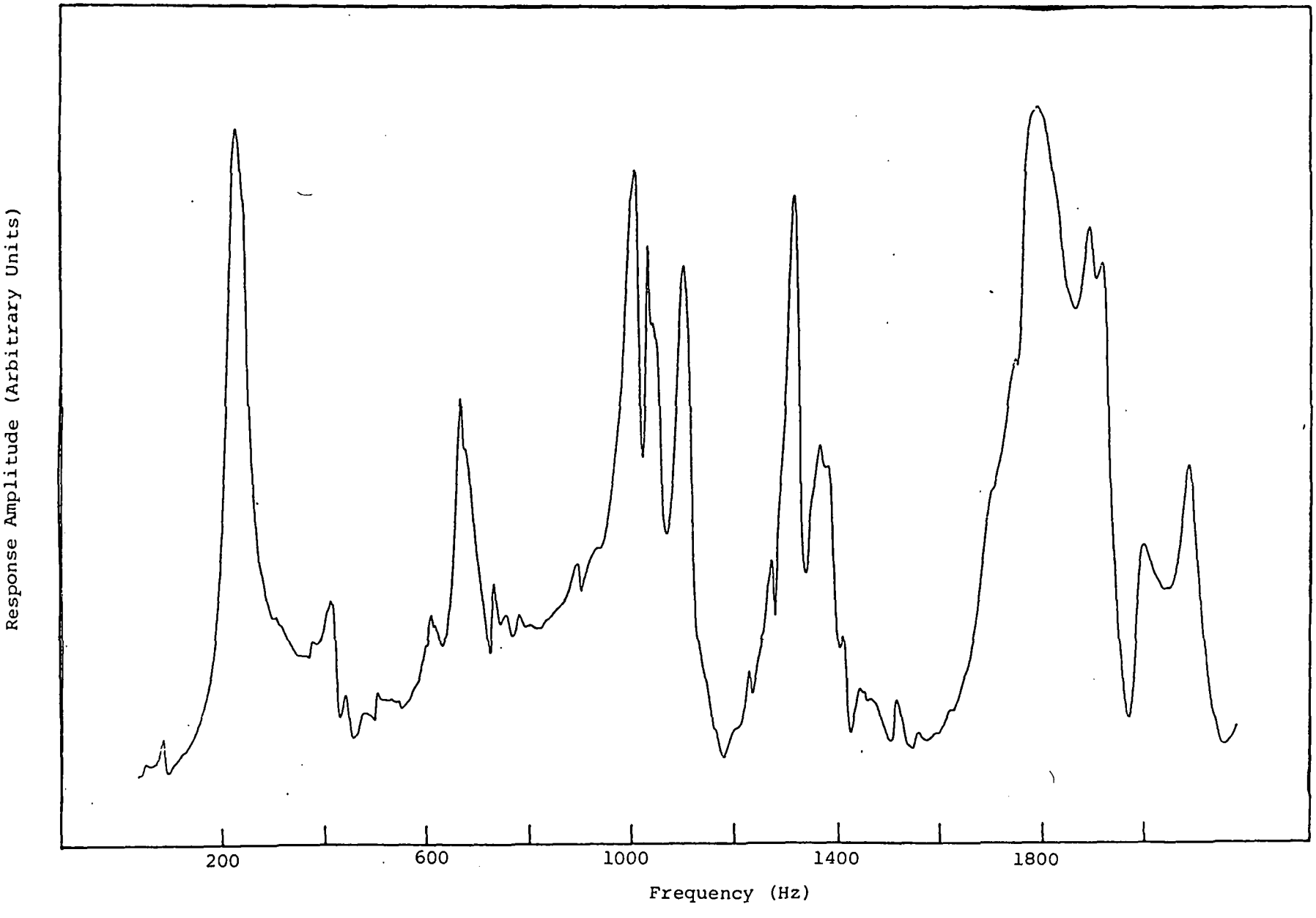

Figure 11. Frequency response of aircraft panel No. 5 with structure borne excitation.

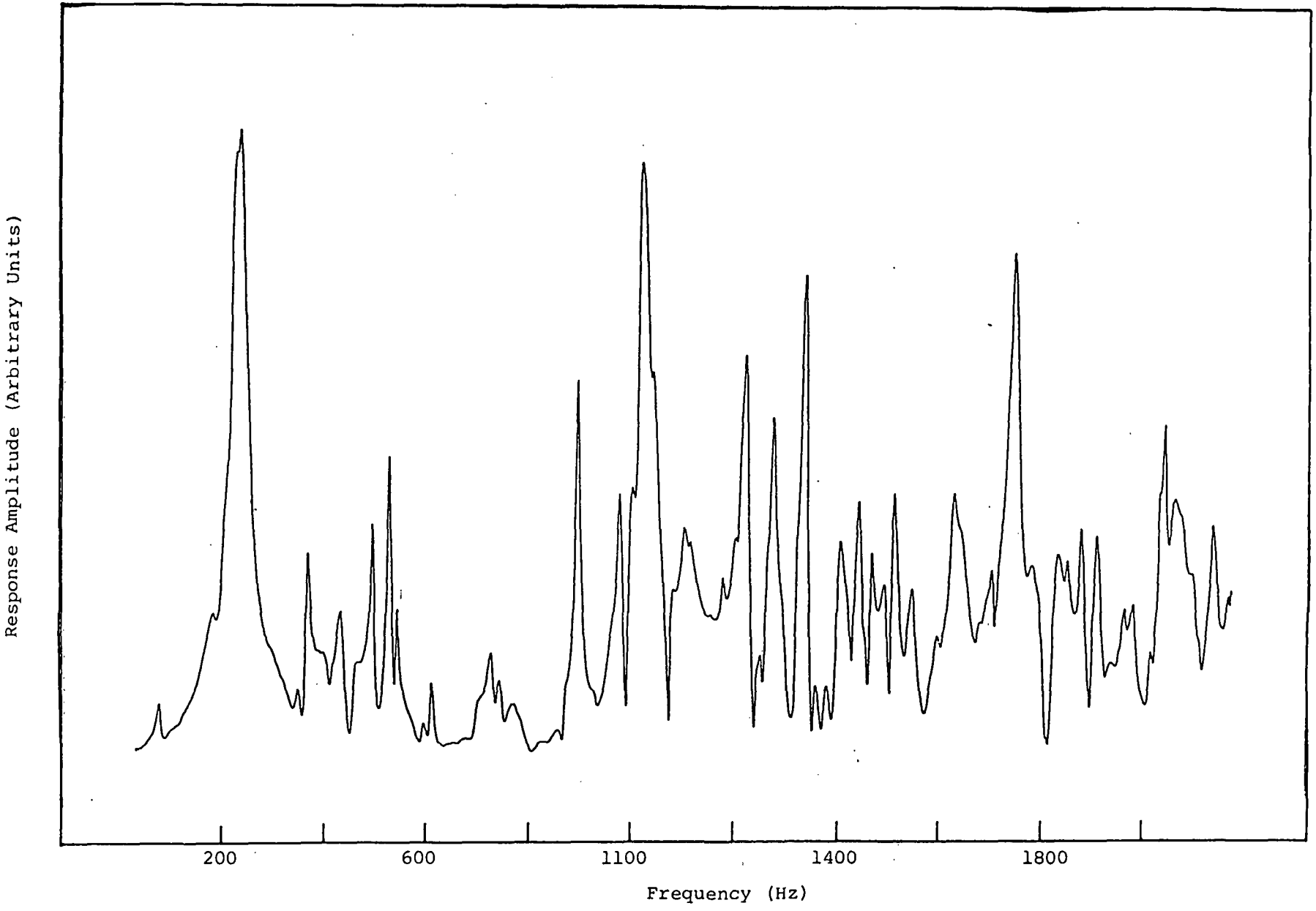

Figure 12. Frequency response of aircraft panel No. 5 with airborne excitation.

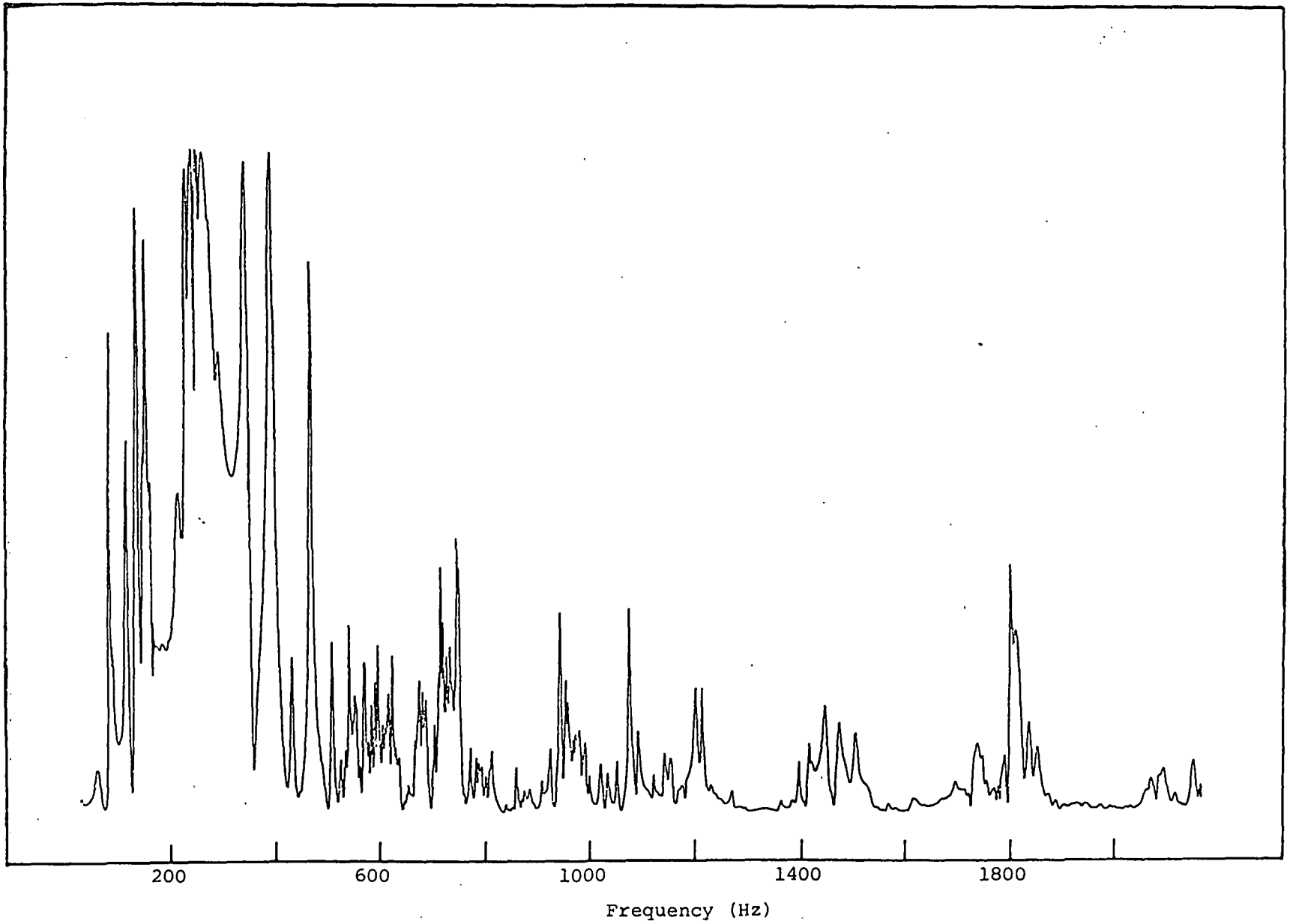

Figure 13. Frequency response of aircraft plane No. 6 with structure borne excitation.

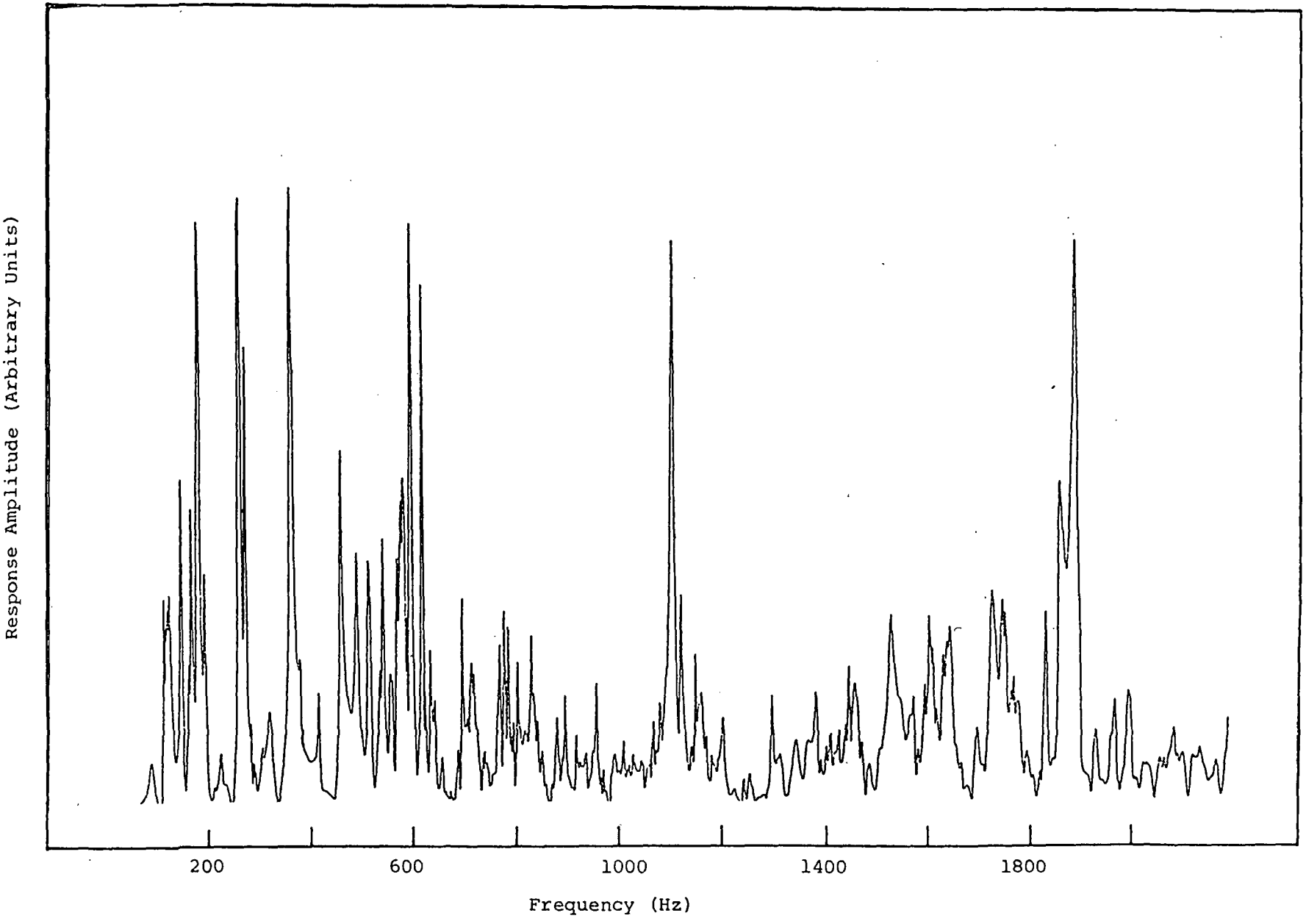

Figure 14. Frequency response of aircraft panel No. 6 with airborne excitation.

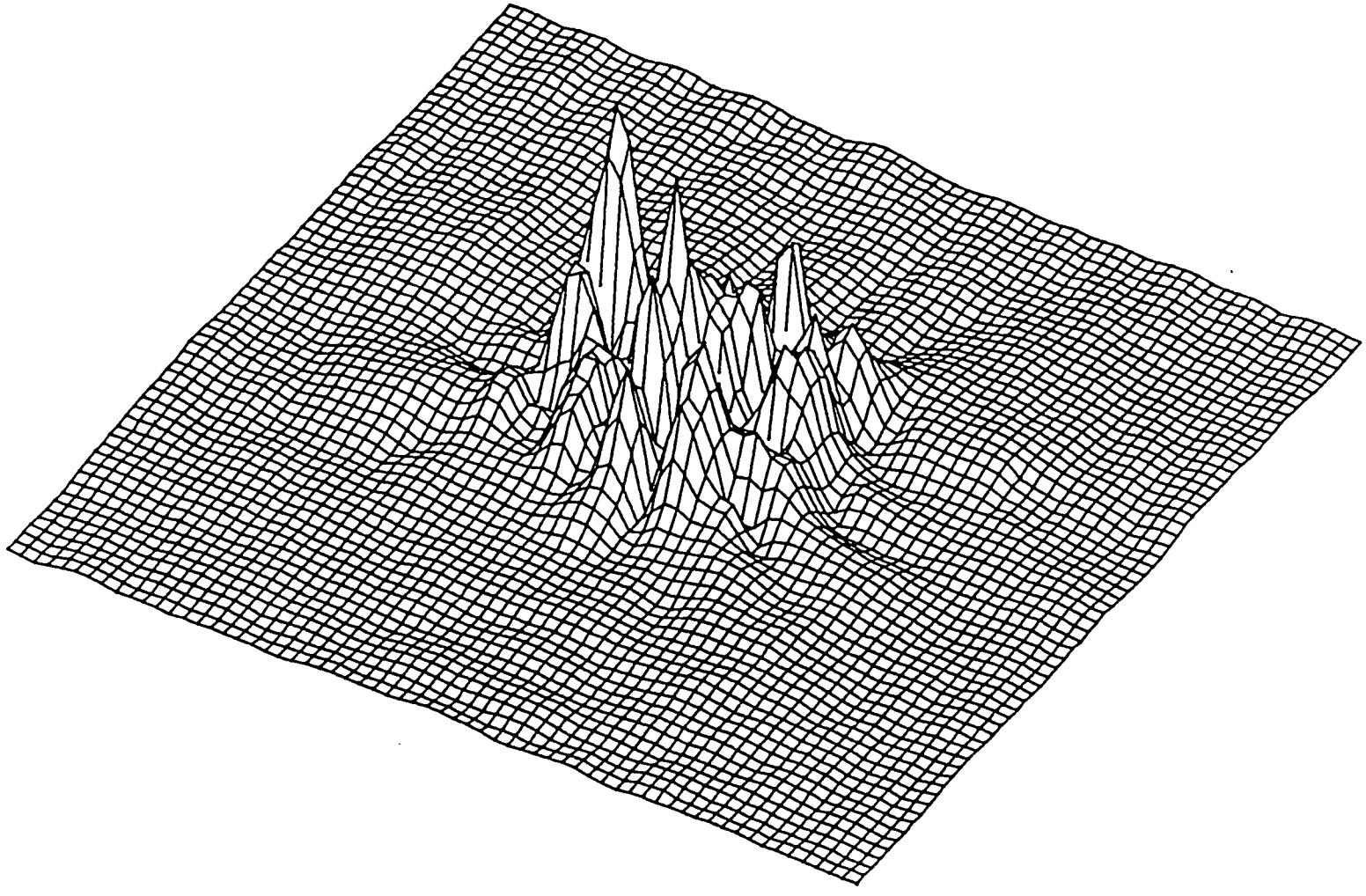

ARS891.HLD PEAK= 0.533E+00

ARL580. HLD PEAK= 0. 546E+00

ORIGINAL PAGE IS
OF POOR QUALITY

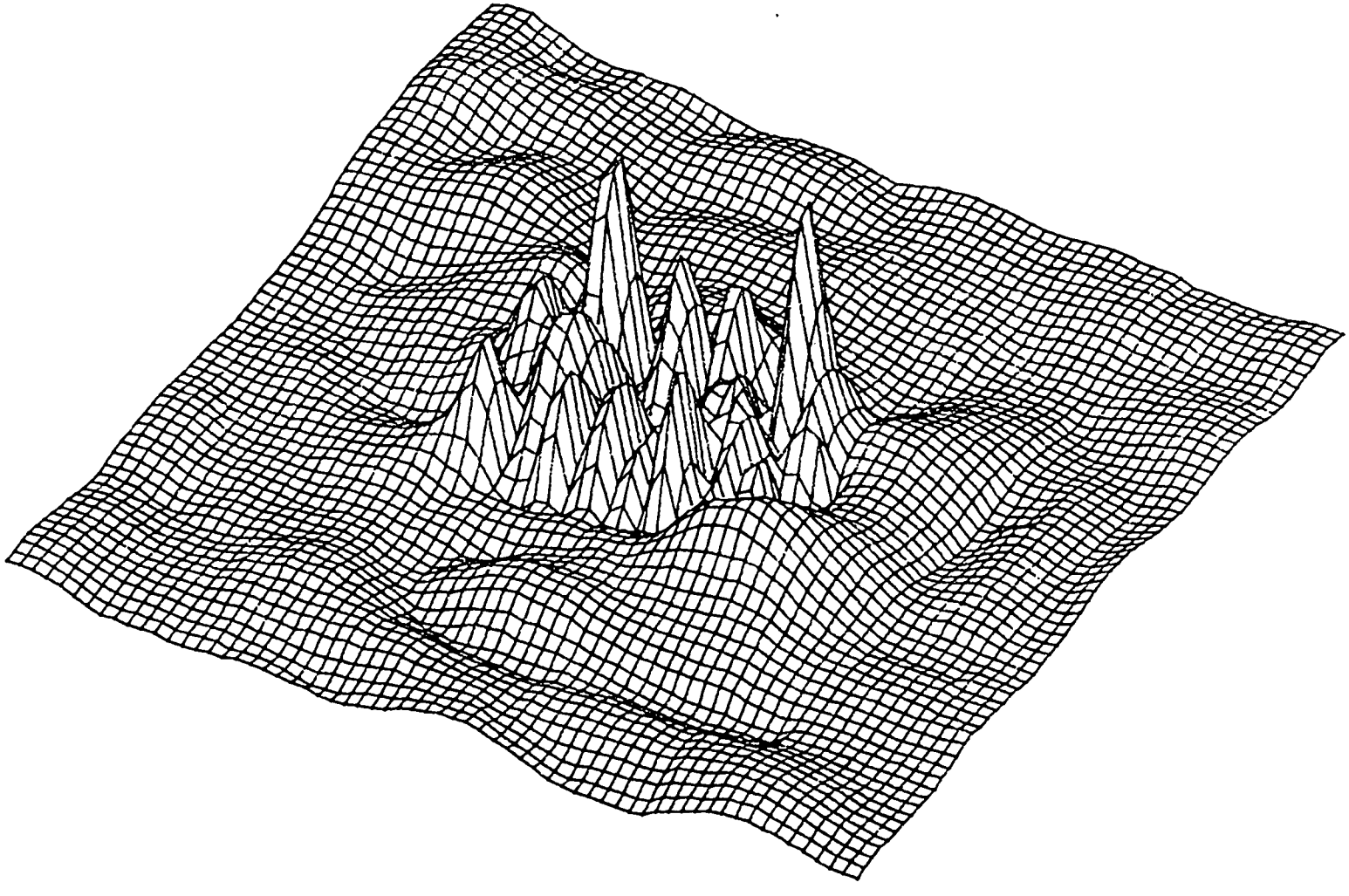

ARL5Ø9. HLD PEAK= Ø. 183E+Ø1

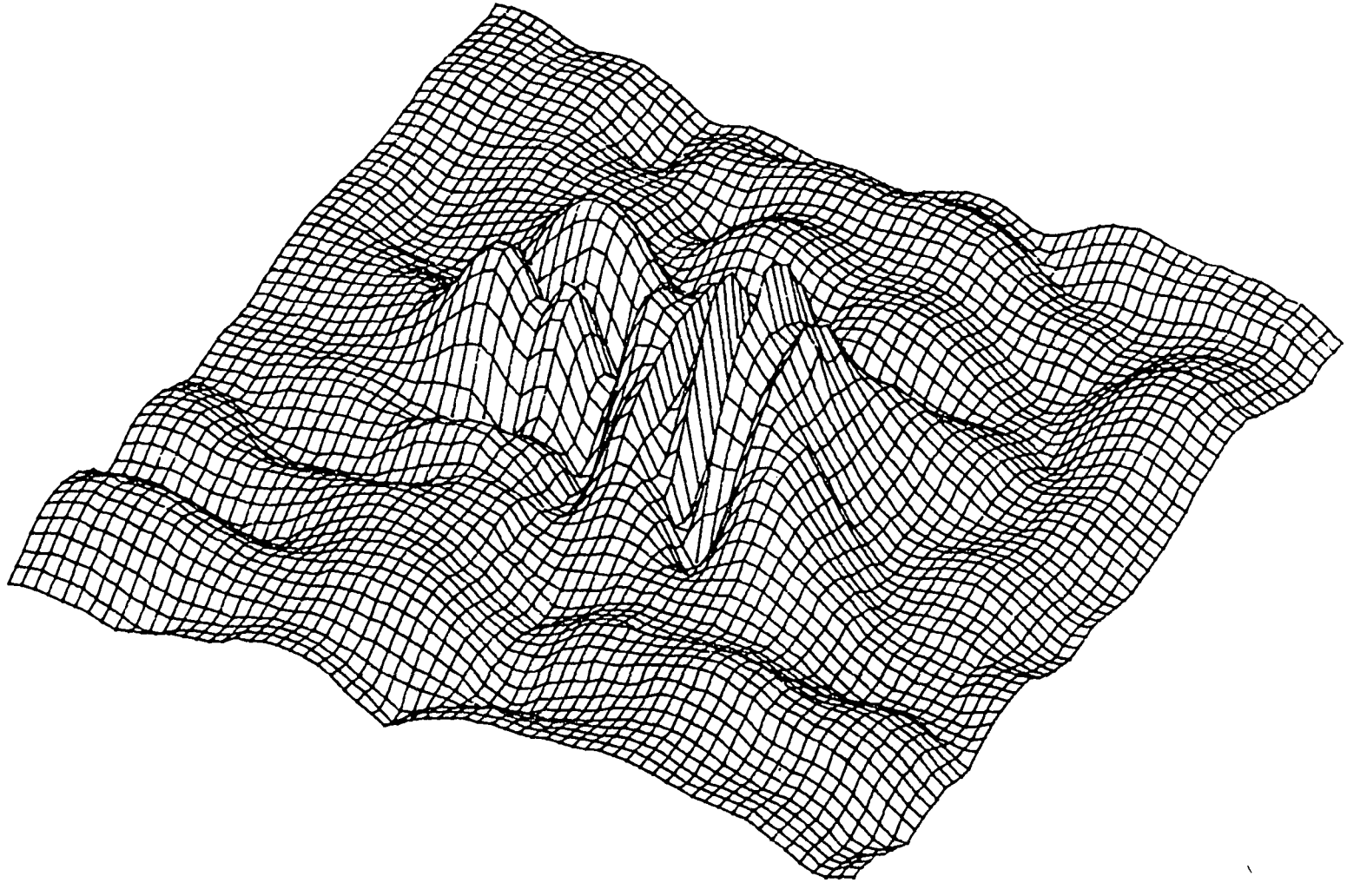

ARL474.HLD PEAK= Ø.115E+Ø1

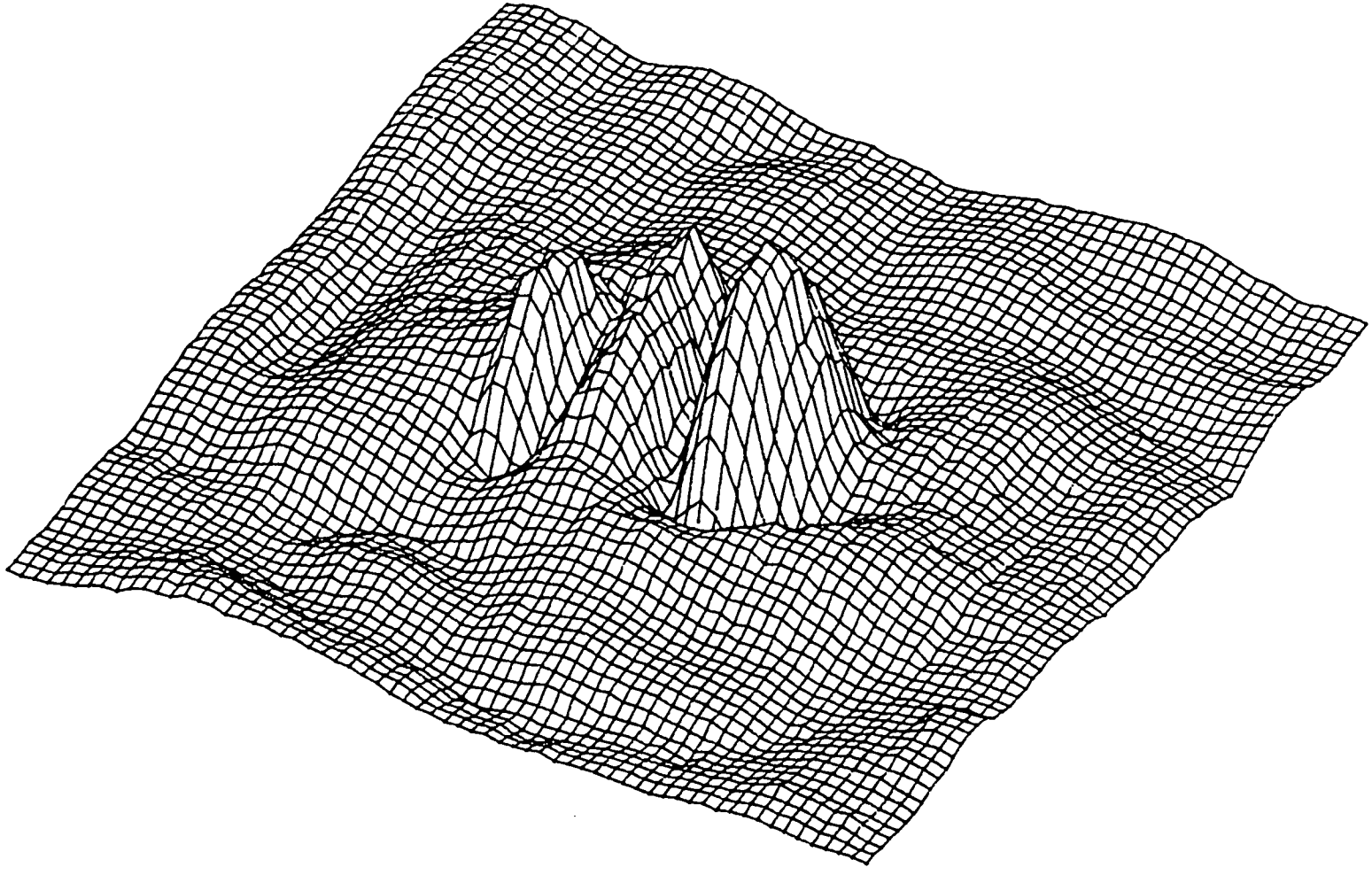

ARL424.HLD PEAK= 0.119E+01

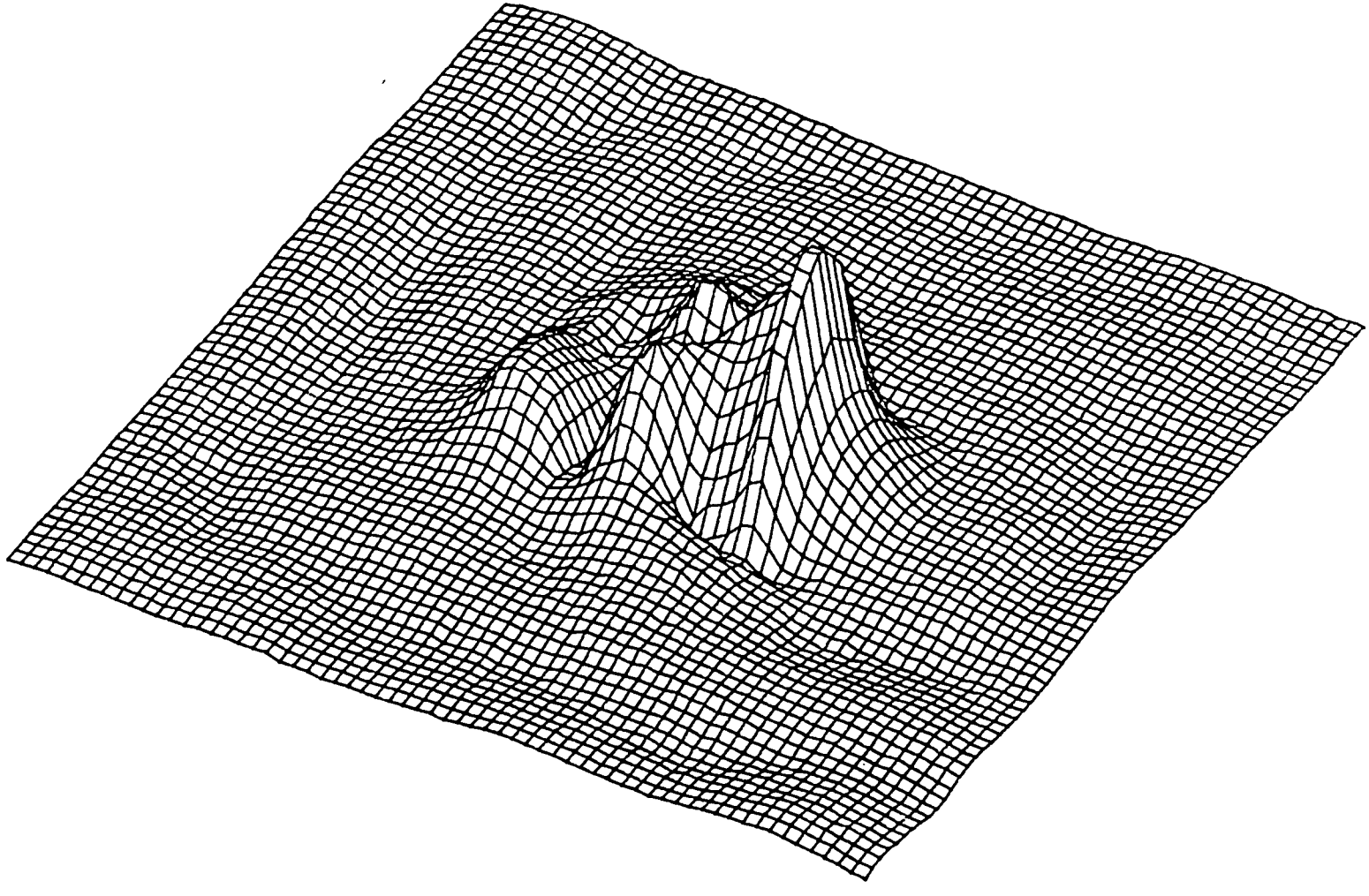

ARL381.HLD PEAK= 0.217E+01

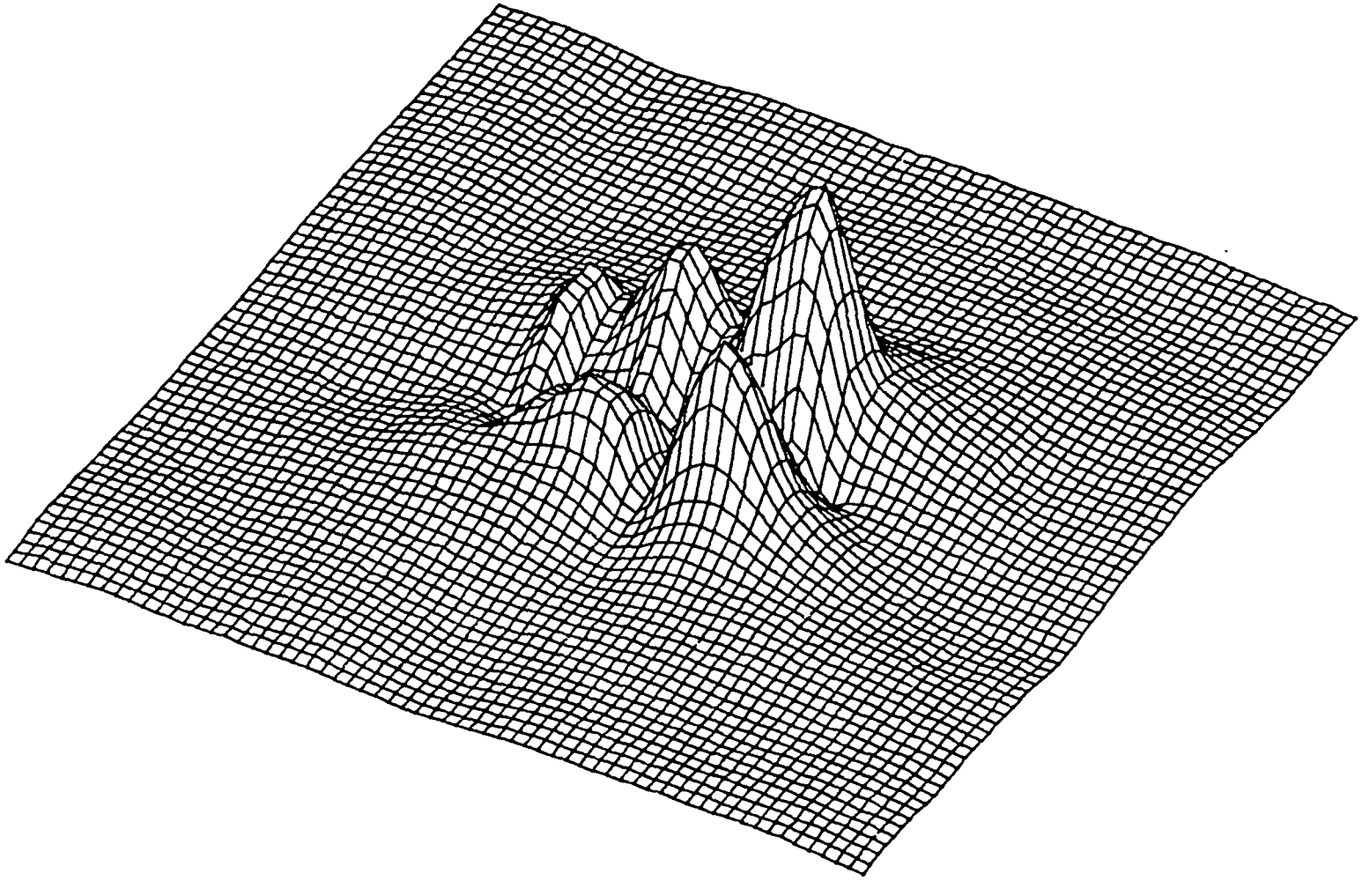

ARL324.HLD PEAK= 0.341E+01

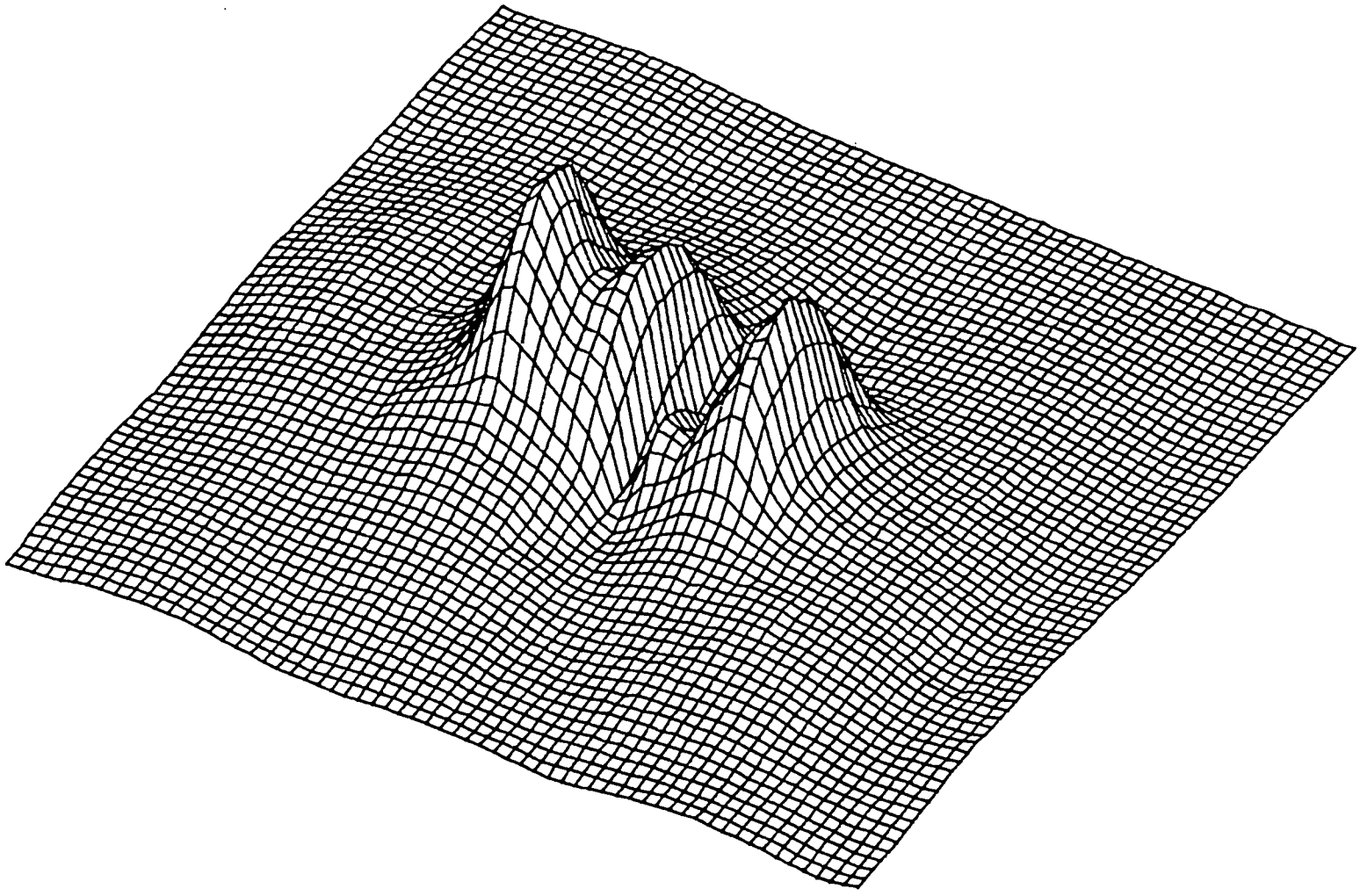

ARL261.HLD PEAK= 0.419E+01

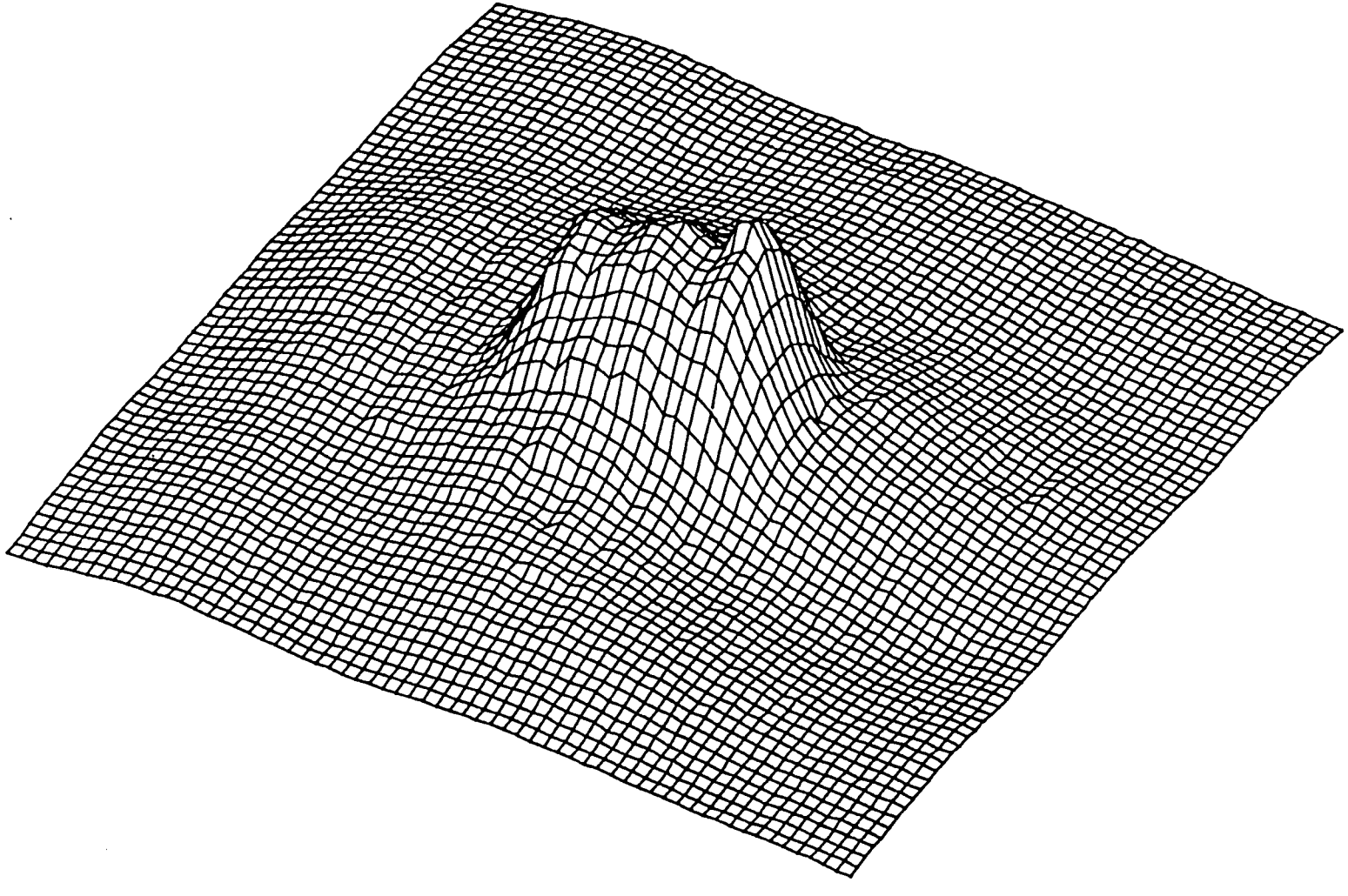

ARL249. HLD PEAK= Ø. 377E+Ø1

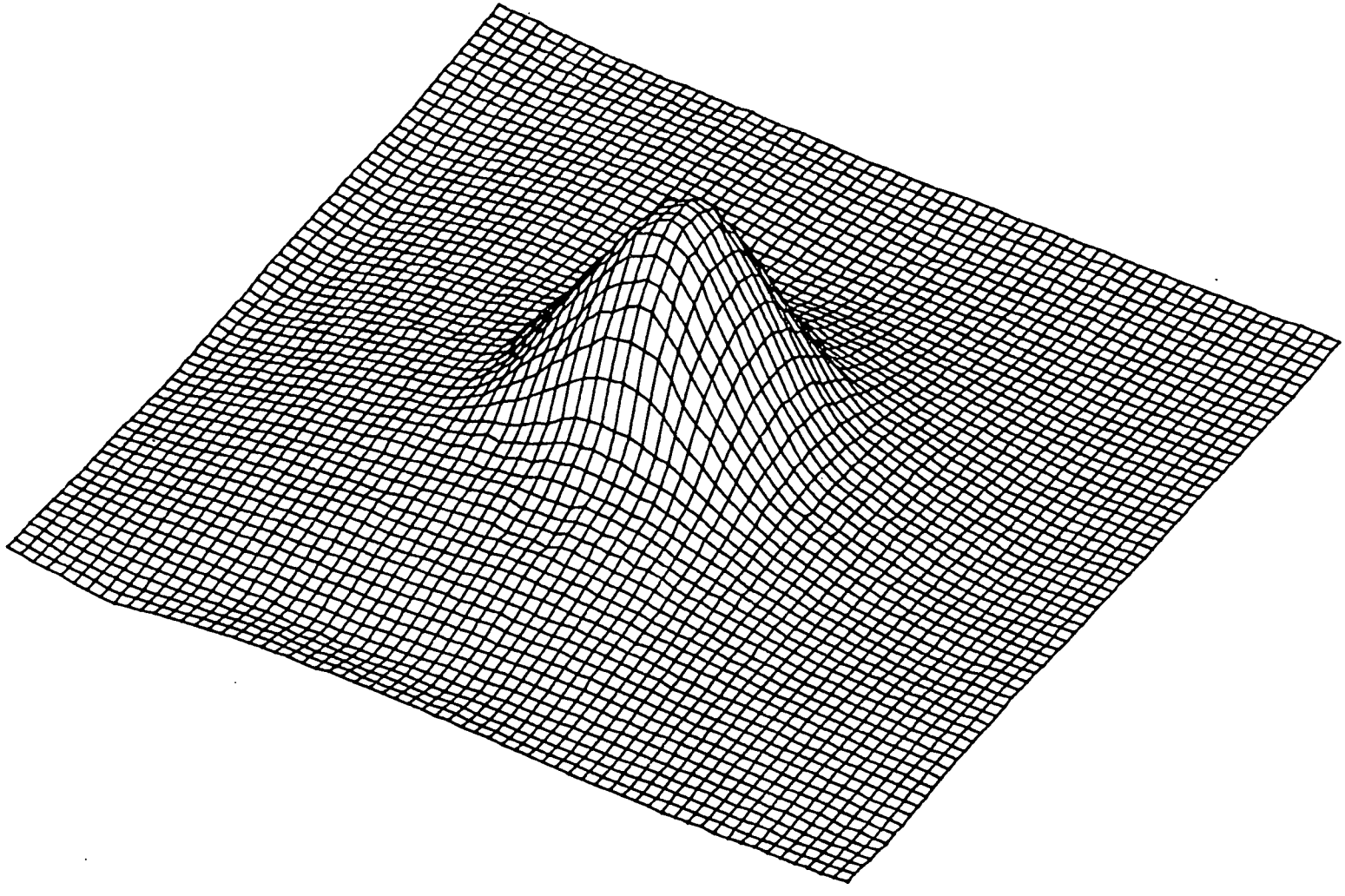

ARL165. HLD PEAK= Ø. 955E+Ø1

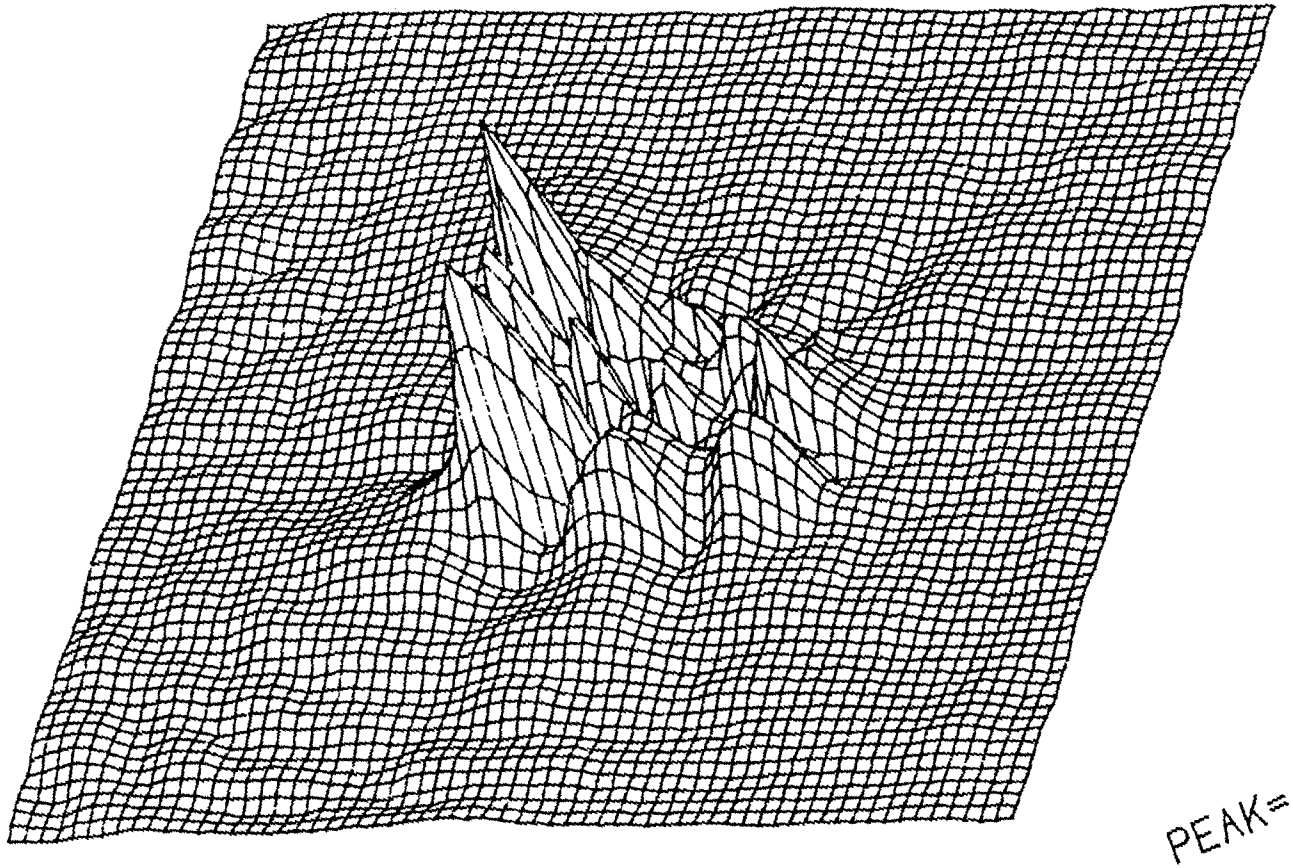

PEAK= 0.470E+01

ARB840.HLD

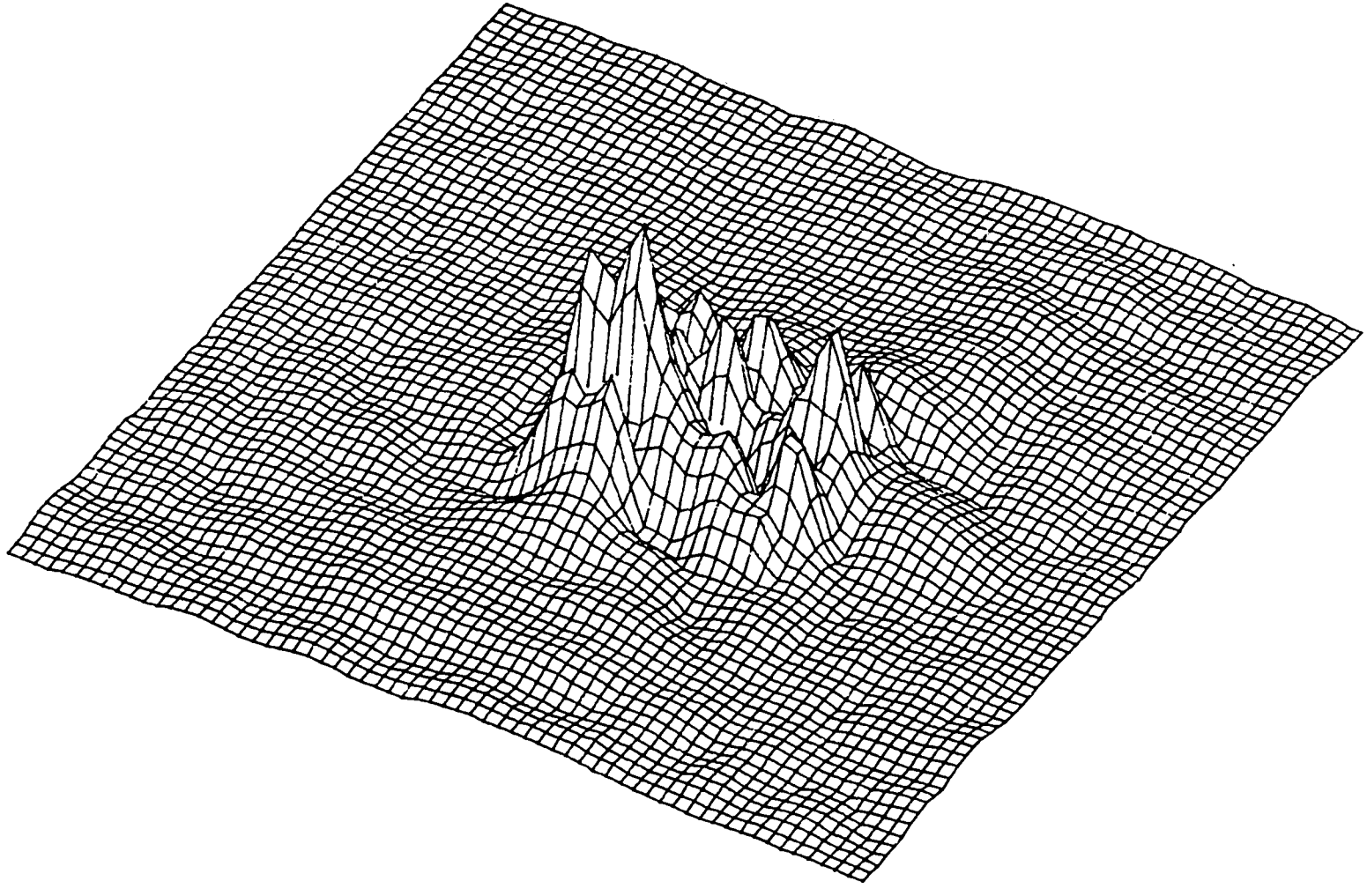

ARB716. HLD PEAK= Ø. 315E+Ø1

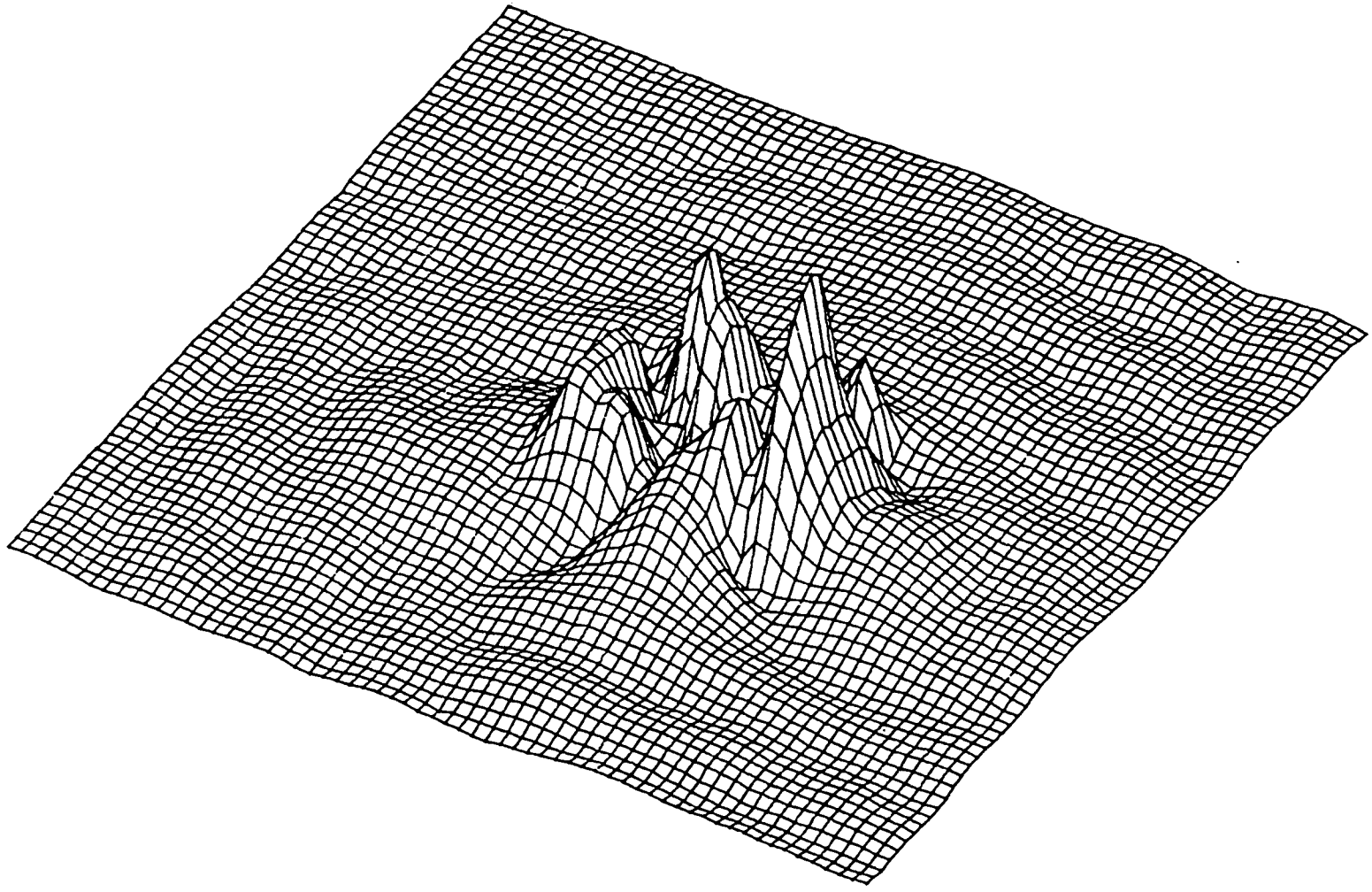

ARB536. HLD PEAK= Ø. 553E+Ø1

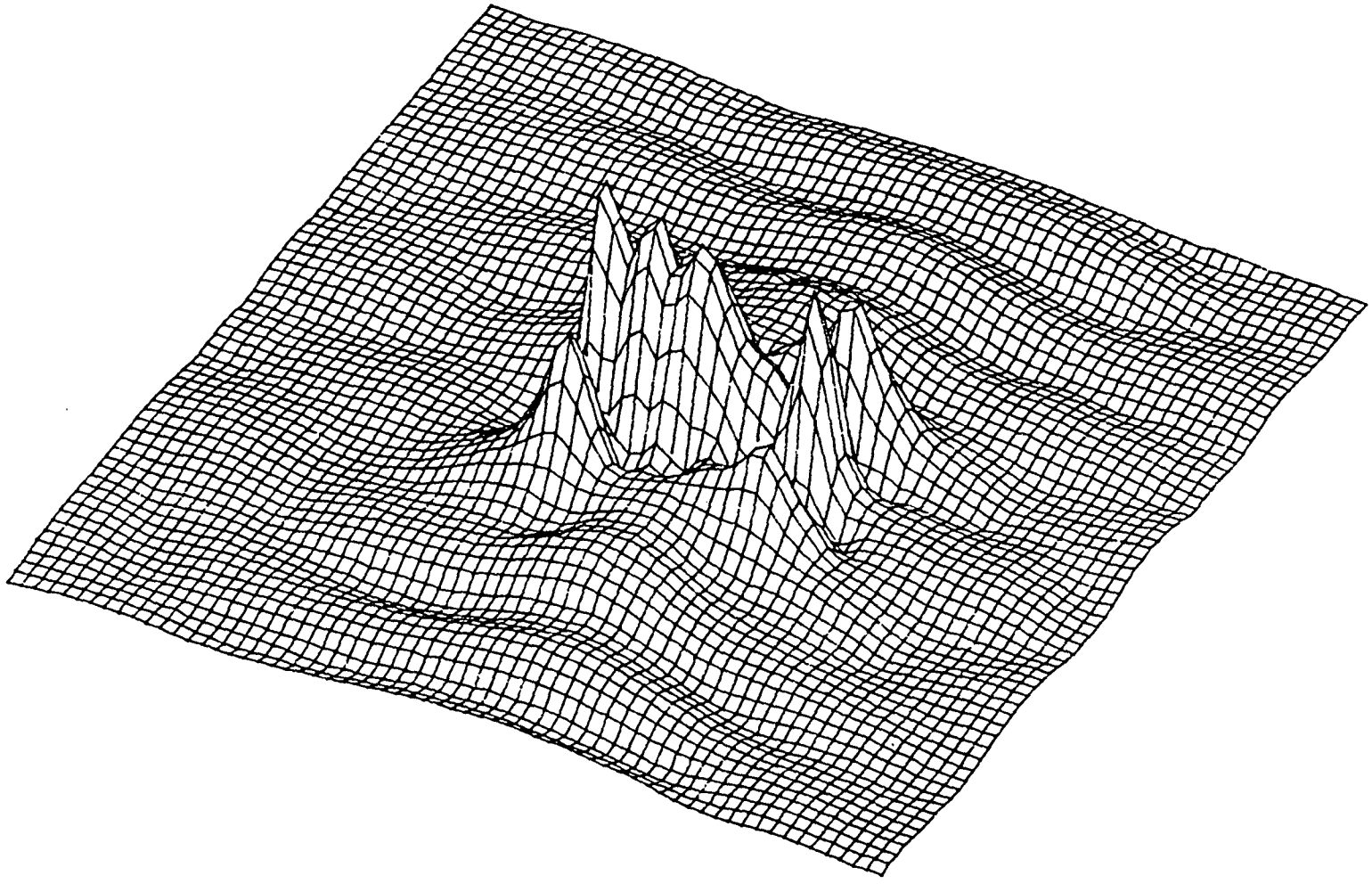

ARB503.HLD PEAK= 0.620E+01

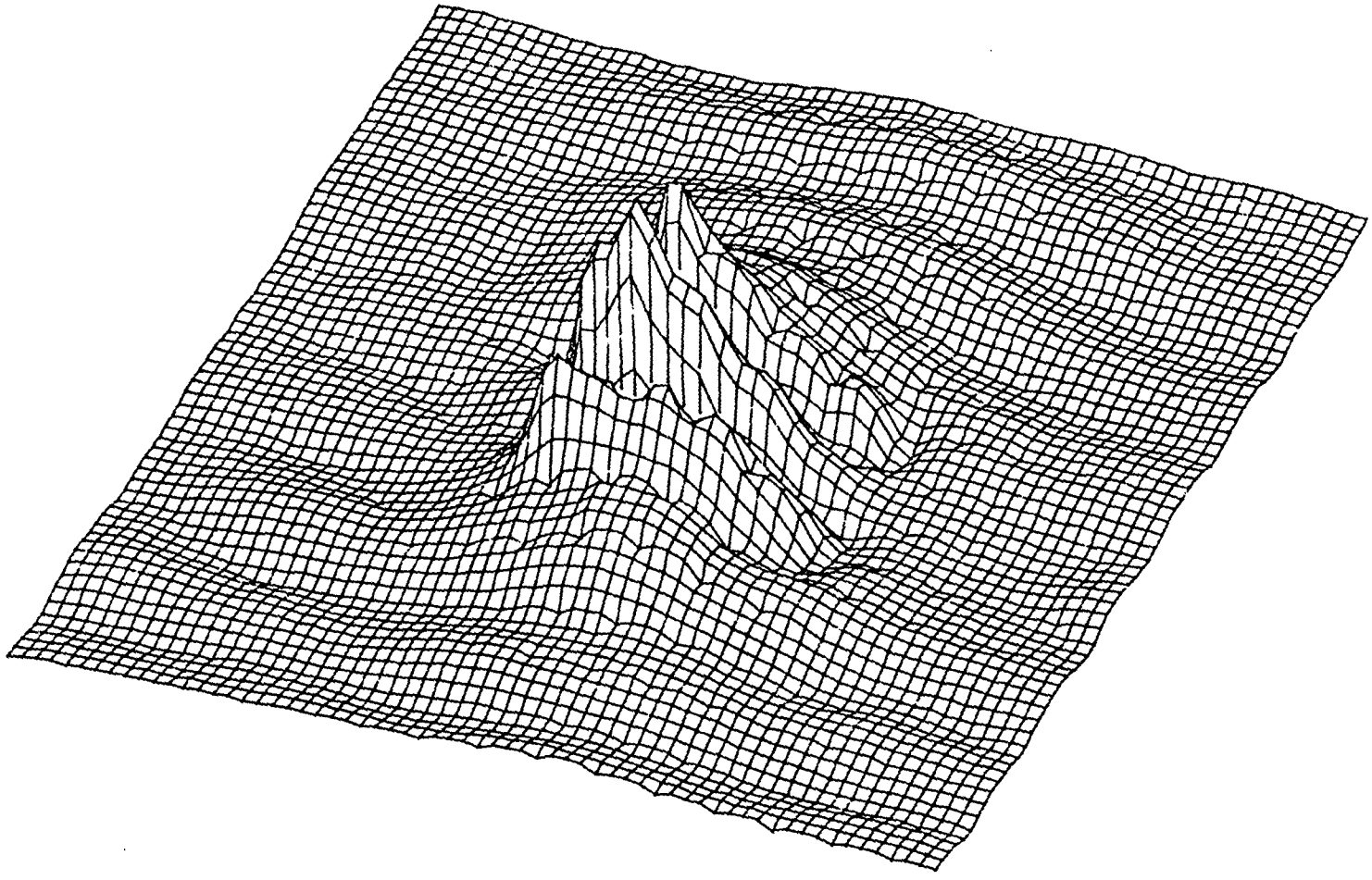

ARB470.HLD

PEAK= 0.534E+01

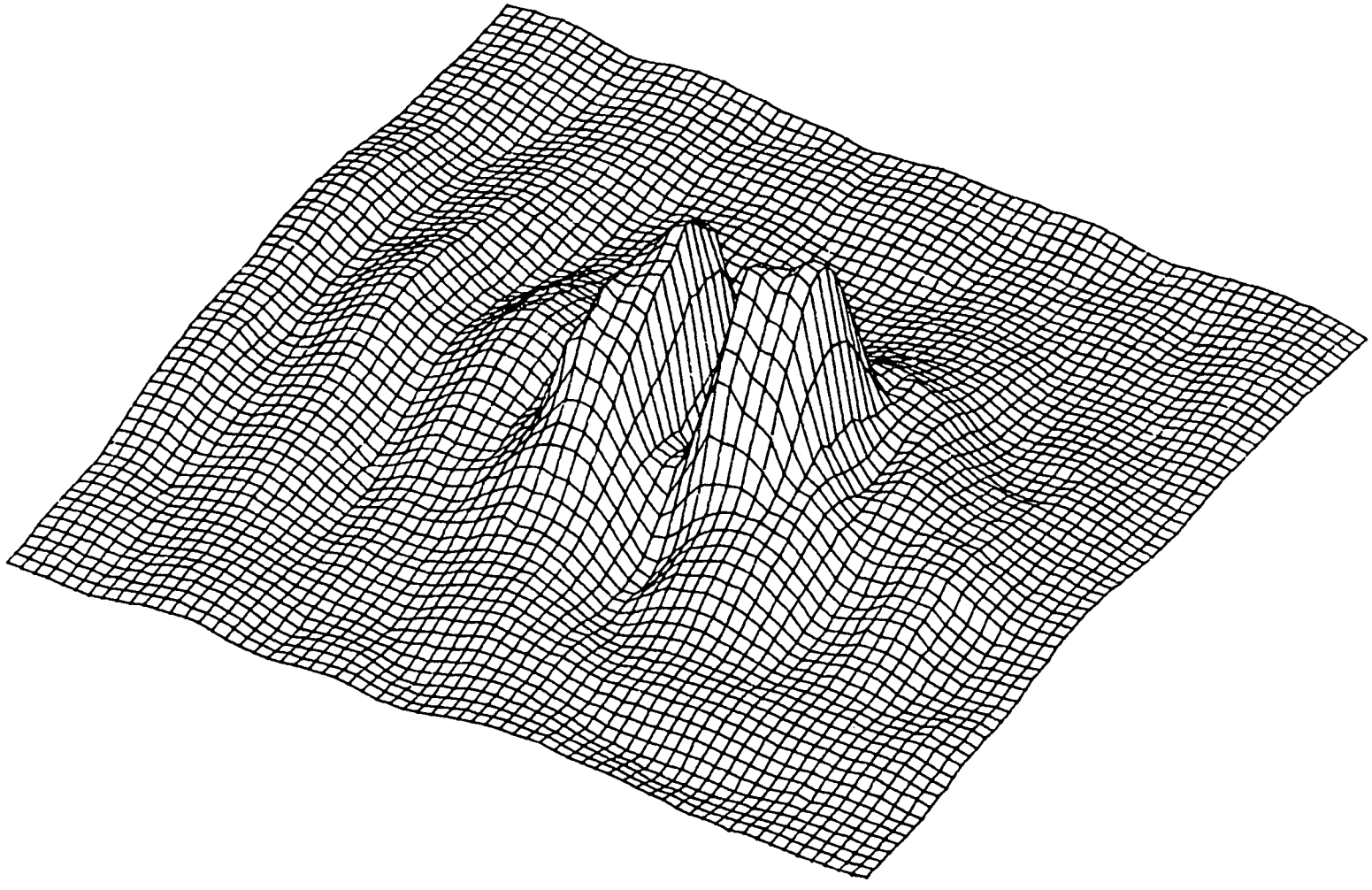

ARB444. HLD PEAK= Ø. 439E+Ø1

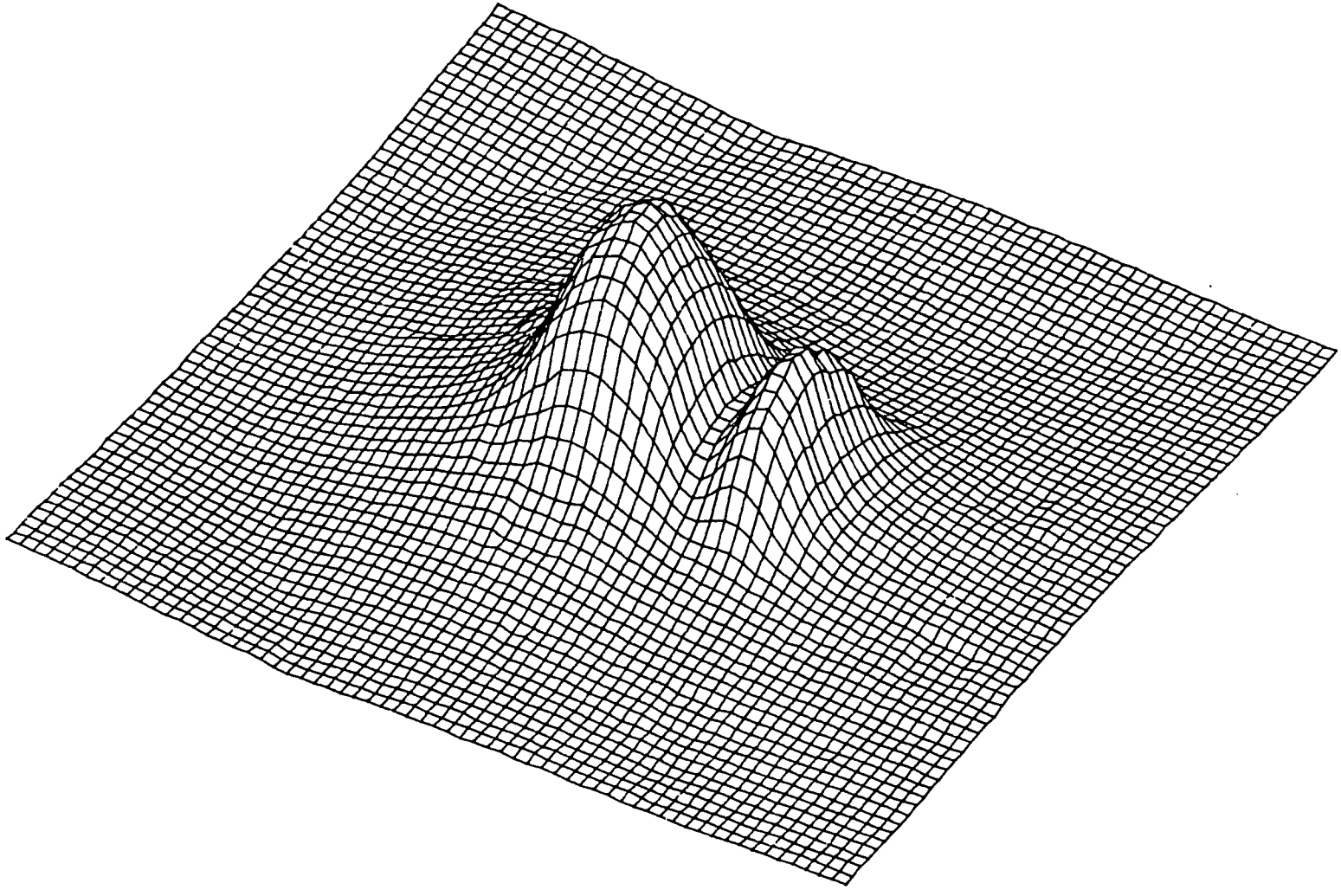

ARB. HLD PEAK= Ø. 467E+Ø1

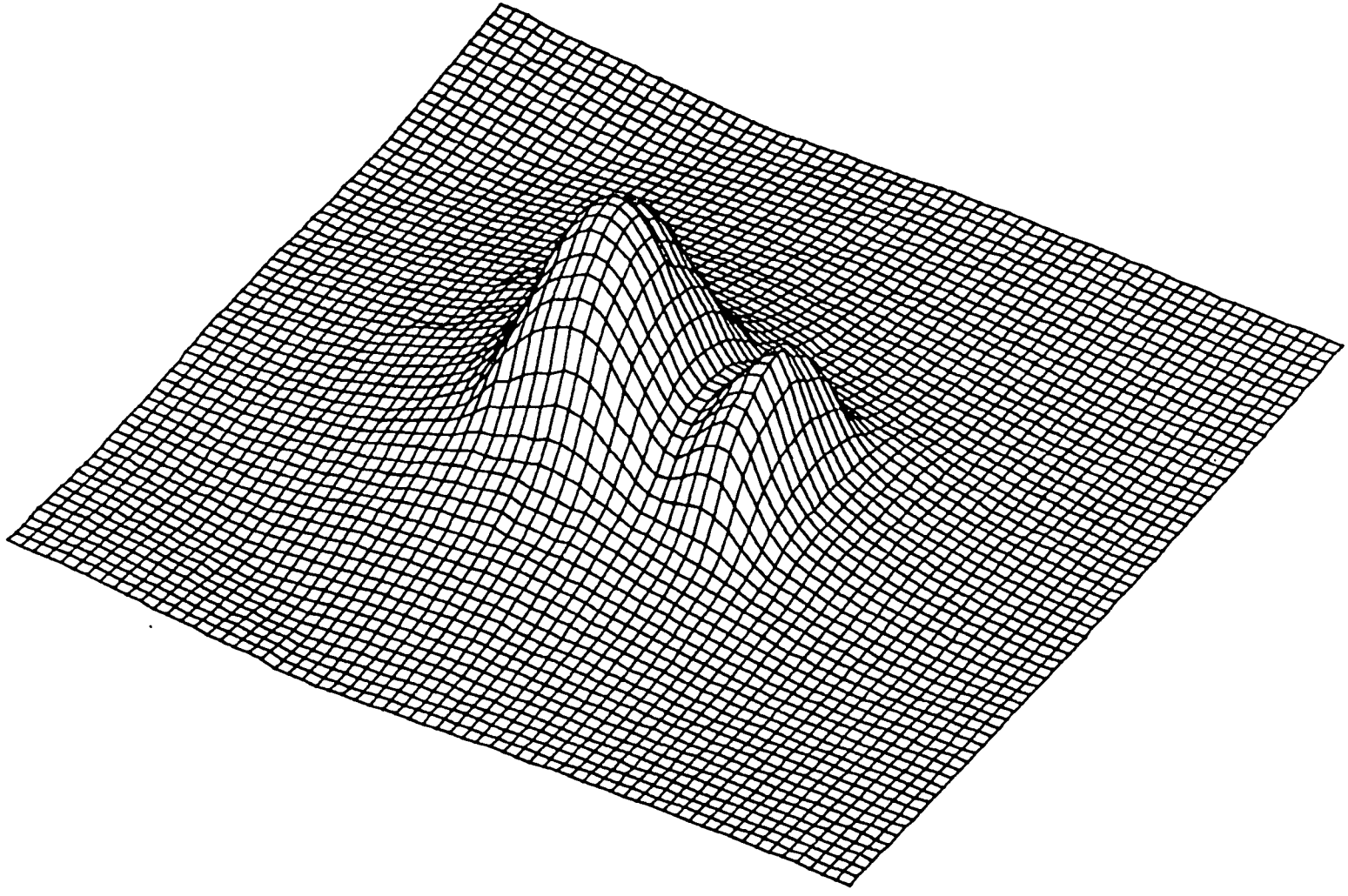

ARB114.HLD PEAK= 0.775E+01

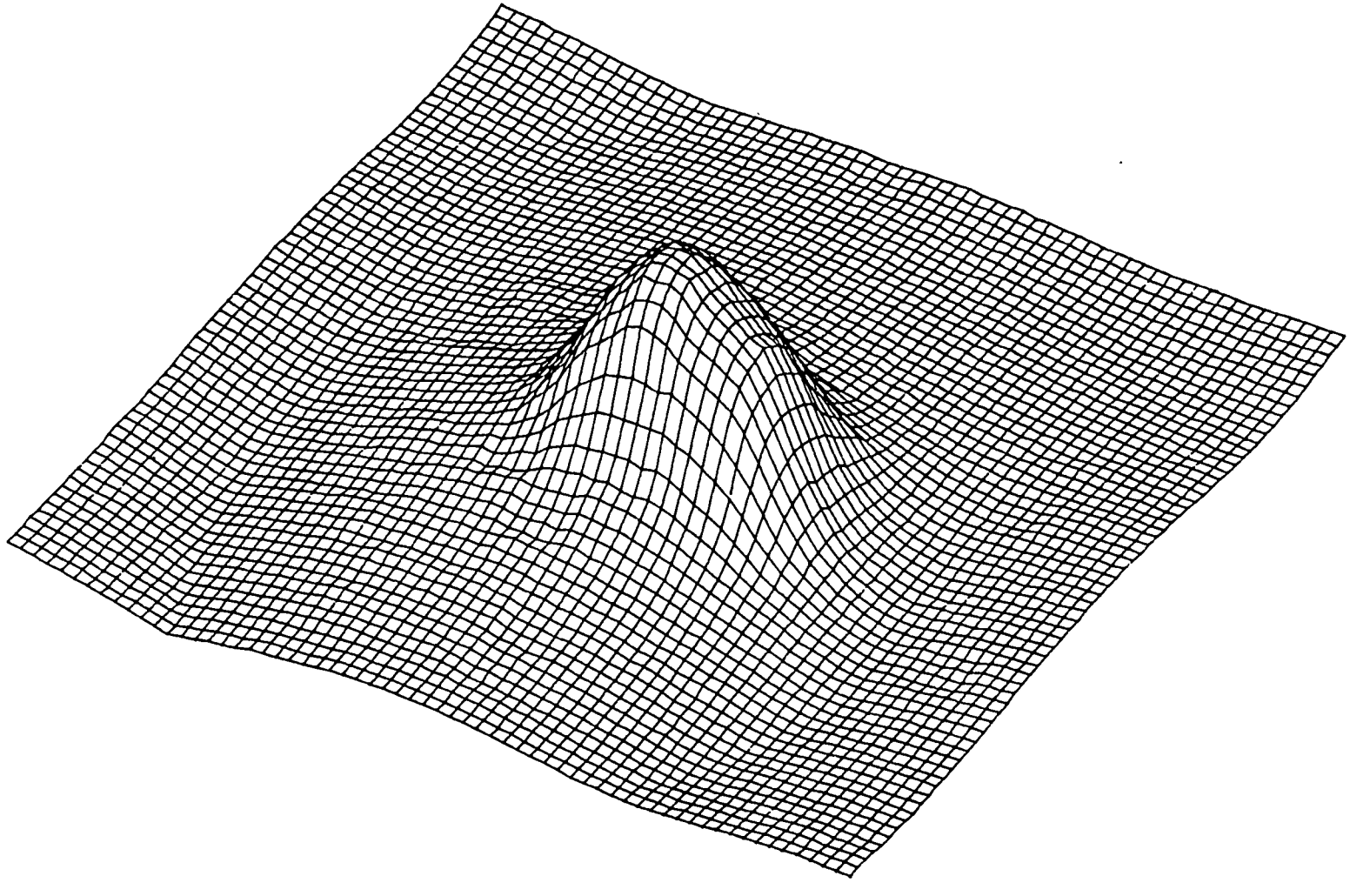

ARB136. HLD PEAK= 0. 108E+02

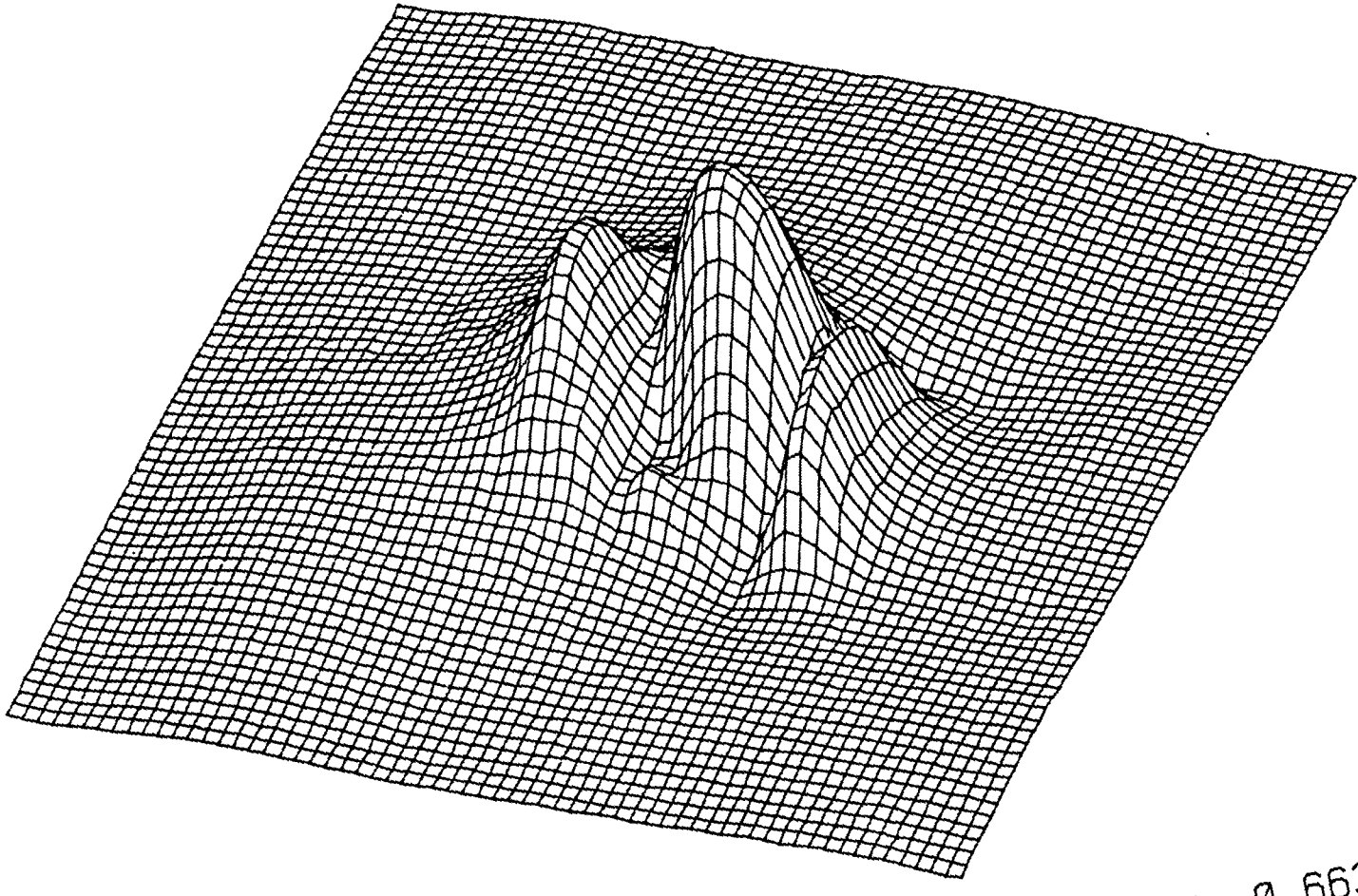

ARB224.HLD

PEAK= Ø.663E+Ø1

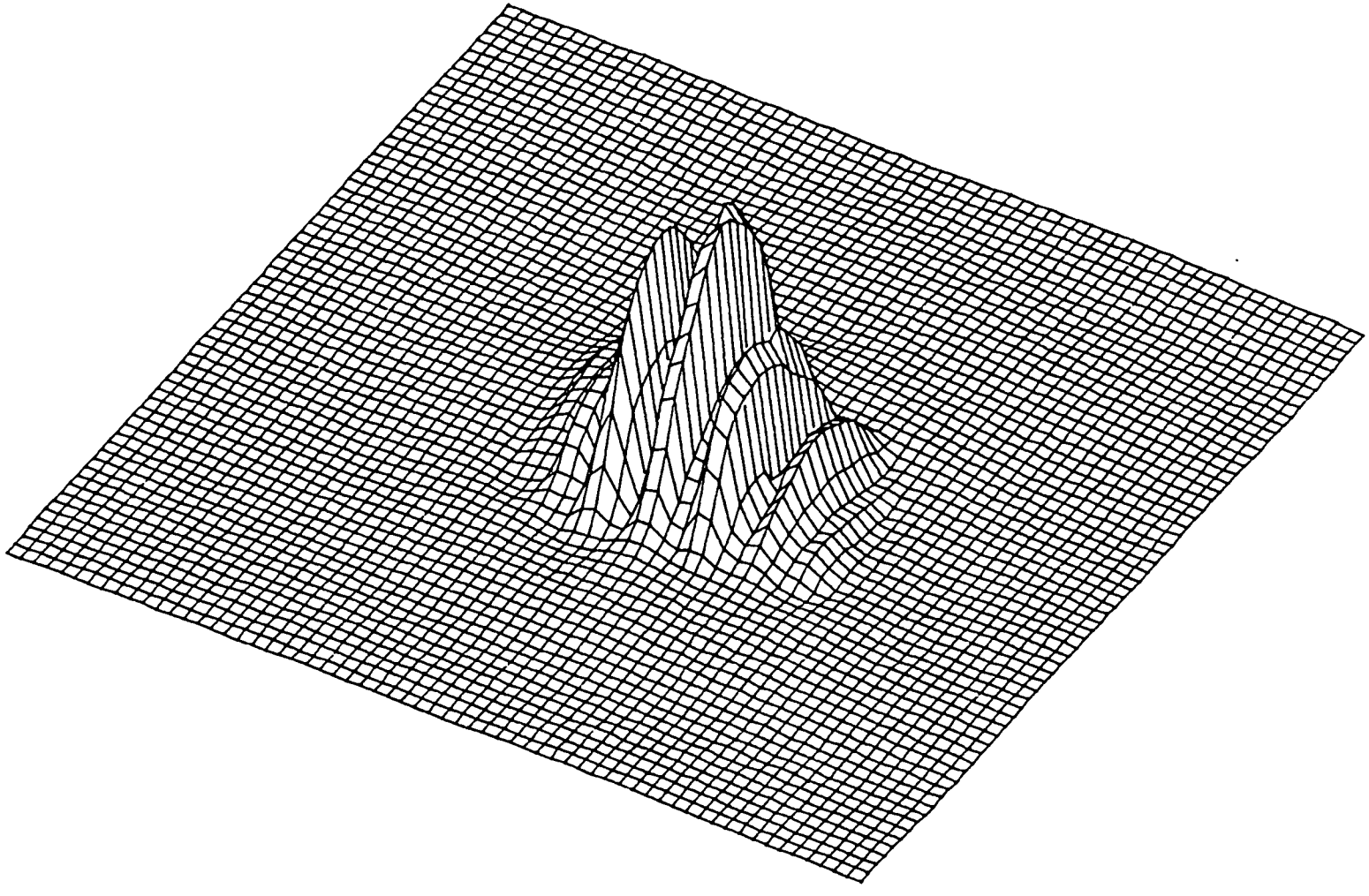

ARB332. HLD PEAK= Ø. 769E+Ø1

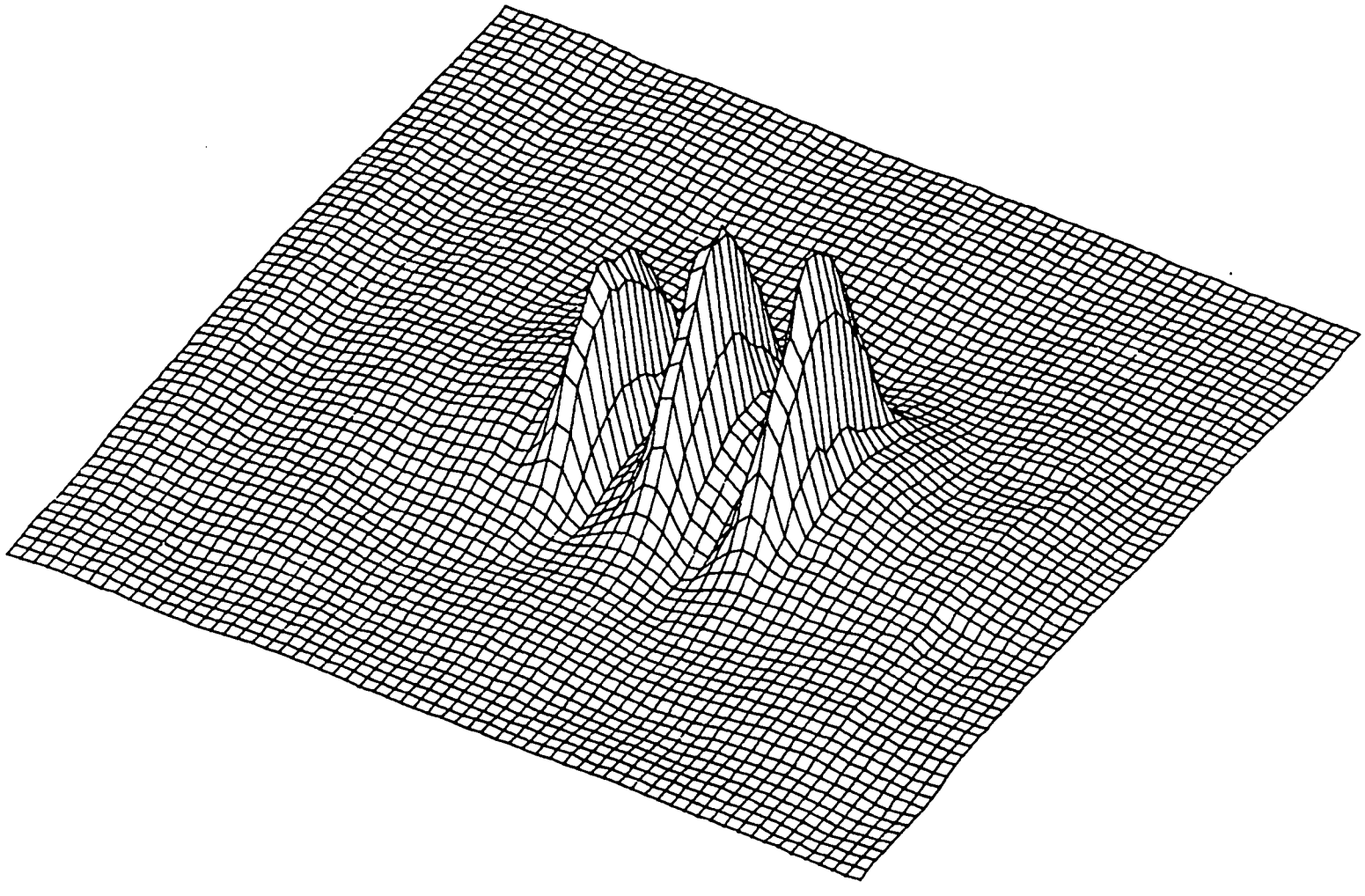

ARB394. HLD PEAK= 0. 401E+01

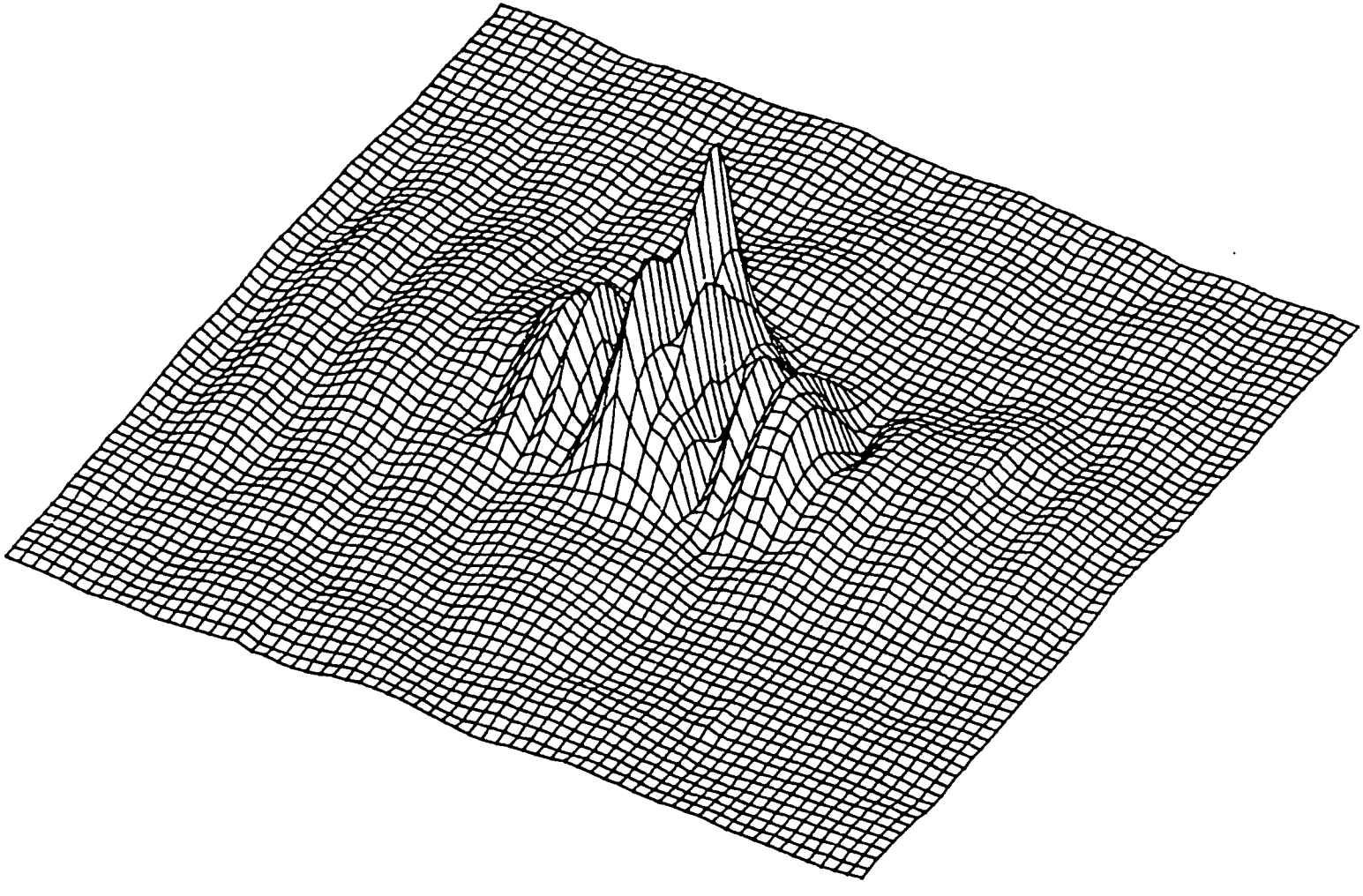

ARM580.HLD PEAK= 0.931E+00

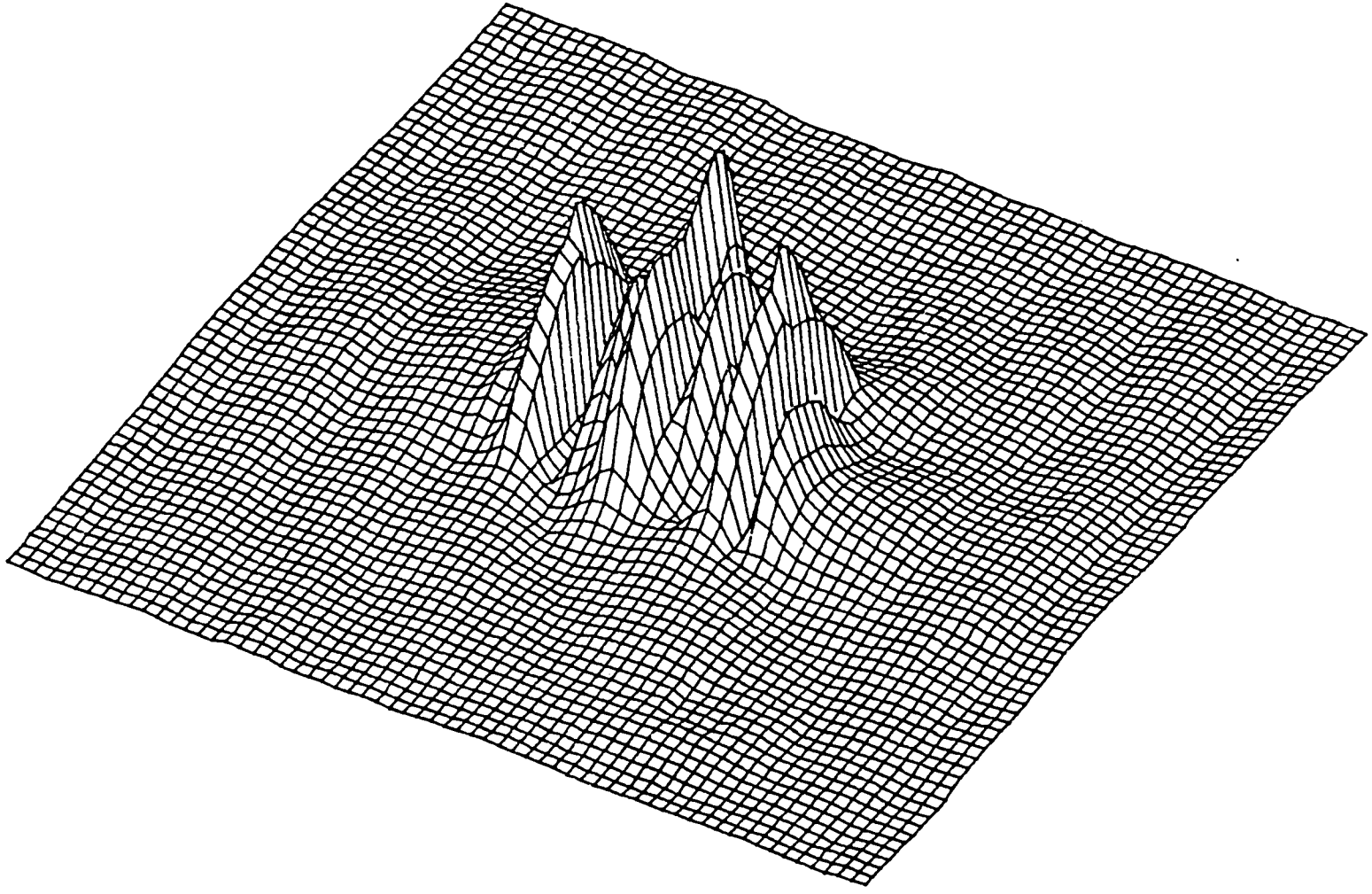

ARM515.HLD PEAK= 0.862E+00

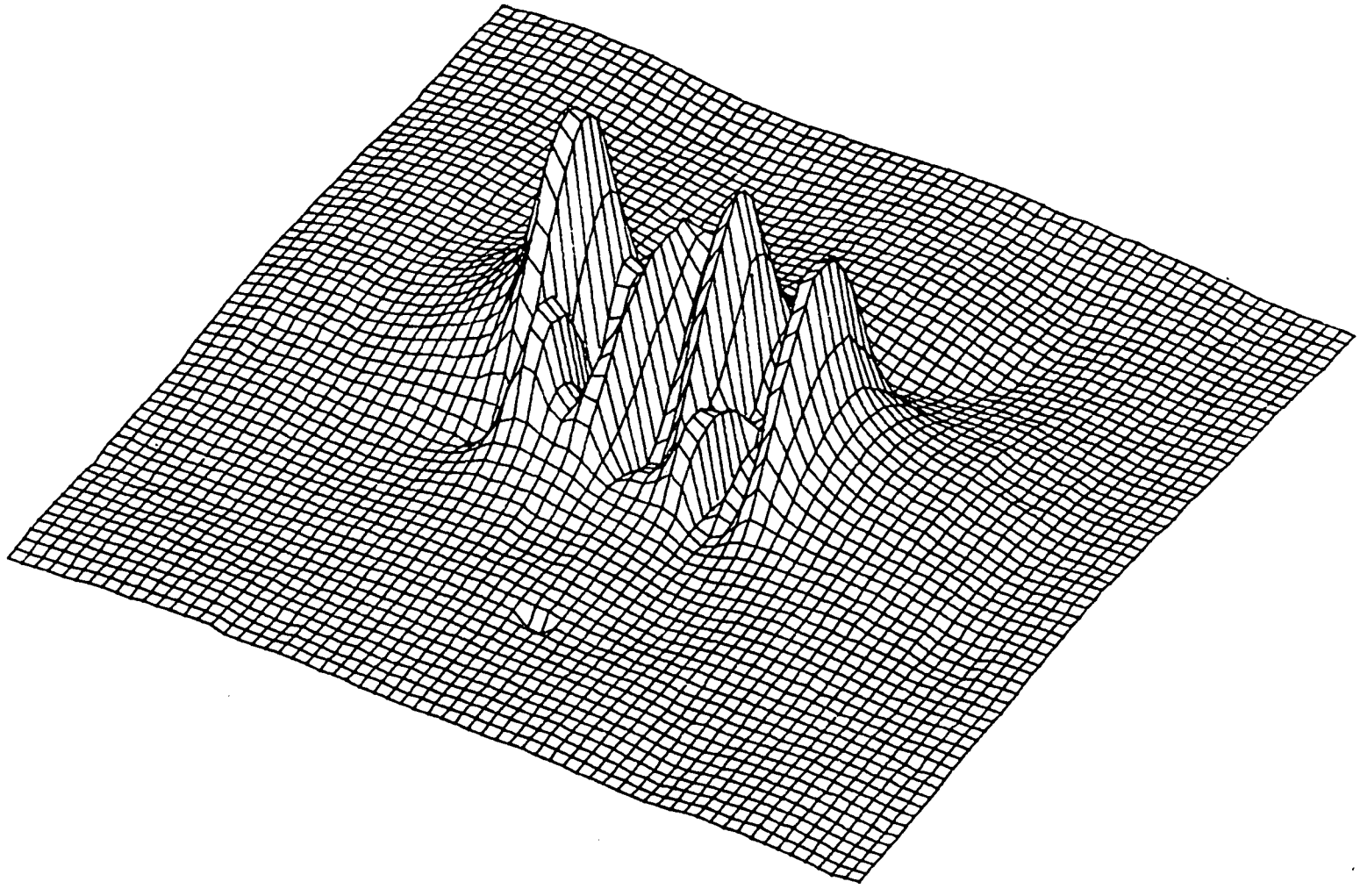

ARM323. HLD PEAK= 0. 567E+00

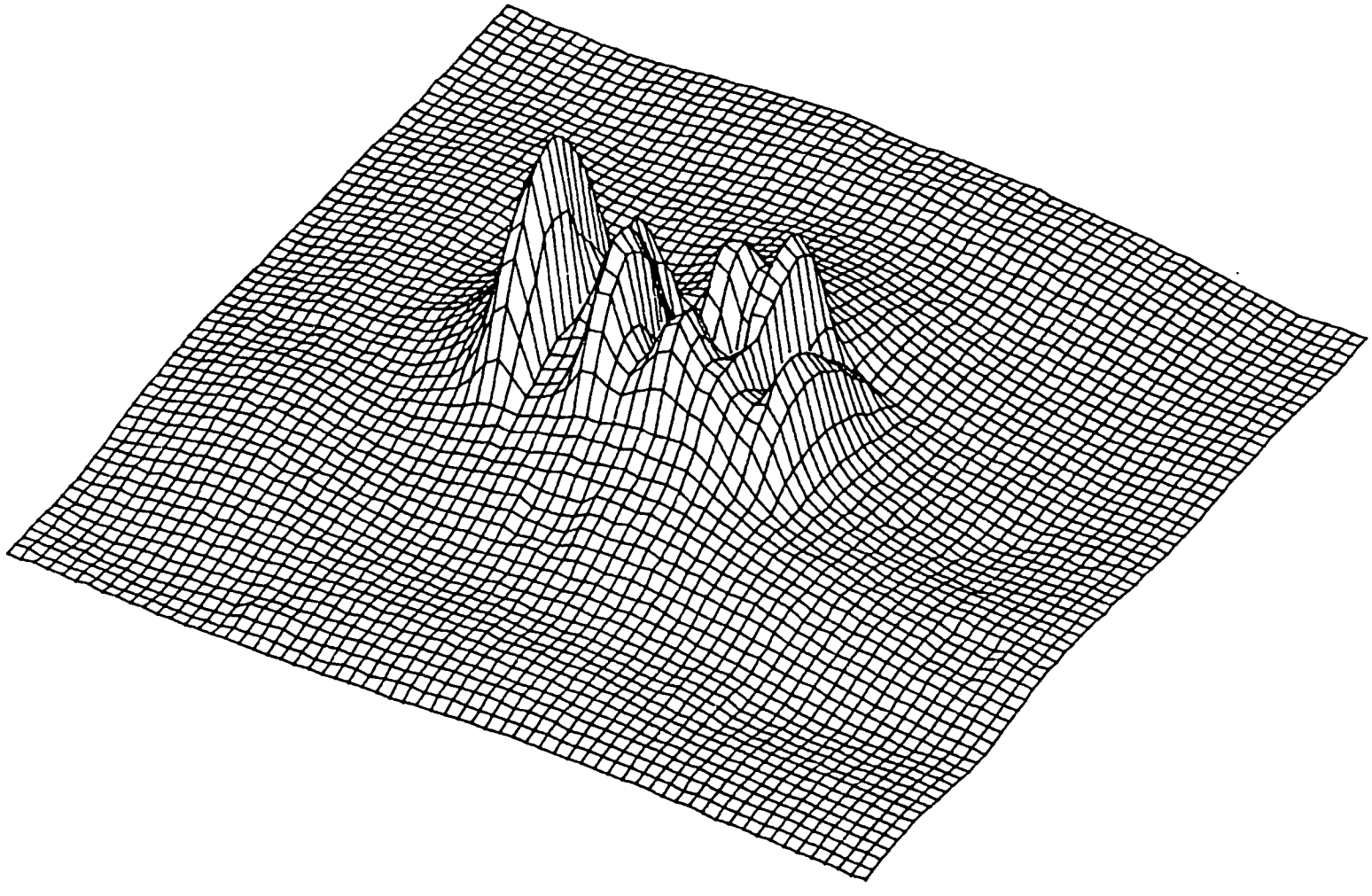

ARM273. HLD PEAK= 0. 658E+00

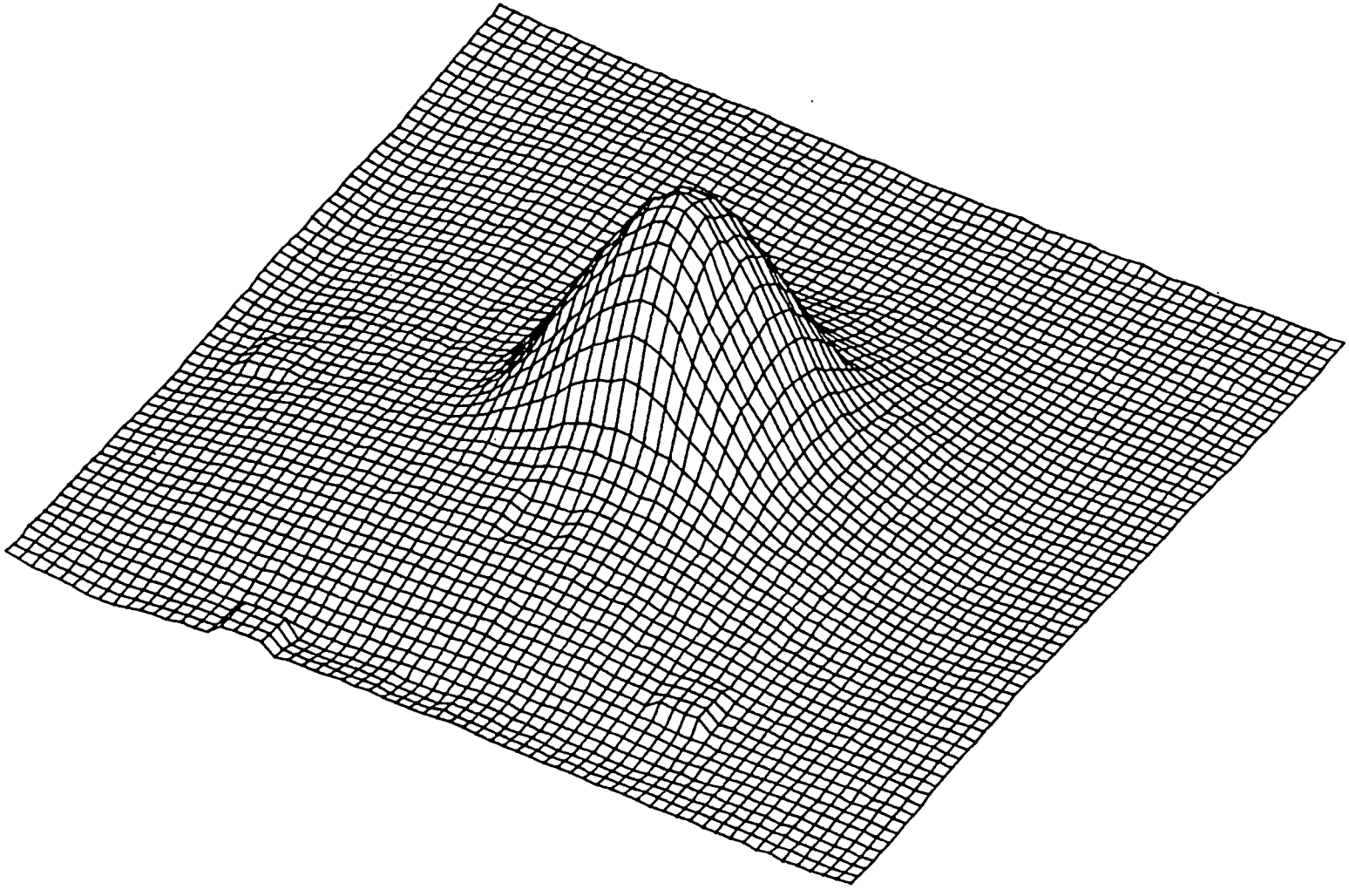

ARM167.HLD PEAK= 0.804E+00

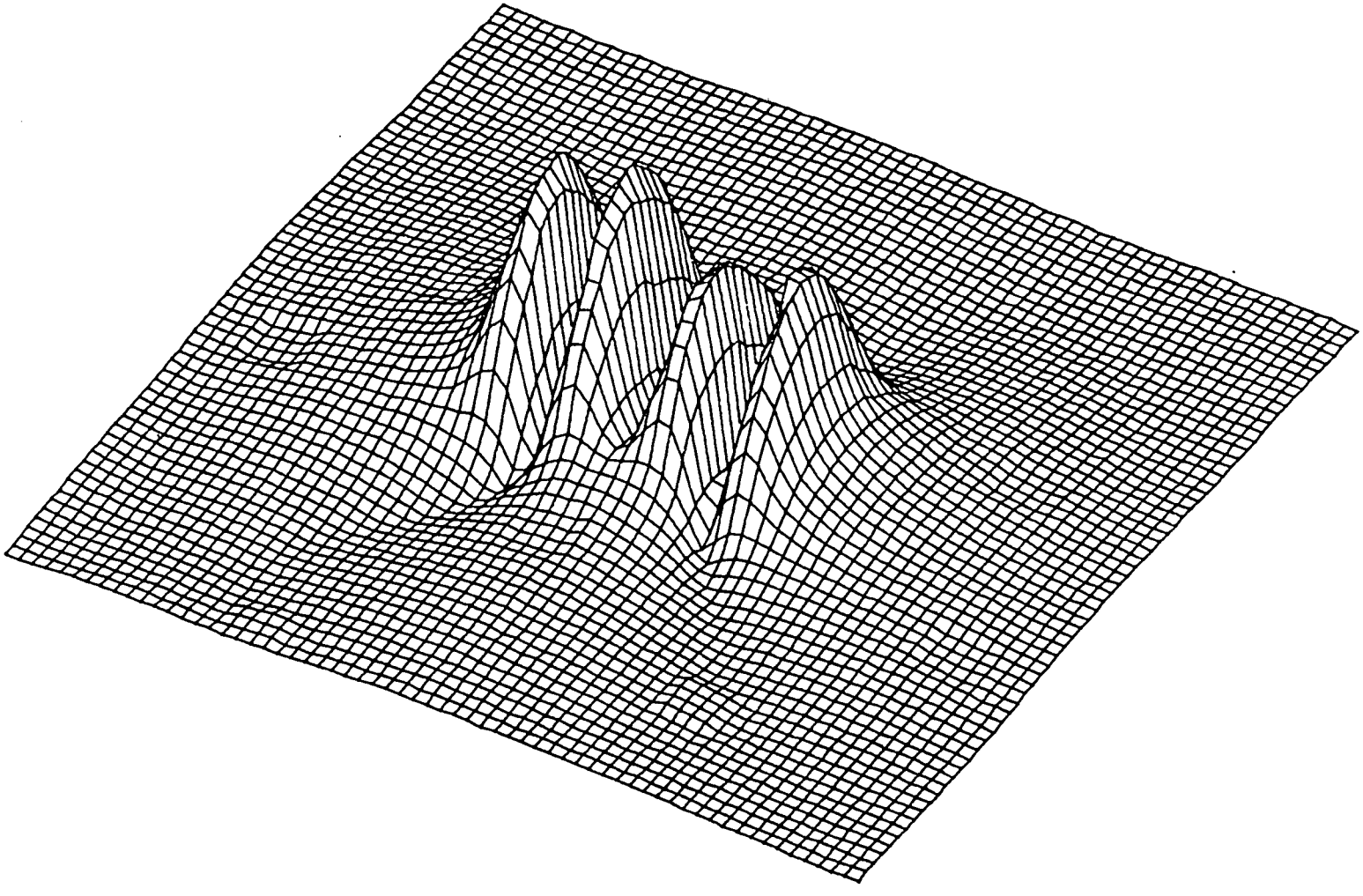

ARM231.HLD PEAK= 0.709E+00

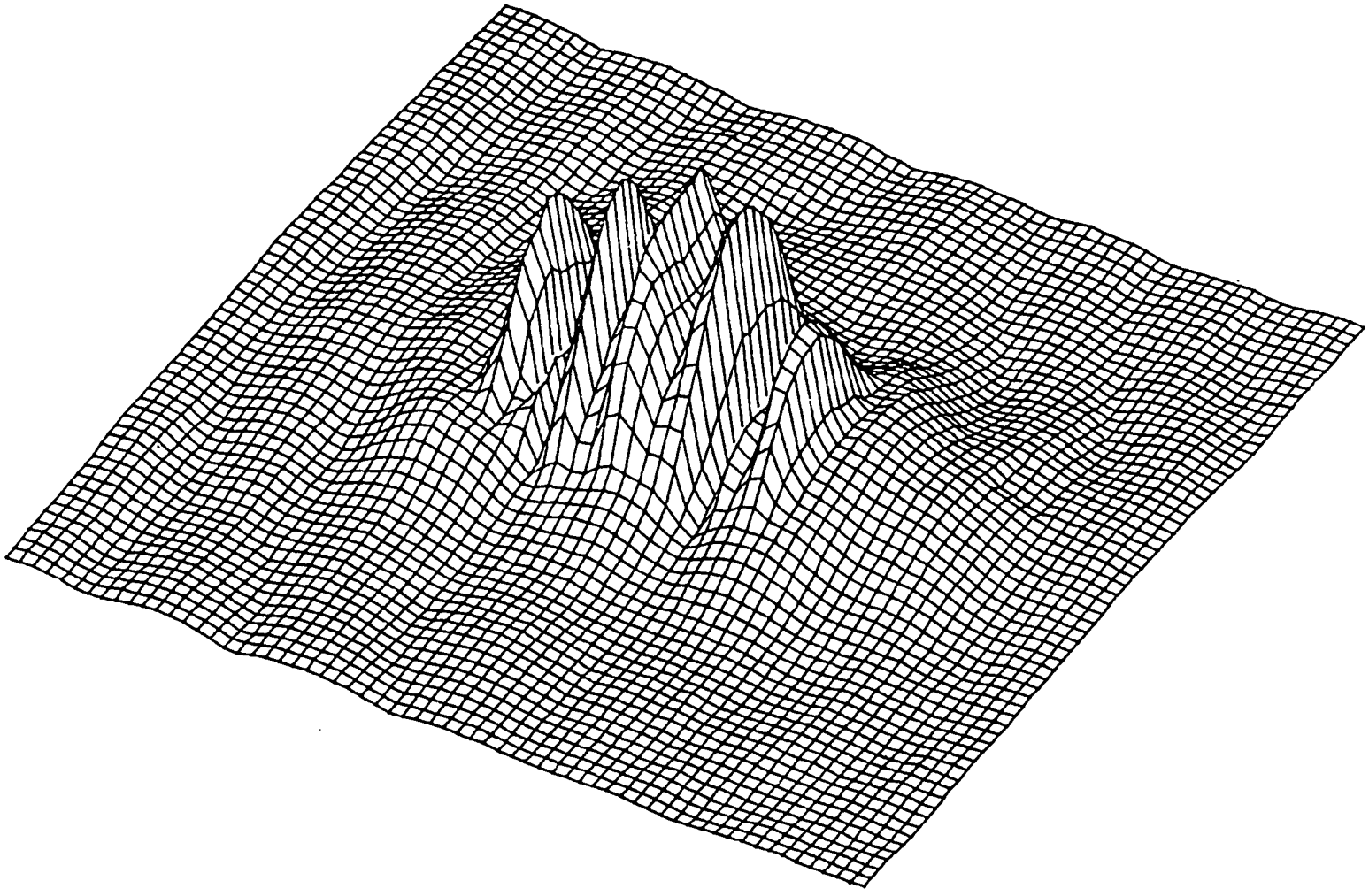

ARM474.HLD PEAK= 0.619E+00

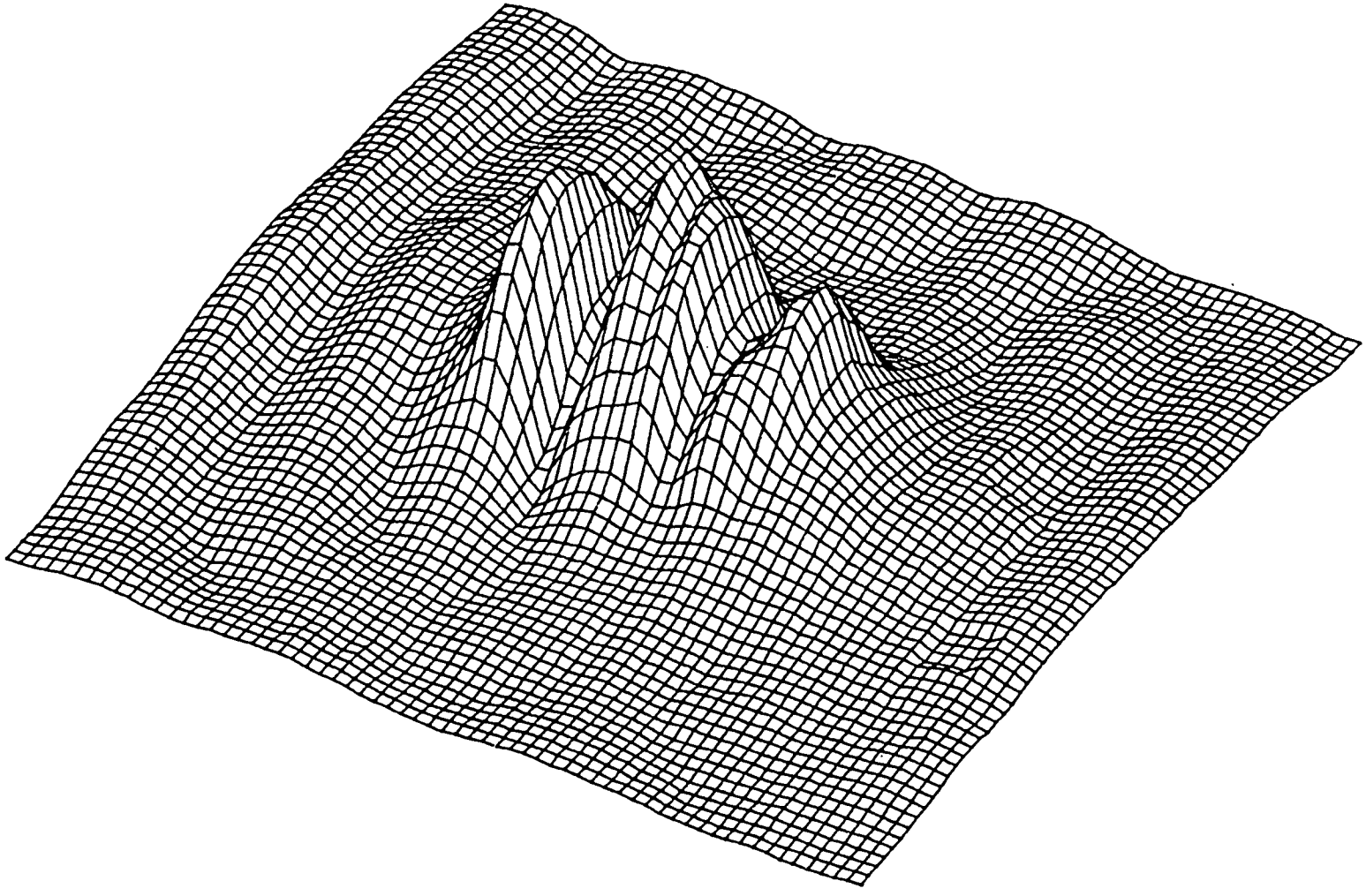

ARM424.HLD PEAK= 0.773E+00

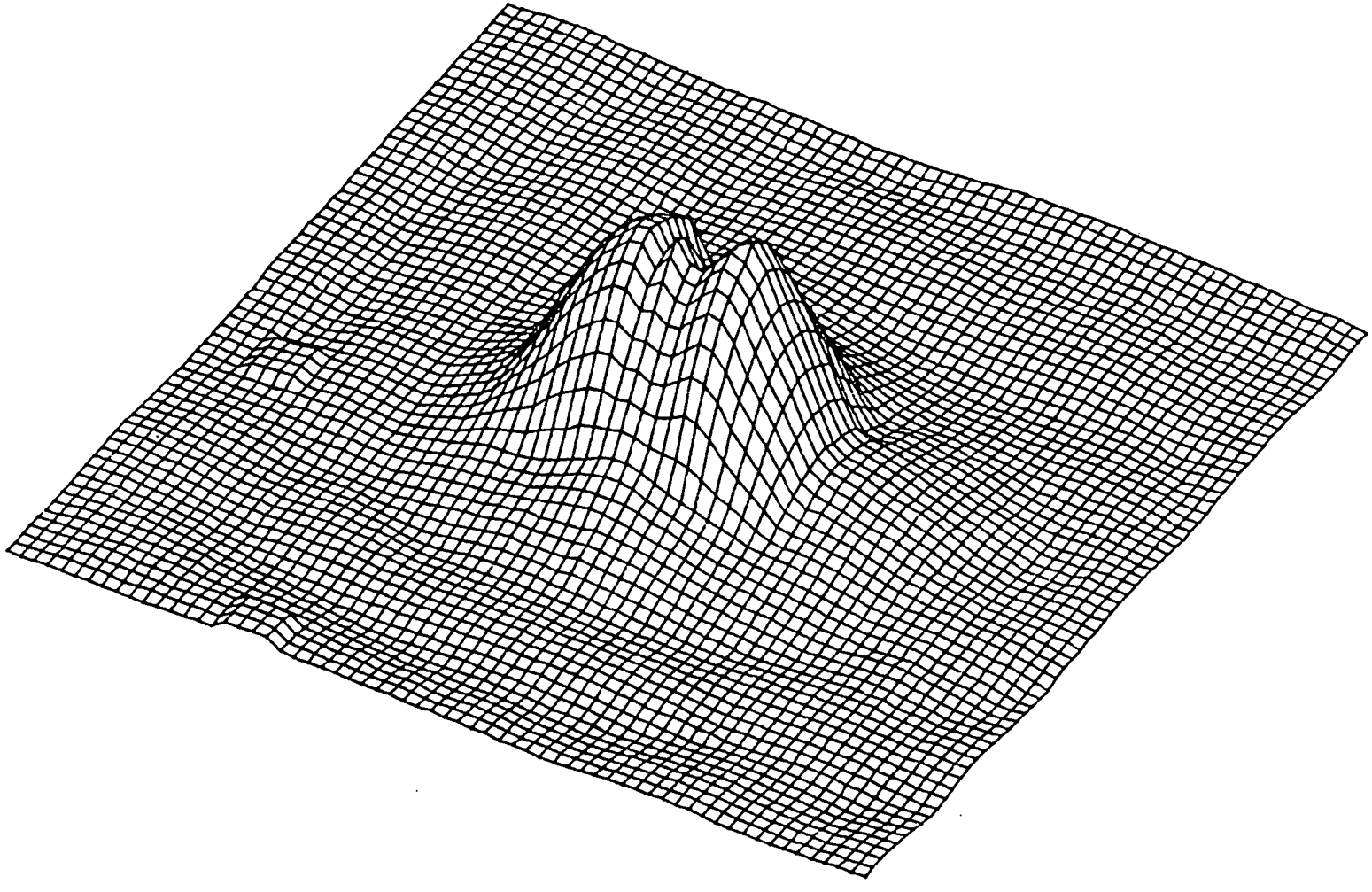

ARM406. HLD PEAK= 0. 440E+00

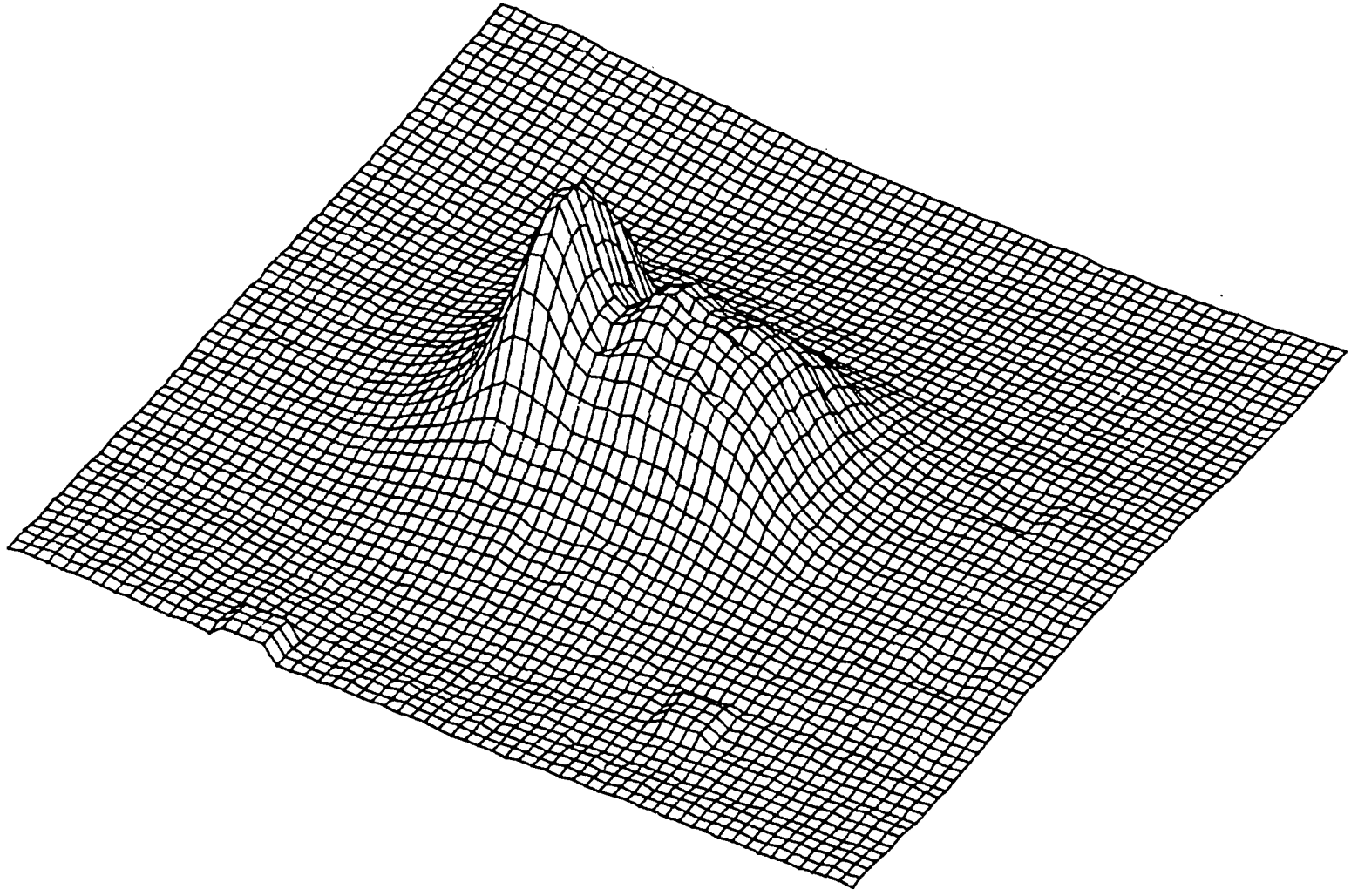

ARS108.HLD PEAK= 0.537E+00

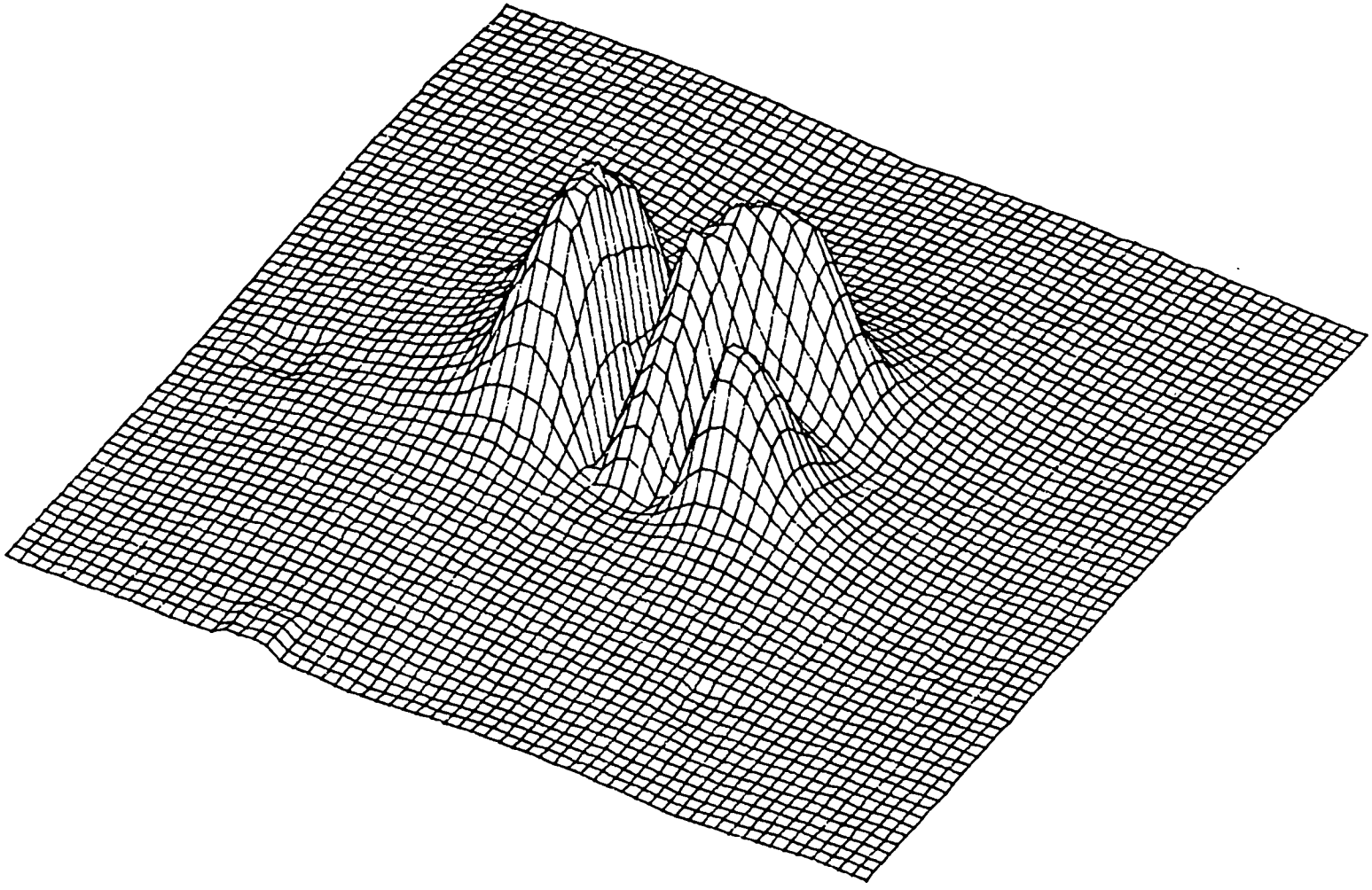

ARS179. HLD PEAK= Ø. 899E+ØØ

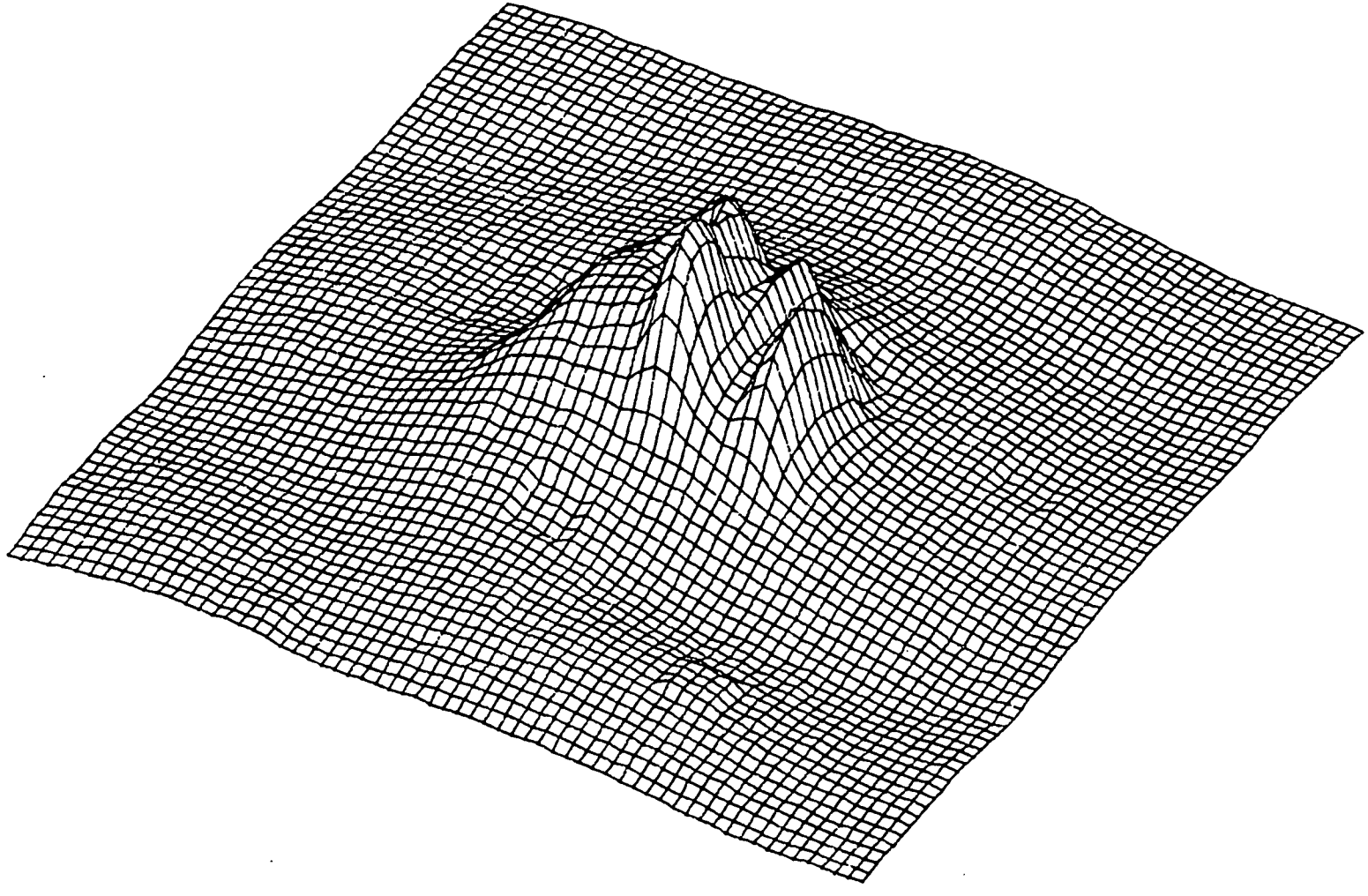

ARS256. HLD PEAK= 0. 551E+00

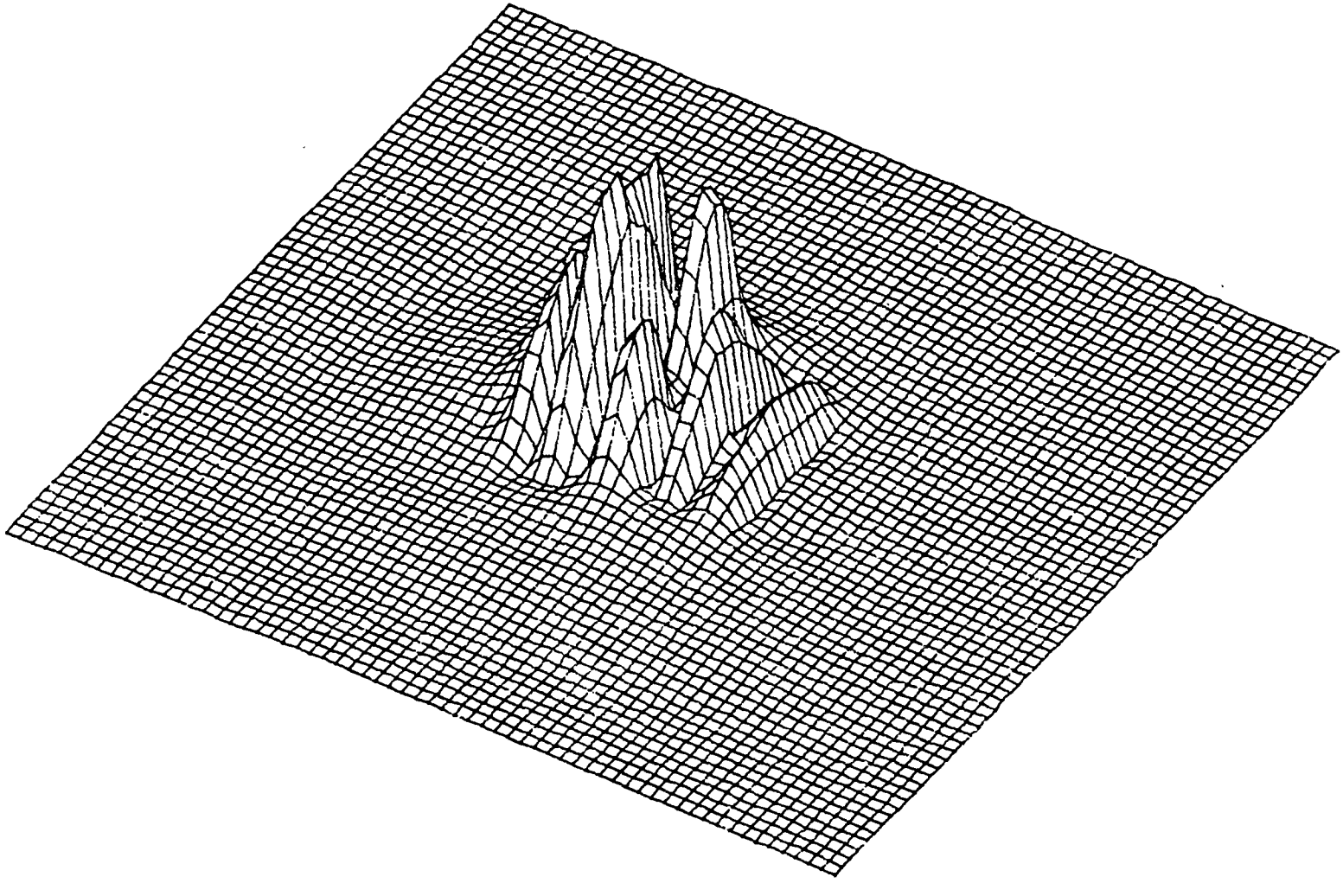

ARS346. HLD

PEAK= Ø. 11ØE+Ø1

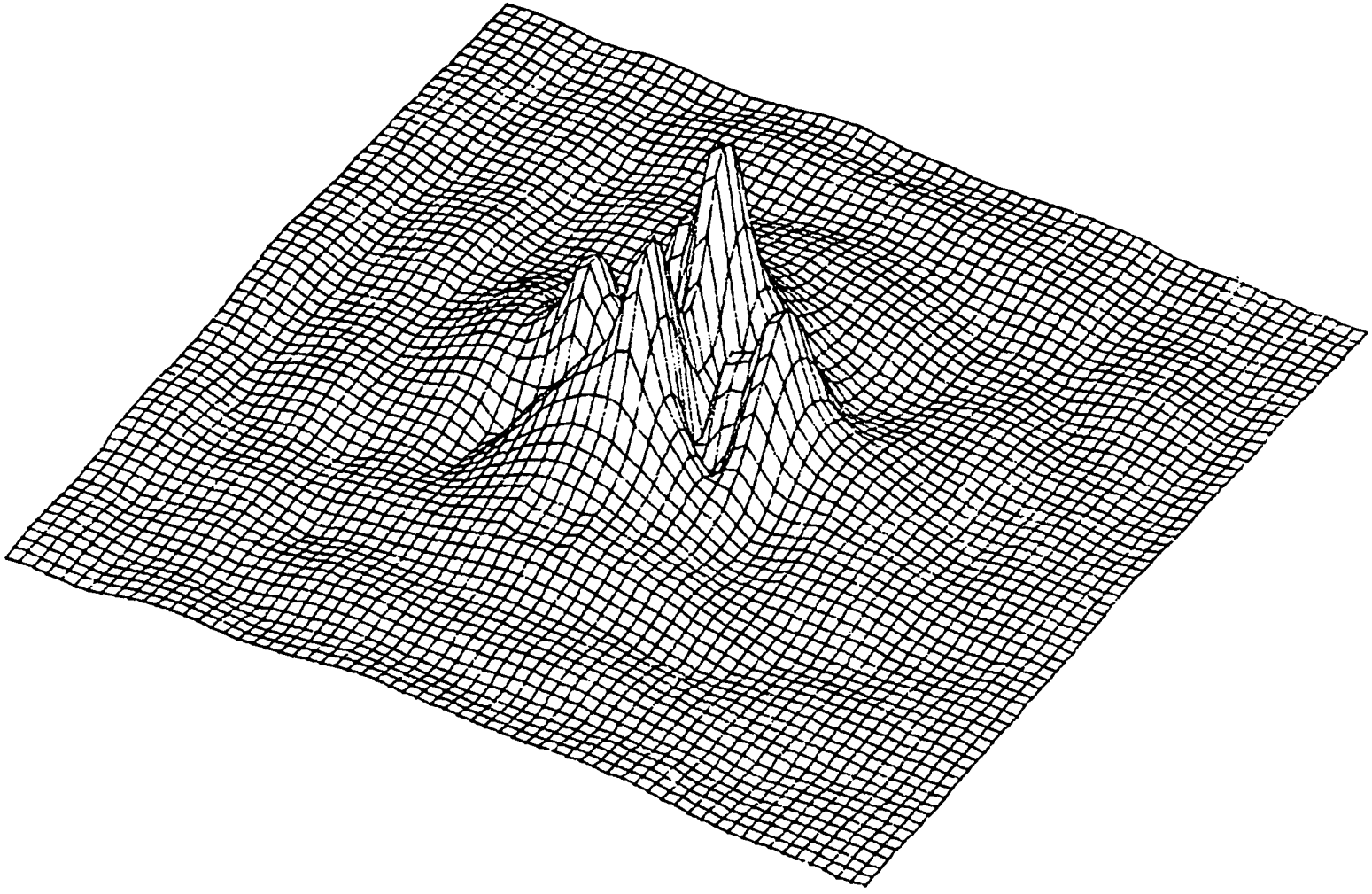

ARS463. HLD PEAK= Ø. 456E+ØØ

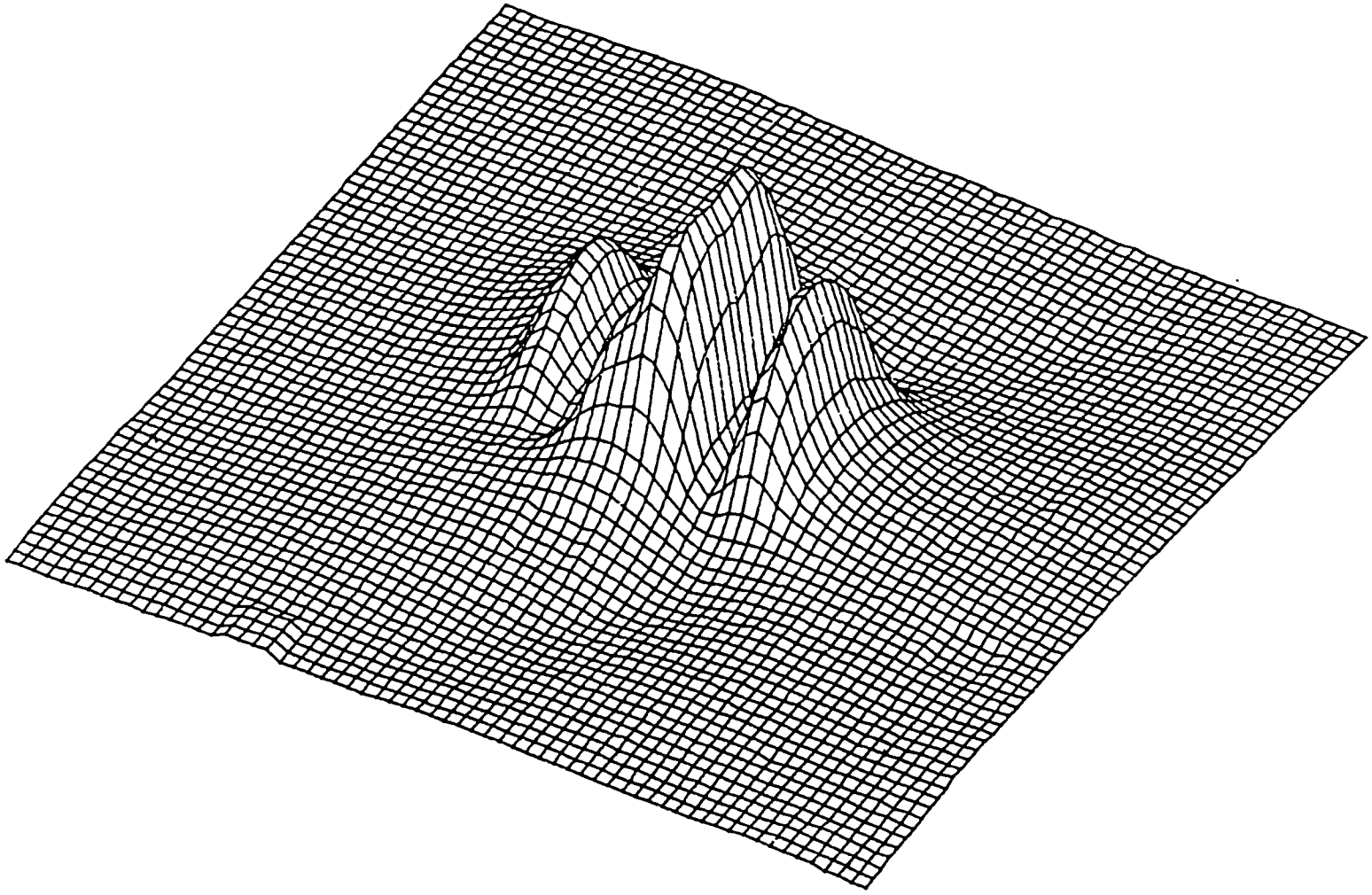

ARS224.HLD PEAK= 0.735E+00

ARS488. HLD

PEAK= Ø. 341E+ØØ

ORIGINAL PAGE IS
OF POOR QUALITY

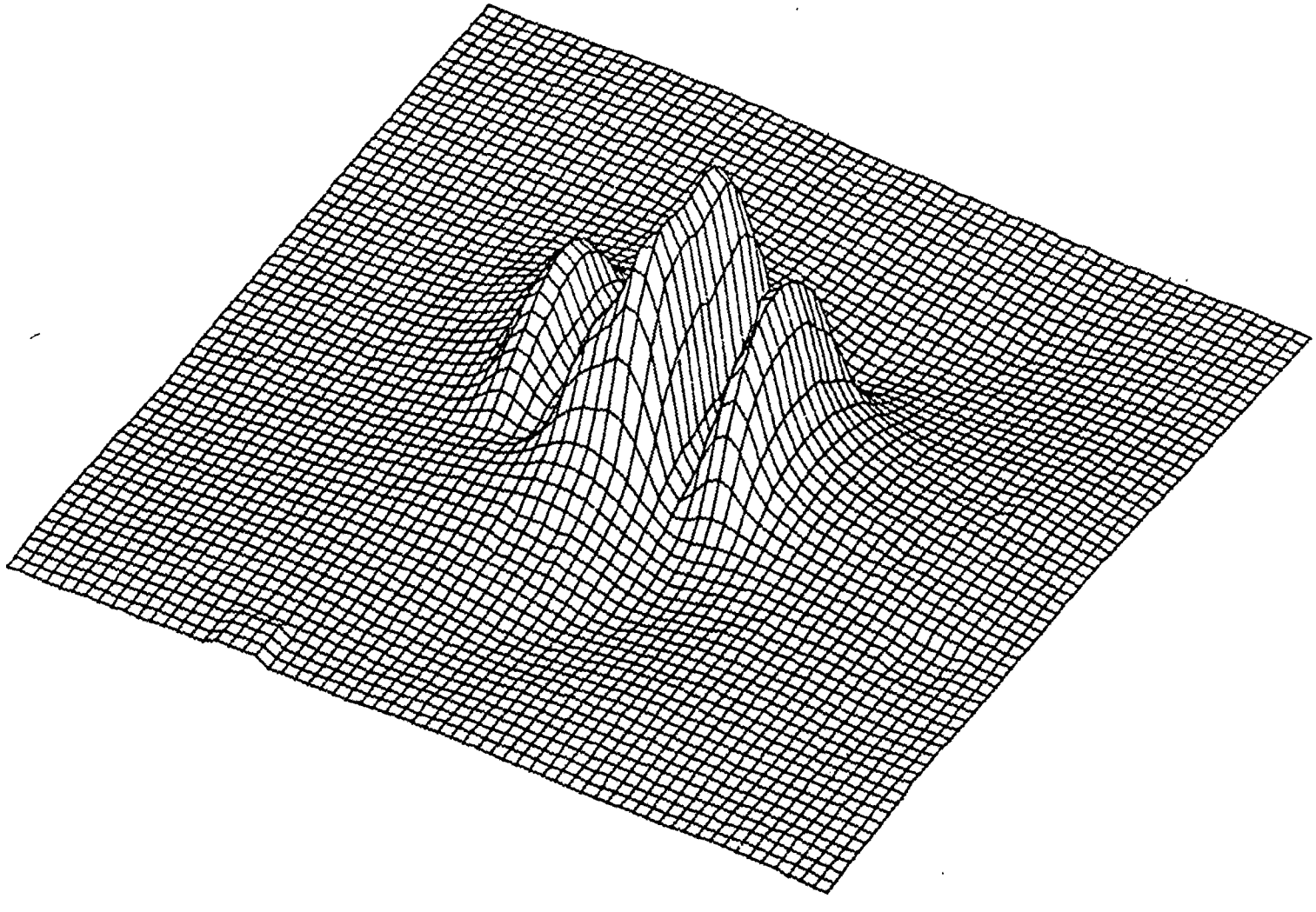

ARS224.HLD PEAK= 0.735E+00

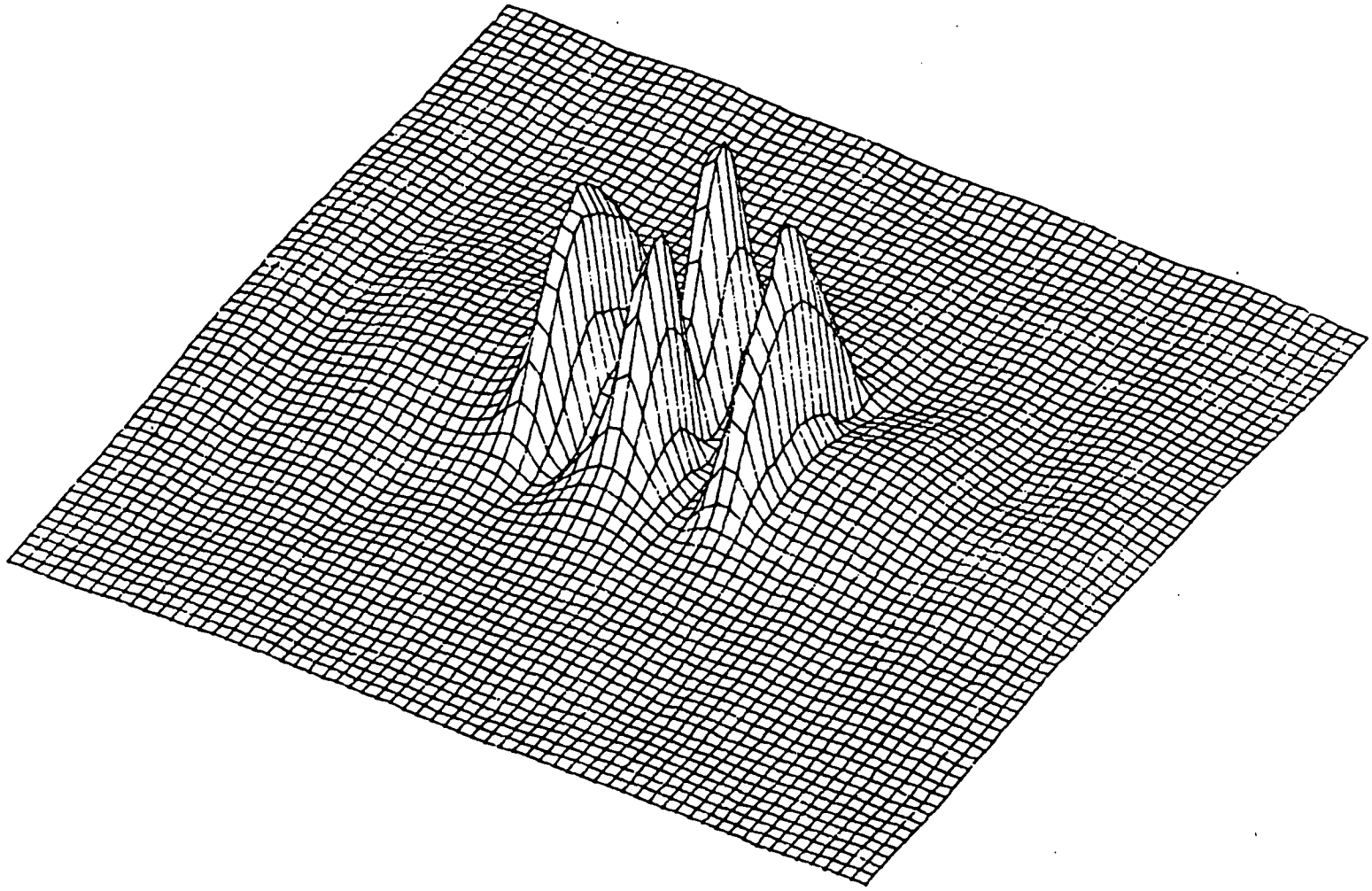

ARS405. HLD PEAK= 0. 926E+00

ORIGINAL PAGE IS
OF POOR QUALITY

ARS134. HLD PEAK= Ø. 738E+ØØ

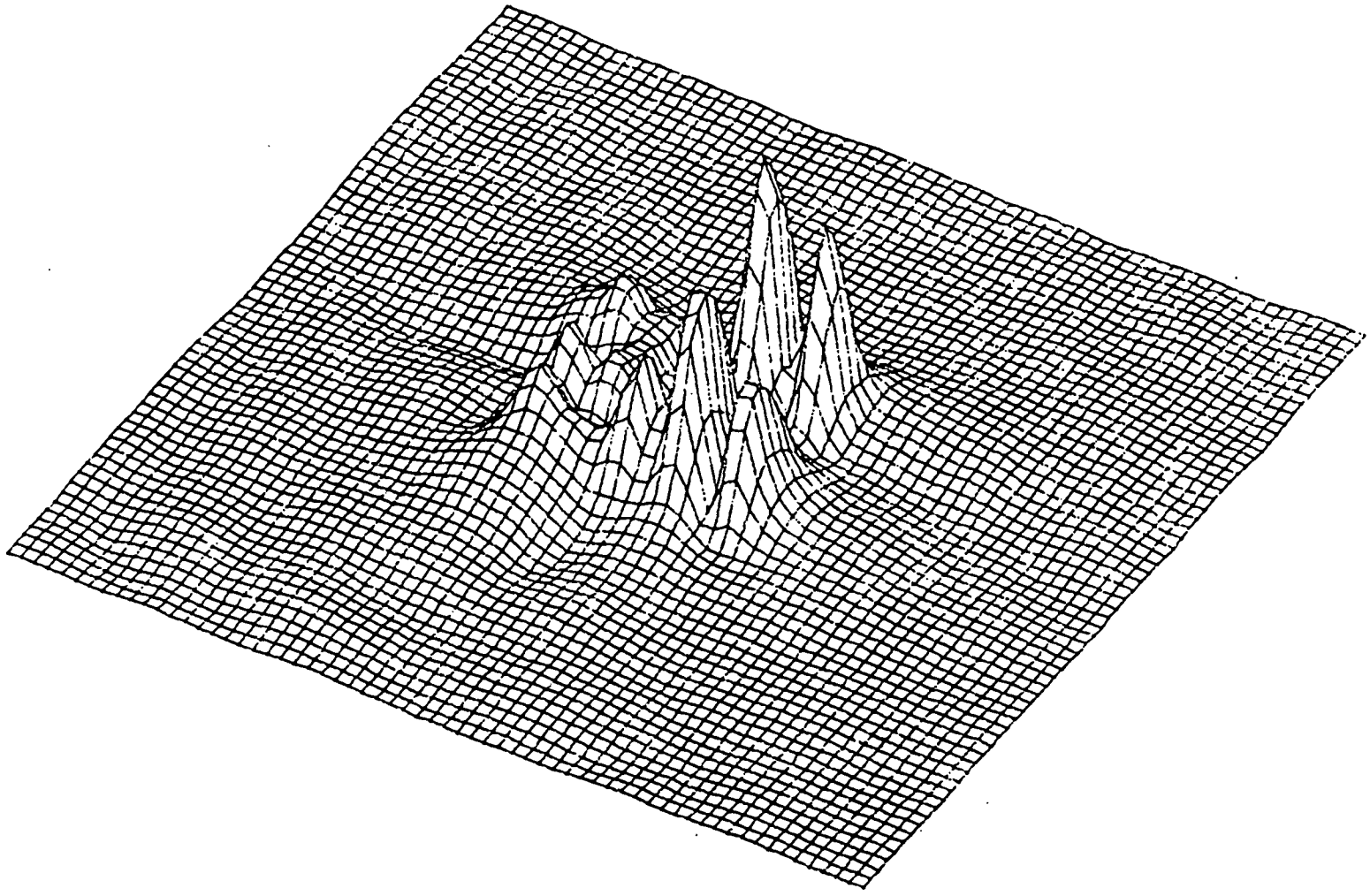

ARS530. HLD PEAK= 0. 625E+00

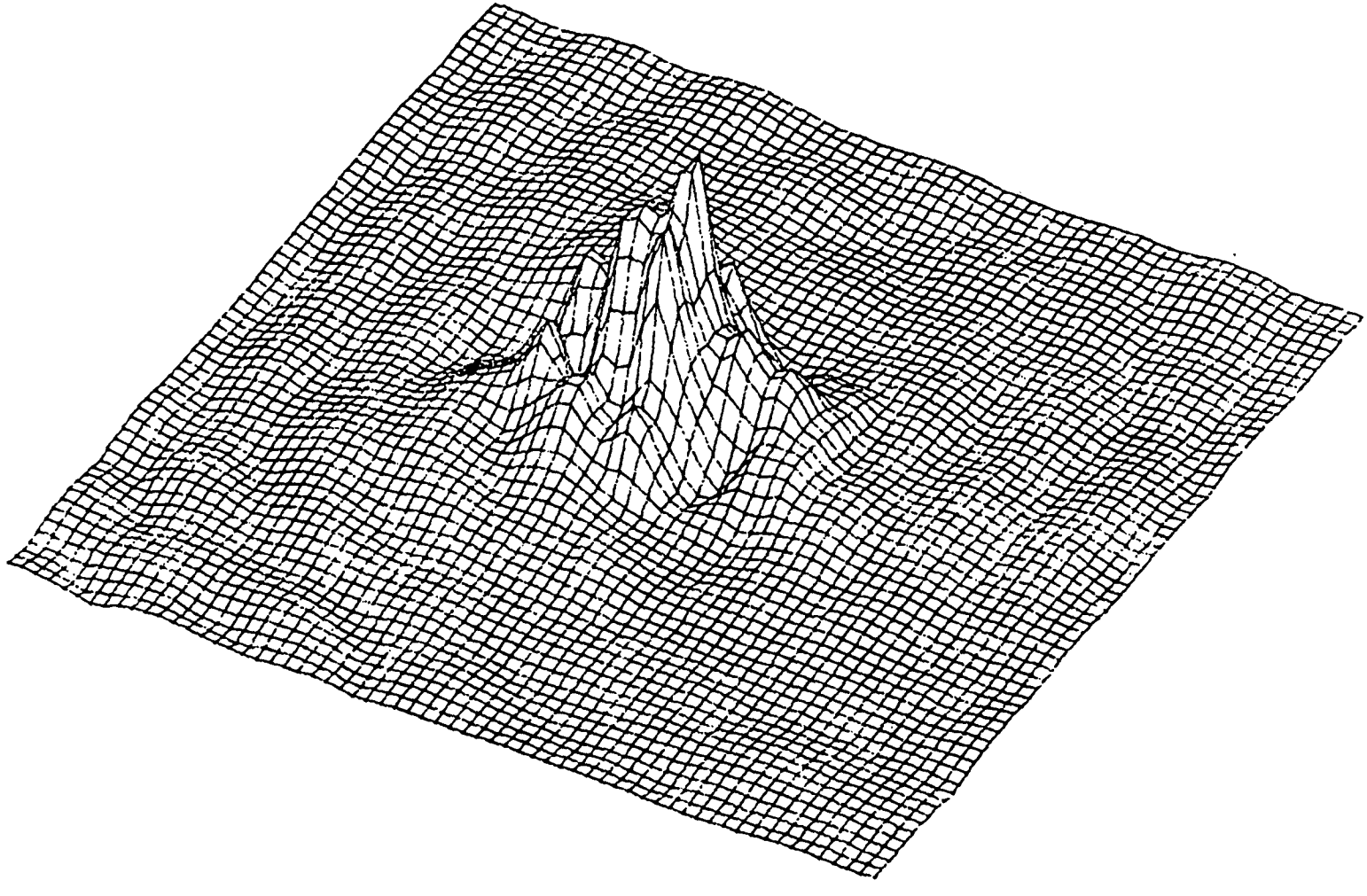

ARS584.HLD PEAK= 0.110E+01

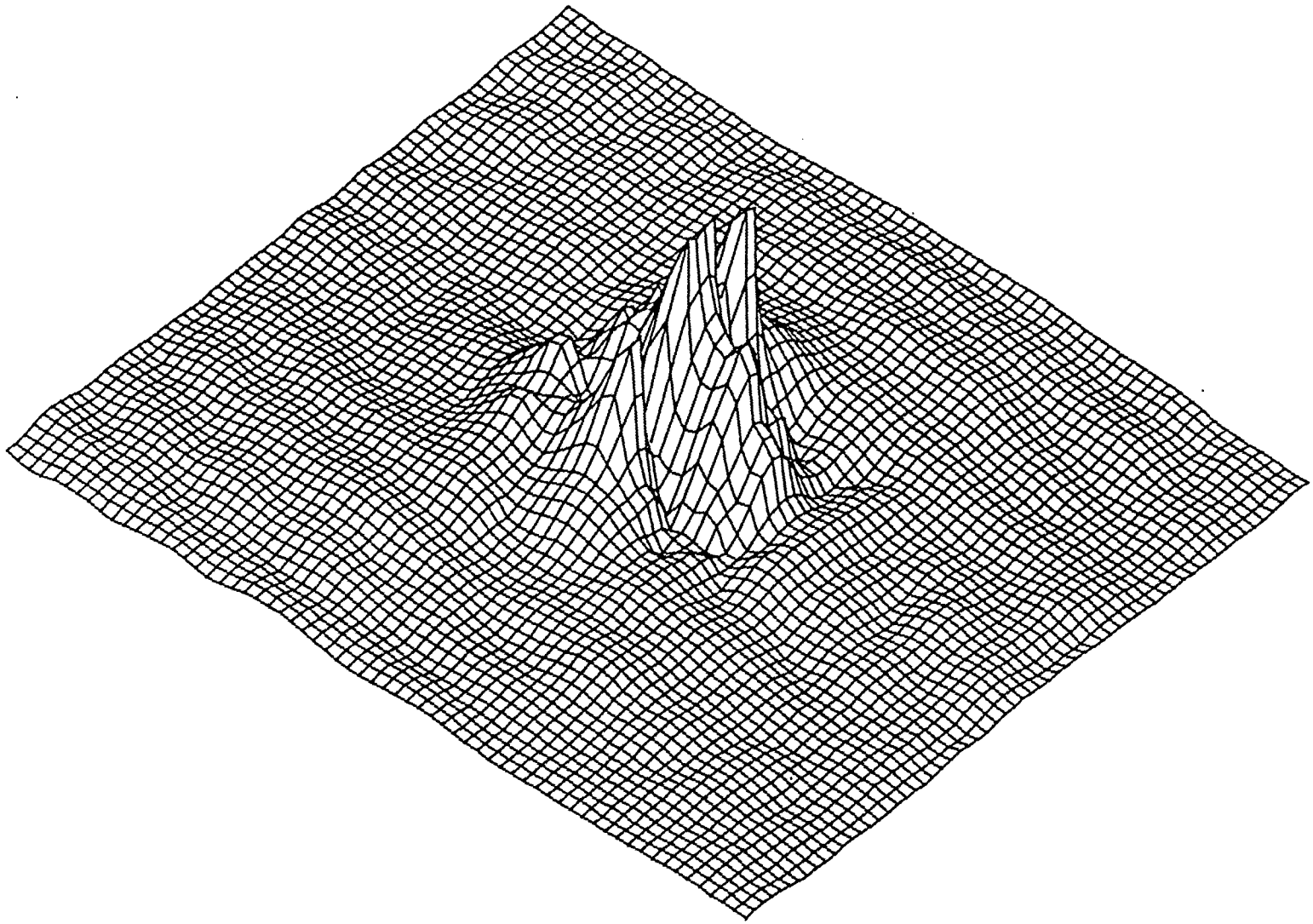

ARS714. HLD

PEAK= Ø.

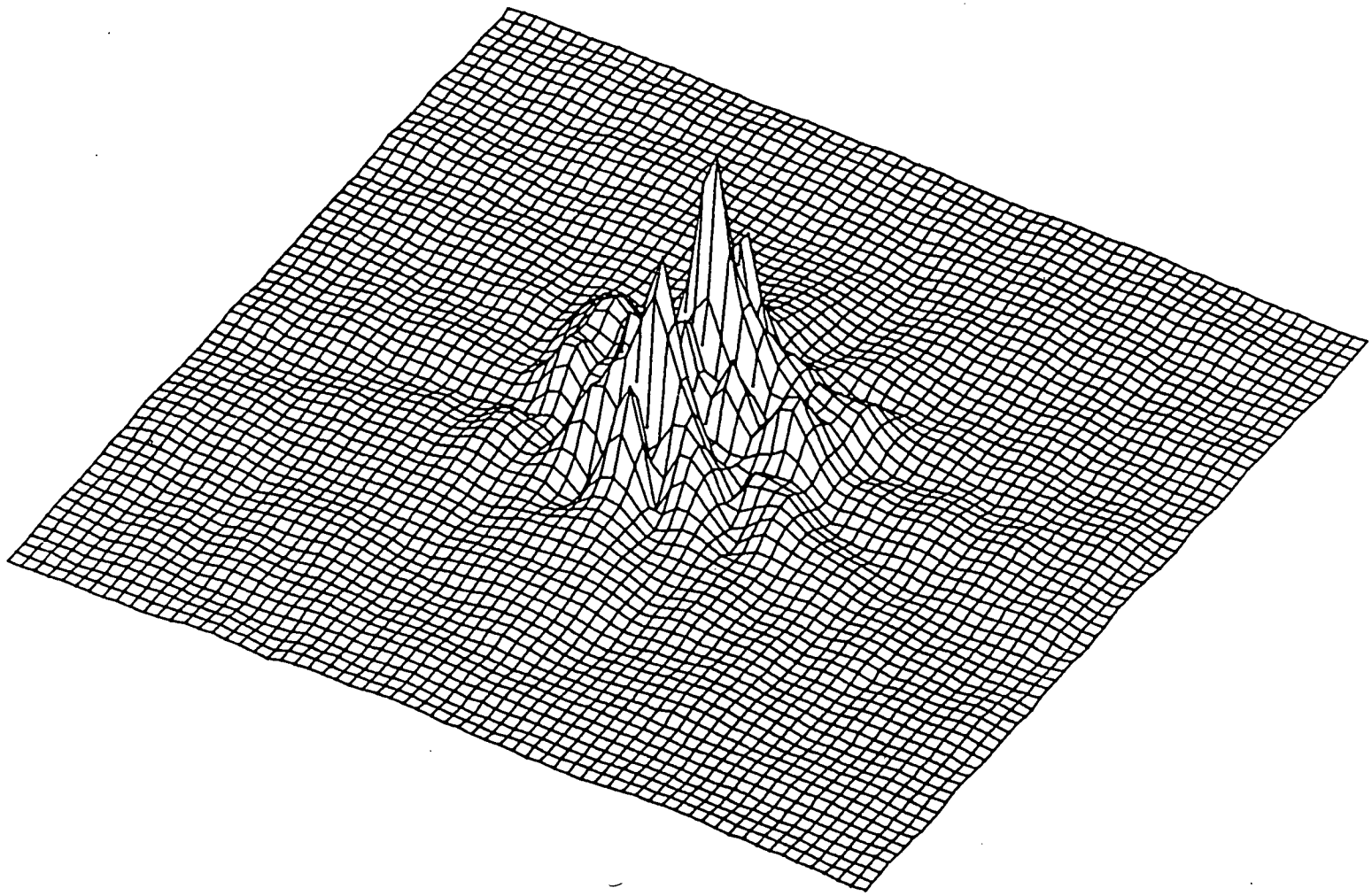

ARS823. HLD PEAK= 0. 109E+01